2,5-Anhydro-D-Mannose End-Functionalized Chitin Oligomers Activated by Dioxyamines or Dihydrazides as Precursors of Diblock Oligosaccharides

Ingrid Vikøren Mo, Marianne Øksnes Dalheim, Finn L. Aachmann,
Christophe Schatz, Bjørn E. Christensen

2,5-Anhydro-D-mannose end-functionalised chitin oligomers activated by dioxyamines or dihydrazides as precursors of diblock oligosaccharides

Ingrid Vikøren Mo[†], Marianne Øksnes Dalheim[†], Finn L. Aachmann[†], Christophe Schatz[‡]*,

Bjørn E. Christensen[†]*

[†]NOBIPOL, Department of Biotechnology and Food Science, NTNU - Norwegian University of Science and Technology, Sem Saelands veg 6/8, NO-7491 Trondheim, Norway

[‡]Laboratoire de Chimie des Polymères Organiques (LCPO), Université de Bordeaux, CNRS, Bordeaux INP, UMR 5629, 33600 Pessac, France

*Corresponding authors

KEYWORDS

chitin • conjugation • hydrazides • oxyamines • dextran • block polysaccharides

ABSTRACT

Diblock oligosaccharides based on renewable resources allow for a range of new, but so far little explored biomaterials. Coupling of blocks through their reducing ends ensures retention of many of their intrinsic properties which otherwise are perturbed in classical lateral modifications.

Chitin ia an abundant, biodegradable, bioactive and self-assembling polysaccharide. However, most coupling protocols relevant for chitin blocks have shortcomings. Here we exploit the highly reactive 2,5-anhydro-D-mannose residue at the reducing end of chitin oligomers obtained by nitrous acid depolymerisation. Subsequent activation by dihydrazides or dioxyamines provides precursors for chitin-based diblock oligosaccharides. These reactions are much faster than for other carbohydrates, and only acyclic imines (hydrazones or oximes) are formed (no cyclic *N*-glycosides). α-Picoline borane and cyanoborohydride are effective reductants of imines, but in contrast to most other carbohydrates they are not selective for the imines in the present case. This could be circumvented by a simple two-step procedure. Attachment of a second block to hydrazide- or aminooxy-functionalised chitin oligomers turned out to be even faster than the attachment of the first block. The study provides simple protocols for the preparation of chitin-*b*-chitin and chitin-*b*-dextran diblock oligosaccharides without involving protection/deprotection strategies.

INTRODUCTION

Block polysaccharides are a new class of engineered polymers based on renewable resources [1, 2]. Among these, diblock polysaccharides, which are composed of two different oligo- or polysaccharide blocks (Figure 1) represent the simplest type. By attaching the blocks at the chain termini their intrinsic properties are minimally perturbed [3, 4]. In this respect they are analogous to synthetic AB type block copolymers. However, the broad range of chemical, physical and biological properties of natural and abundant polysaccharides is very different from most synthetic blocks. Examples include solubility, crystallinity, interactions with ions, pH responses, and above all, biodegradability. This work focuses on the preparation of chitin-based diblock

oligosaccharides by using the dihydrazide/dioxyamine copper-free and aniline-free conjugation methodology recently applied to chitosan oligosaccharides having a *N*-acetyl-D-glucosamine (GlcNAc) residue at the reducing end [5]. Here we take advantage of chitins with a reactive 2,5-anhydro-D-mannose residue at the reducing end. In contrast to alkyne/azide click chemistry, where each block needs to be modified prior to coupling [6-9], our methodology takes advantage of the native reducing end for attachment of blocks to bivalent dihydrazides and dioxyamines (Figure 1).
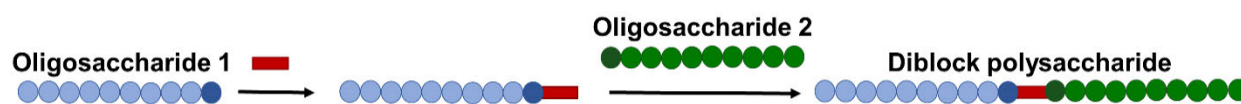

Figure 1: Preparation of a diblock polysaccharide by a two-step strategy. First a bivalent linker is attached to the reducing end of oligosaccharide 1. Oligosaccharide 2 is subsequently attached.

Chitin is a component of the exoskeleton of shrimp and crabs and is available in large quantities as a by-product in aquaculture. It is exclusively composed of β-1,4-linked GlcNAc (A) residues, and consequently, the fraction of acetylated units (F_A) is 1. Chitin has self-assembly properties and becomes water insoluble and crystalline above DP 6. In contrast to chitosans, which can be obtained by partial de-*N*-acetylation of chitin ($F_A < 1$), it is not responsive to changes in pH. Chitin can be degraded by chitinases or by chemical methods to form chitooligosaccharides, which may have biological effects including eliciting defence responses in plants and anticancer properties in animals [10-13]. Enzymatically degradable chitin-cellulose[14] and chitin-poly(propylene glycol)[15] diblocks have been described in the literature. However, their synthesis involved protection/deprotection of hydroxyls and diisocyanate coupling via the natural reducing ends.

Nitrous acid (HONO) depolymerisation of chitosan (Figure 2a) is a commonly used alternative to enzymatic degradation or acid hydrolysis to prepare chitooligosaccharides with a 2,5-

anhydro-D-mannose (M) residue at the reducing end [16, 17]. The HONO only affects the D-glucosamine (GlcN, D) residues of the chitosan, and hence, chitin oligomers (A_nM) can be obtained by using an excess HONO to the fraction of D residues ($F_D = 1 - F_A$). The pending aldehyde of the M residue (Figure 2b) makes such oligomers particularly reactive. This has been exploited to prepare self-branched chitosans [18] as well as a range of end-activated chitosan oligomers for subsequent preparation of chitosan-based copolymers [3, 19-21]. In contrast, block polysaccharides exploiting A_nM chitin oligomers have to our knowledge not been explored.
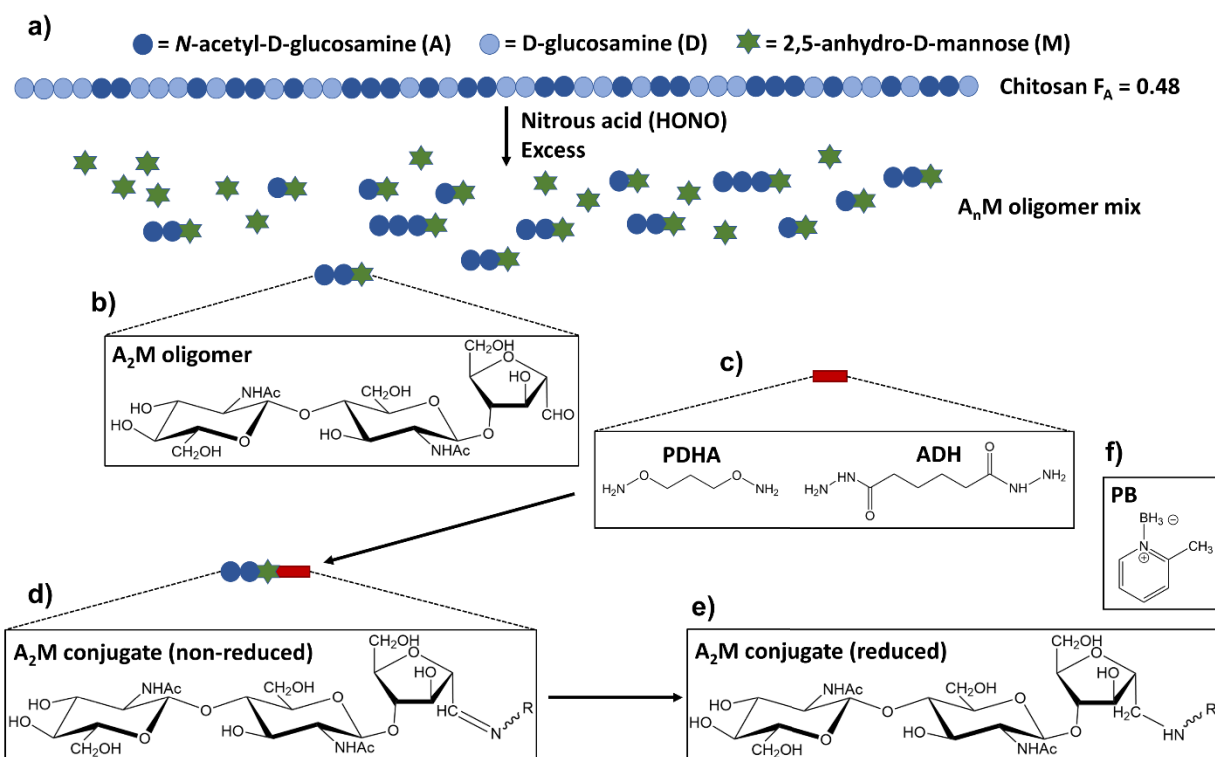
Figure 2: a) Preparation of chitin oligomers (AnM) by degradation of chitosan (e.g. $F_A = 0.48$) using an excess nitrous acid (HONO) **b)** Chemical structure of an A2M oligomer **c)** Chemical structure of PDHA and ADH **d)** Chemical structure of a non-reduced A2M conjugate **e)** Chemical structure of a reduced A2M conjugate **f)** Chemical structure of PB.

Here we report the conjugation of chitin oligomers of the type A_nM (where n refers to the number of A residues, hence the degree of polymerisation (DP) = n+1) to adipic acid dihydrazide (ADH) and O,O'-1,3-propanediyl-bishydroxylamine (PDHA) as the first step to form activated chitin oligomers (A_nM-ADH and A_nM-PDHA) (Figure 2b-d). The study includes the irreversible reduction of conjugates to form stable secondary amine conjugates (Figure 2e) using Picoline borane (PB) as reductant (Figure 2f) [5, 22-25]. In the second step we explore, in a similar way, the attachment of a second oligosaccharide block to both ADH- and PDHA-activated A_nM to prepare two different chitin-based diblocks with antiparallel chains: A_nM-*b*-MA_n and A_nM-*b*-$Dext_m$. $Dext_m$ refers to dextran oligomers with *m* residues. Dextran is a neutral and flexible polysaccharide composed of D-glucose residues linked by α-1,6-linkages, with some short branches [26, 27]. The diblocks were purified by gel filtration chromatography (GFC) and characterized by NMR. The outcome of the study includes kinetic and structural data for each conjugation step as well as protocols for preparing activated oligosaccharides and pure diblock polysaccharides, the latter forming a basis for future structure-function studies.

MATERIALS AND METHODS

Materials

The high molecular weight chitosan (F_A = 0.48) was an in-house sample prepared by homogenous partial de-*N*-acetylation of chitin [28]. The fraction of acetylated units (F_A) was confirmed by ^{1}H-NMR spectroscopy [28]. Dextran T-2000 (M_w = 2 000 000 g/mol) was obtained from Pharmacia Fine Chemicals. Adipic acid dihydrazide (ADH), O,O'-1,3-propanediylbishydroxylamine dihydrochloride (PDHA) and 2-methylpyridine borane complex

(α-Picoline borane, PB) were obtained from Sigma-Aldrich. All other chemicals were obtained from commercial sources and were of analytical grade.

Gel filtration chromatography (GFC)

Preparative and analytical gel filtration chromatography (GFC) were used for fractionation of chitin oligosaccharides and fractionation of products, respectively, as described earlier [5]. In brief, both systems were composed of Superdex 30 columns (BPG 140/950 (140 mm x 95 cm) and HiLoad 26/600 (26 mm x 60 cm), respectively) connected in series, continuously eluting ammonium acetate (AmAc) buffer (0.15 M, pH 4.5 and 0.1 M, pH 6.9, respectively). Fractionation was monitored on-line using a refractive index (RI) detector and fractions were collected and pooled according to elution times. The pooled fractions were reduced to appropriate volumes, dialyzed (MWCO = 100-500 Da) against ultrapure Milli-Q (MQ) water until the measured conductivity of the water was < 2 µS/cm and freeze-dried or freeze-dried directly without dialysis.

NMR spectroscopy

Samples for NMR characterization were dissolved in D_2O (450-600 µL, approx.10 mg/mL). For some samples, 1% sodium 3-(trimethylsilyl)-propionate-d_4 (TSP, 3 µL) was added as an internal standard. Samples for the time course NMR experiments were prepared in deuterated NaAc-buffer (500 mM, pH = 3.0, 4.0 or 5.0, 2 mM TSP).

All homo- and heteronuclear NMR experiments were carried out on a Bruker Ascend 14.1 Tesla 600 MHz or a Bruker Ascend 18.8 Tesla 800 MHz spectrometer (Bruker BioSpin AG,

Fällanden, Switzerland), both equipped with Avance III HD electronics and a 5 mm Z-gradient CP-TCI cryogenic probe.

Characterization of oligomers, purified conjugates or other products was performed by obtaining 1D ^{1}H NMR spectra at 300K on the 600 MHz spectrometer. Time course experiments were performed by obtaining 1D ^{1}H-NMR spectra at specific time points at 300 K on the 600 MHz spectrometer. Chemical shift assignments were performed at 298 K on the 800 MHz spectrometer by obtaining the following homo- and heteronuclear NMR spectra: 1D proton, 2D double quantum filtered correlation spectroscopy (DQF-COSY), 2D total correlation spectroscopy (TOCSY) with 70 ms mixing time, 2D ^{13}C heteronuclear single quantum coherence (HSQC) with multiplicity editing, 2D ^{13}C Heteronuclear 2 Bond Correlation (H2BC), 2D ^{13}C HSQC-[^{1}H,^{1}H]TOCSY with 70 ms mixing time on protons and 2D heteronuclear multiple bond correlation (HMBC) with BIRD filter to suppress first order correlations.

All spectra were recorded, processed and analysed using TopSpin 3.5pl7 software (Bruker BioSpin).

Preparation of chitin oligomers by nitrous acid degradation

Chitosan (F_A = 0.48, 20 mg/mL) was dissolved in acetic acid (AcOH, 2.5 vol%) by stirring overnight. Dissolved oxygen was removed by bubbling the solution with N_2 gas for 15 minutes. After cooling the solution to approx. 4 °C, a freshly prepared $NaNO_2$-solution (20 mg/mL, 30% excess mole $NaNO_2$: mole D-units) was added in three portions with 45-minute intervals. The reaction mixture was agitated in the dark at 4 °C overnight on a shaking device to ensure complete degradation. The degradation mixture was centrifuged using an Allegra X-15R centrifuge (Beckman Coulter) equipped with a SX4750A rotor (30 min, 4750 rpm) and the pellet

was washed with AcOH (2.5 vol%). The washing and centrifugation steps were repeated three times to remove insoluble high molecular weight chitin oligomers. The supernatant (containing water-soluble low molecular weight chitin oligomers) was filtered (5 and 45 µm) and freeze-dried. The water-soluble chitin oligomers (DP < 10) were fractionated according to degree of polymerization (DP) using the preparative GFC system (0.15 M AmAc, pH 4.5). Oligomer fractions were dialyzed (MWCO = 100-500) against MQ-water until the measured conductivity was < 2 µS/cm and freeze-dried. Purified oligomers were characterized by 1D ^{1}H-NMR (600 MHz spectrometer).

Preparation of dextran oligomers by acid degradation

Dextran T-2000 (M_w = 2,000,000, 50 mg/mL) was dissolved in MQ-water over night. HCl (0.1 M) was added to give a final concentration of 0.05 M HCl and 25 mg/mL dextran. Degradation was performed at 95 ℃ for 12 hours. The degradation mixture was fractionated using the preparative GFC system to obtain dextran oligomers ($Dext_m$) of specific DP (m = DP). $Dext_m$ oligomers were purified by dialysis as above and characterized by 1D ^{1}H-NMR (600 MHz spectrometer).

Conjugation and reduction studied by time course NMR

Time course NMR experiments were performed as described earlier [5]. In brief, chitin oligomers (A_nM) or dextran oligomers ($Dext_m$) (20.1 mM) and 2 equivalents ADH or PDHA (40.2 mM) were dissolved separately in deuterated NaAc-buffer (500 mM, pH = 3.0, 4.0 or 5.0, 2 mM TSP) and transferred to a 5 mm NMR tube. For the time course reduction experiments, 3 equivalents (60.3 mM) PB or 3 or 10 equivalents (60.3 or 201 mM) $NaCNBH_3$ were added directly to the NMR tube with equilibrium mixtures of conjugates. Concentrations given in parenthesis are final

concentrations after mixing. Mixing of reagents in the NMR tube or addition of reducing agent served as time zero (t = 0). 1D ^{1}H-NMR spectra were recorded at desired time-points (600 MHz spectrometer, 300 K) and the course of the reactions was tracked by integration of the spectra. Samples were held at room temperature between recordings. Equilibrium yields and yields from the reduction of conjugates in the NMR tube were obtained by integration of the ^{1}H-NMR spectra.

For experiments where a large excess of PB (20 equivalents) was used, equilibrium mixtures with non-reduced conjugates were removed from the NMR tube and reduced in a separate vial.

Preparative protocol for reduced conjugates (activated chitin oligomers)

Chitin oligomers (A_nM, 20.1 mM) and 10 equivalents of ADH or PDHA (201 mM) were dissolved in NaAc-buffer (500 mM, pH 4.0) to which 3 or 20 equivalents of PB (60.3 mM or 420 mM), respectively were added after > 6 hours. The reduction was performed at room temperature for 24 or 48 hours for A_nM-ADH or A_nM-PDHA conjugates, respectively. Reactions were terminated by dialysis (MWCO = 100-500 Da) against 0.05 M NaCl until the insoluble PB was dissolved, and subsequently freeze-dried. Conjugates were purified by GFC (analytical scale) and freeze-dried directly several times to remove the volatile GFC buffer (0.1 M AmAc). Purified conjugates were characterized by NMR spectroscopy (600 MHz spectrometer). Chemical shift assignment for the purified A_2M-PDHA conjugate was performed by homo- and heteronuclear NMR spectroscopy (800 MHz spectrometer).

Preparation of chitin diblock structures using a substoichiometric amount of ADH or PDHA

Chitin oligomers (A_nM, 20.1 mM) and 0.5 equivalents of PDHA or ADH (10.05 mM) were dissolved in deuterated NaAc-buffer (500 mM, pH 4.0) and the conjugation was studied by time course NMR as described above. Reduction with 3 or 20 equivalents PB, fractionation and characterization of products were performed as described for the preparative protocol, however with a longer reduction time (96 hours) for the diblocks formed with PDHA.

**Preparation of diblock structures from activated chitin oligomers**

Purified chitin oligomer conjugates (A_nM-ADH or A_nM-PDHA, 20.1 mM) were reacted with equimolar concentrations of chitin oligomers (A_nM) or dextran oligomers ($Dext_m$) to form diblock structures (in 500 mM deuterated NaAc-buffer, pH 4.0, RT). The conjugation of the second block was monitored by time course ^{1}H-NMR until equilibrium was reached. Reduction of chitin diblocks (A_nM-*b*-MA_n) was performed as described for the preparative protocol using 3 equivalents PB. Due to slow reduction of $Dext_m$ conjugates, reduction was performed using 20 equivalents (402 mM) PB at 40 ℃ for 96 hours for the A_nM-PDHA-$Dext_m$ diblocks and 144 hours for the A_nM-ADH-$Dext_m$ diblocks. Fractionation and characterization of products were performed as above. Yield of diblock structures were obtained by integration of the GFC chromatogram.

RESULTS AND DISCUSSION

Preparation and characterization of chitin oligomers

Chitin oligomers of the type A_nM were obtained by degrading chitosan using an excess nitrous acid (HONO) to the fraction of D residues. The mixture of water-soluble chitin oligomers was fractionated by GFC (Supporting Information, S1). Purified oligomers were characterized by ^{1}H-

NMR (Figure 3), and key resonances were annotated according to literature [17]. The reducing end 'aldehyde' proton appears as a doublet at 4.9 ppm due to complete hydration in water to the corresponding gem-diol [17]. The minor resonances around 5 ppm (marked as M' in Figure 3) were tentatively assigned to alternative forms of the M residue predicted in the literature [29]. These alternative forms (< 15 %) are not easily detected, and in particular not quantified for longer oligomers of the D_nM type (where n is the number of contiguous uninterrupted D residues) [19] due to weak reducing end resonances. Also, a major difference between A_nM and D_nM oligomers is the requirement for excess HONO in the preparation of the former which may possibly influence the formation of these alternative M forms.
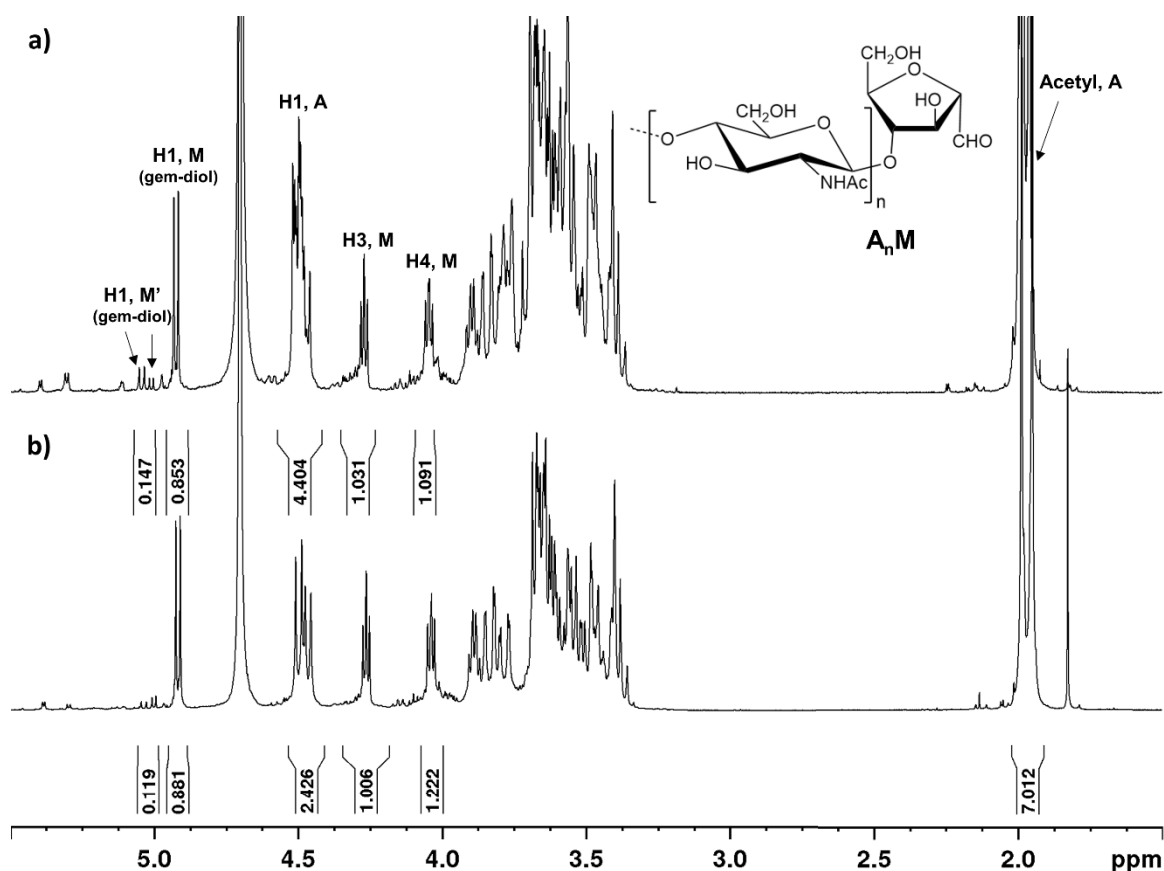
Figure 3: ^{1}H-NMR characterization of purified **a)** A_4M and **b)** A_2M oligomers in D_2O (600 MHz).

Reaction with ADH and PDHA

The conjugation of the trisaccharide A_2M to ADH or PDHA (2 equivalents) was studied in detail by time course NMR at pH 3.0, 4.0 and 5.0 (Supporting information, S2). ^{1}H-NMR spectra of the equilibrium mixtures for the conjugation reactions at pH 4.0 are given in Figure 4. In agreement with the literature [19], only E-/Z-hydrazones or oximes were formed. Minor resonances close to the main resonances for the E- and Z-hydrazones or oximes were attributed to the conjugation of oligomers with alternative forms of the M residue (marked as H1 M' in Figure 4).
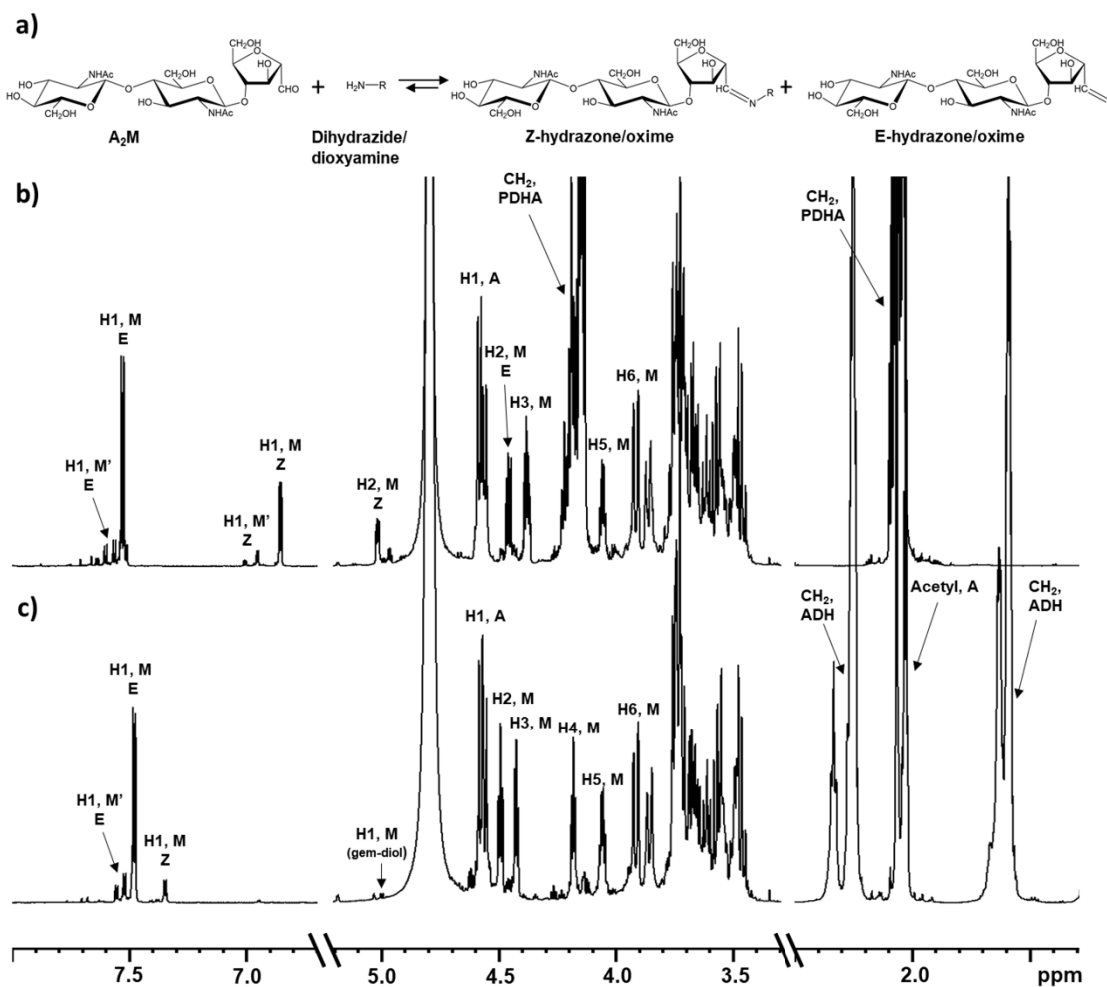
Figure 4: a) General reaction scheme for the conjugation of A_2M to ADH (dihydrazide) or PDHA (dioxyamine), **b)** and **c)** ^{1}H-NMR spectra of the equilibrium mixtures obtained for the conjugation of A_2M to PDHA and ADH, respectively.
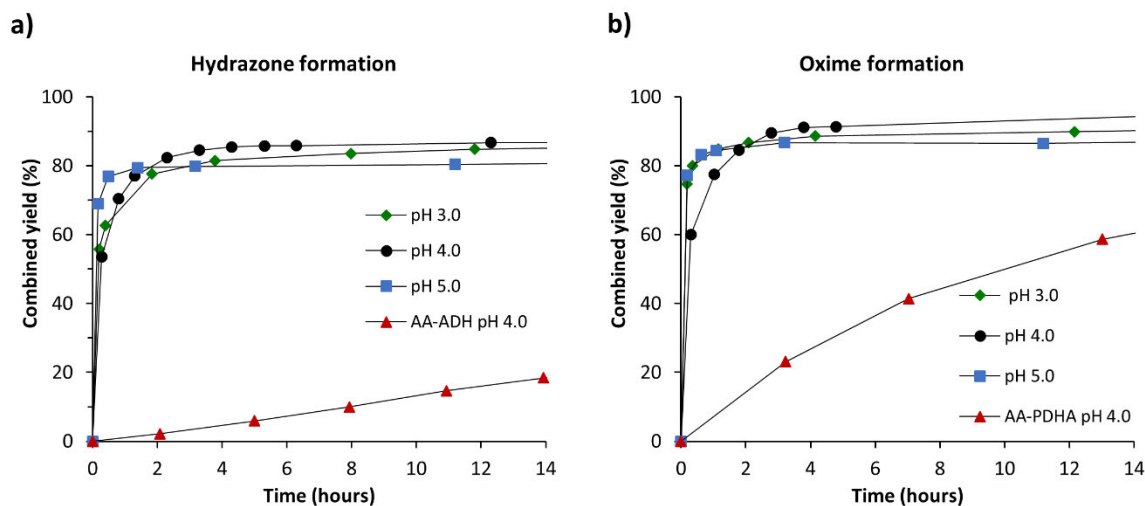
Kinetics

Kinetic plots for the conjugation of A_2M to ADH (hydrazone formation) and PDHA (oxime formation) are given in Figures 5a and 5b, respectively. The combined yield is the sum of E- and Z- hydrazones/oximes for all the forms of the M residue. Compared to chitosan oligomers with GlcNAc (A) at the reducing end [5], A_nM oligomers reacted much faster with both ADH and

13

PDHA under otherwise identical conditions (results obtained for AA [5] included in Figure 5).
With two equivalents of ADH or PDHA, reactions were essentially complete after 4-6 hours.

Reaction modelling is a powerful tool to simulate reactions, and to predict the effects of e.g.
changing the concentration of reactants. We have previously shown that the conjugation of
chitosan oligomers (with A at the reducing end) to ADH and PDHA, was first order with respect
to each reactant in the range 2 to 10 equivalents [5]. In contrast to these oligomers, the model for
A_nM becomes simpler because cyclic *N*-glycosides are not formed. The model is detailed in
Supporting information, S3. The outcome of the modelling is estimated rate constants for the
formation and dissociation of E-/Z-hydrazones and oximes. Rate constants for best fits are given
in Table 1. We also included the times to reach 50% and 90% of the combined equilibrium yields
($t_{0.5}$ and $t_{0.9}$) (Table 1). This provides a clearer picture when comparing different reactions and
reaction protocols, and also follows the method devised for other conjugation reactions [5, 31]. In
general, all experimental data gave relatively good fits, except a slight deviation in the range
between 85 and 100 % conversion, which can tentatively be attributed to the minor population of
alternative forms of the M residue reacting somewhat more slowly (Supporting information, S4).
It may also be noted that the rate constants for the dissociation of E- and Z- conjugates needed to
have the same value in order to obtain the good fits for the data to the model. The kinetics,
equilibrium constants, and reaction yield depended slightly on pH, with pH 5.0 giving the fastest
reactions in both cases (Table 1). However, pH 4.0 was used in further conjugations due to the
pH dependence for the reduction step (see below).

Figure 5: Reaction kinetics for the conjugation of A_2M oligomers (20.1 mM) to 2 equivalents of **a)** ADH (hydrazone formation) and **b)** PDHA (oxime formation) at pH 3.0, 4.0 and 5.0. Kinetics for the conjugation of AA at pH 4.0 [5] is included for comparison.

Table 1: Kinetic parameters obtained from the modelling of the conjugation of A (A_nM) to B (ADH, PDHA or A_4M-ADH) using different equivalents of B. E: E-hydrazone/oxime. Z: Z-hydrazone/oxime. Two different models were applied. The first model estimates the individual rate constants for the formation and dissociation of E (k_1 and k_{-1}) and Z (k_2 and k_{-2}), whereas the second model considers the total (E+Z) as a single reaction product, providing times needed to reach 50% and 90% ($t_{0.5}$ and $t_{0.9}$) of the equilibrium yield.

	Equivalents			A+B $\leftrightarrow$ E		A+B $\leftrightarrow$ Z		$t_{0.5}$	$t_{0.9}$	Equilibrium yield
A	B	B	pH	k_1 [h^{-1}]	k_{-1} [h^{-1}]	k_2 [h^{-1}]	k_{-2} [h^{-1}]	[h]	[h]	[%]
A_2M	ADH	2	3.0	3.1×10^{-2}	4.0×10^{-1}	4.1×10^{-3}	4.0×10^{-1}	0.22	0.78	85
A_2M	ADH	2	4.0	1.8×10^{-2}	2.0×10^{-1}	2.5×10^{-3}	2.0×10^{-1}	0.38	1.37	87
A_2M	ADH	2	5.0	4.1×10^{-2}	7.0×10^{-1}	5.8×10^{-3}	7.0×10^{-1}	0.16	0.55	81
A_2M	PDHA	2	3.0	2.8×10^{-2}	2.5×10^{-1}	1.2×10^{-2}	2.5×10^{-1}	0.21	0.75	91

|										
A_2M	PDHA	2	4.0	2.4×10^{-2}	2.2×10^{-1}	1.0×10^{-2}	2.2×10^{-1}	0.24	0.87	91
A_2M	PDHA	2	5.0	3.5×10^{-2}	4.5×10^{-1}	1.6×10^{-2}	4.5×10^{-1}	0.16	0.56	88
A_5M	ADH	2	4.0	3.0×10^{-2}	3.5×10^{-1}	4.0×10^{-3}	3.5×10^{-1}	0.23	0.82	86
A_5M	PDHA	2	4.0	2.3×10^{-2}	8.0×10^{-2}	1.0×10^{-3}	8.0×10^{-2}	0.27	0.97	96
A_2M	ADH	0.5	4.0	4.0×10^{-1}	9.0×10^{-1}	5.8×10^{-2}	9.0×10^{-1}	0.06	0.28	73
A_2M	PDHA	0.5	4.0	1.2×10^{-1}	6.0×10^{-2}	5.2×10^{-2}	6.0×10^{-2}	0.22	1.21	88
A_4M	A_4M-ADH	1	4.0	7.3×10^{-2}	1.5×10^{-1}	1.1×10^{-2}	1.5×10^{-1}	0.35	1.57	74

The table includes kinetic data for a higher DP, in this case the hexamer A_5M. As for the chitosan oligomers studied previously [5], the reaction kinetics appeared to be essentially independent of DP in the range studied. It may be noted that A_nM become gradually less soluble in the buffer when n > 5. Hence, longer oligomers can therefore not be easily be prepared and studied by the present method.

Reduction

Most conjugations of this type are combined with an irreversible reduction step to obtain stable secondary amine conjugates. It was recently confirmed that PB can be a good alternative to sodium cyanoborohydride ($NaCNBH_3$) for similar conjugations of chitosan oligomers with natural reducing ends [5], prompting us to attempt a similar approach here. Besides being less toxic, PB also spontaneously decomposes more slowly (about 20 times) than $NaCNBH_3$ under the given conditions (Supporting information, S5). Although PB has low solubility in the aqueous buffer at room temperature, stirring was shown to increase the reduction rate, suggesting the reduction also takes place at the surface of the undissolved particles [5, 32].

The high reactivity of the pending aldehyde (*gem*-diol) of the M residue, prompted us to first investigate possible reduction of A_nM oligomers, which would render the oligomers unreactive

for further conjugation. The reduction by PB was therefore assayed by time course NMR in the

pH range 3.0 – 5.0. Reduction by $NaCNBH_3$ at pH 4.0 was included for comparison. Kinetic data

are shown in Figure 6. NMR spectra are given in the Supporting information, S6. Complete

reduction by PB was obtained after approximately 20, 12 and 40 hours for pH 3.0, 4.0 and 5.0,

respectively. Data were further fitted to a kinetic model assuming the rate of reduction (assumed

irreversible) is proportional to the concentrations of each reactant. The rate constants are given in

Table 2. With $NaCNBH_3$ reduction was complete after less than 12 hours at pH 4.0. These results

contrast with those of natural reducing ends such as the AA disaccharide, where no detectable

reduction was observed under the same conditions (Supporting information, S6). Hence, both

reductants result in significant reduction of the A_nM oligomers, which directly influences the

protocols for reductive amination, as discussed below.
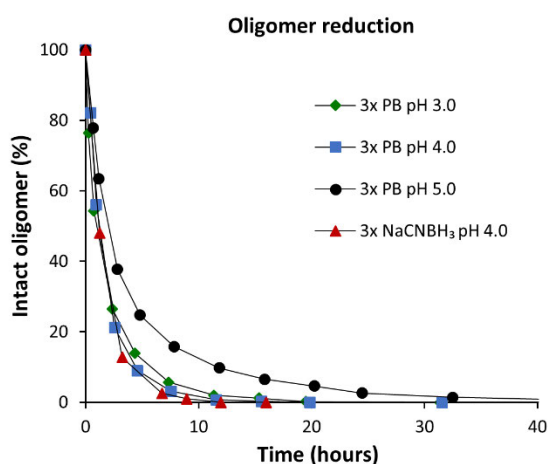
Figure 6: Reaction kinetics for the reduction of A_nM oligomers at pH 3.0, 4.0 and 5.0 using 3

equivalents (3x) PB at RT. Reduction at pH 4.0 using 3 equivalents $NaCNBH_3$ at RT, is included

in the figure for comparison. NMR spectra are shown in Supporting information, S6.

The reduction of A_nM conjugates (oximes and hydrazones) was subsequently investigated by adding PB (3 equivalents) to the corresponding reaction mixtures after equilibrium was reached (i.e. after > 12 hours). Bases for the time course NMR analyses were the reduced intensity of the E- and Z-resonances, as well as emergence of methylene proton resonances of the secondary amine in the ^{1}H-NMR spectra (Supporting information, S7). Kinetic plots are given in Figure 7.
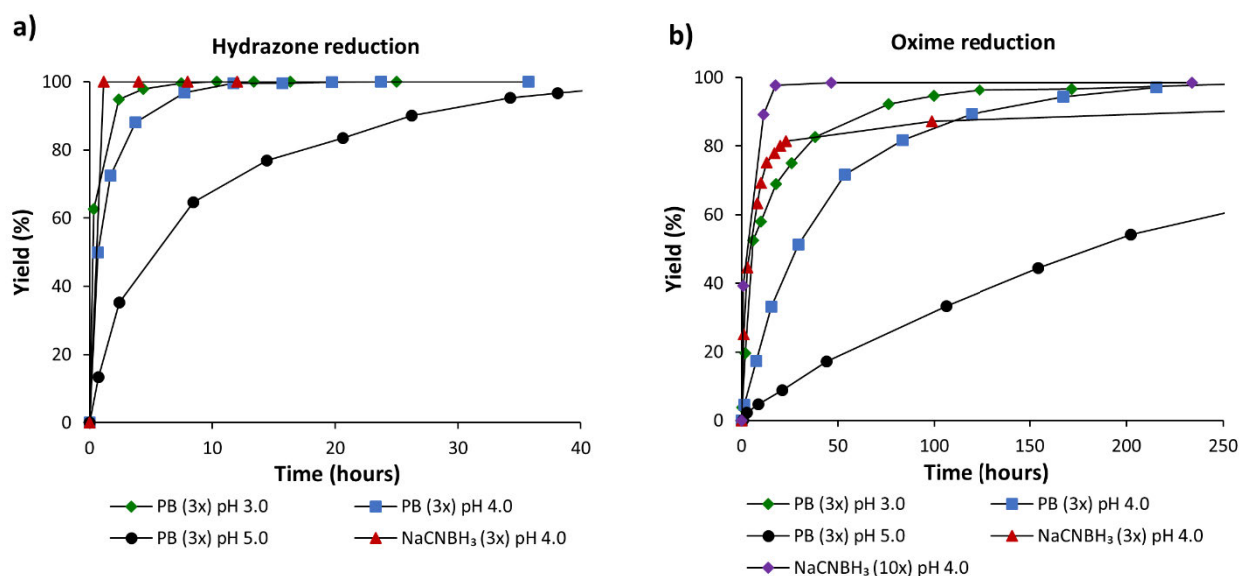
Figure 7: Reaction kinetics for the reduction of **a)** A_nM-ADH conjugates (hydrazone reduction) and **b)** A_nM-PDHA conjugates (oxime reduction) at pH 3.0, 4.0 and 5.0 using 3 equivalents (3x) PB at RT. Reduction of conjugates at pH 4.0 using 3 or 10 equivalents $NaCNBH_3$ at RT, is included in the figures for comparison.

Hydrazone (A_nM-ADH) reduction with PB (Figure 7a) is indeed very fast in this system, and clearly fastest at pH 3.0, where complete reduction of conjugates is obtained after about 10 hours at RT. The reduction here is slightly slower at pH 4.0, and much slower at pH 5.0. The same pH dependence is also observed for oxime (A_nM-PDHA) reduction (Figure 7b), except that the

reduction is generally much slower, being complete after about 150 – 200 hours. The pH-dependence of hydrazone and oxime reduction by PB has to our knowledge not been studied in detail, but we attribute the faster reduction at lower pH to the formation of reducible iminium ions by protonation. Hydrazone and oxime reduction by $NaCNBH_3$ (pH 4.0) was also investigated. Complete hydrazone reduction was obtained after approximately one hour with 3 equivalents of $NaCNBH_3$ (Figure 7a). Oxime reduction was slower under the same conditions, however, with an initial rate similar to that of PB at pH 3.0 (Figure 7b). Due to the rapid decomposition of $NaCNBH_3$ in the buffer, 3 equivalents were insufficient to reach completion, levelling off at approx. 90% yield. In contrast to PB, which is poorly soluble at higher concentrations, 10 equivalents of $NaCNBH_3$ could be completely dissolved, enabling monitoring of the oxime reduction. As expected, the rate of reduction increased correspondingly, and resulted in complete reduction in less than 20 hours (Figure 7b).

The kinetic data in Figure 7 could be fitted to the model for the reductive amination using the previously obtained rate constants for the formation and dissociation of hydrazones or oximes (Table 1), as well as the rate constants for aldehyde reduction (Table 2). Hence, the rate of hydrazone or oxime reduction (assumed being irreversible and E- and Z-forms being equally reactive), became the only adjustable kinetic parameter. In general, reasonably good fits were obtained (Supporting information, S8). The obtained rate constants for the reductions are given in Table 2. Interestingly, somewhat better fits were obtained by lowering the rate constants for A_nM reduction compared to reactions with A_nM and PB alone. The reason for this is presently not clear.

Table 2: Rate constants obtained for the reduction of hydrazones and oximes by PB (3x) assuming both isomers (E-/Z-forms) of the conjugates are reduced with the same rate. Rate constants for the reduction of oligomers by PB are included for comparison.

	Rate constants [h^{-1}]		
pH	3.0	4.0	5.0
AnM (unreacted oligomer)	1.1 x10^{-2}	1.5 x10^{-2}	7.0 x10^{-3}
AnM-ADH (hydrazone)	4.0 x10^{-2}	1.5 x10^{-2}	3.0 x10^{-3}
AnM-PDHA (oxime)	1.5 x10^{-3}	4.2 x10^{-4}	8.0 x10^{-5}*

* Inaccurate (initially fast, then slow)

Preparative protocols for reduced A$_n$M-ADH/PDHA conjugates

The results above provide the necessary information to develop protocols for preparative work. The most important is to maximise the conversion, but also to minimise the formation of disubstituted ADH or PDHA, e.g. A$_n$M-ADH-MA$_n$ [5], as they are not reactive towards a second block. Assuming equal reactivity of both ends of ADH or PDHA, the statistical amount of disubstituted (DS) species, is given by the expression

$$DS \ = \ S * \left(\frac{[A_nM]}{[-NH_2]} \right)^2$$

where S is the molar fraction of substituted amine, [A$_n$M] is molar concentration of A$_n$M, and [-NH$_2$] the molar concentration of reactive amine (twice that of [ADH] or [PDHA]). For example, 2 equivalents (40.2 mM) ADH and a S of 0.87 (from Table 1) give 5% disubstituted ADH, which reduces to 0.2% with 10 equivalents (201 mM). Hence, a large excess of ADH or PDHA is recommended, even when 2 equivalents gives acceptable conjugation yields (Supporting information S9). Although possibly interesting in other contexts, disubstituted species prevent further attachment of a second (different) block.

Because of the rapid reduction of unreacted A_nM oligomers, the reducing agent should be added after 4-6 hours of conjugation. As shown above, 3 equivalents of PB and a reduction time of 24 hours (RT) is sufficient for quantitative reduction of A_nM-ADH conjugates. To overcome the slower reduction of oximes, 20 equivalents PB and a reaction time of 48 hours is needed to give complete reduction of A_nM-PDHA conjugates (Supporting information S9). Alternatively, 10 equivalents of $NaCNBH_3$ and a reaction time of 20 hours is sufficient for quantitative reduction of PDHA conjugates, whereas 3 equivalents and less than 1 hour gives complete reduction of ADH conjugates. A_5M-ADH and A_5M-PDHA conjugates were prepared by the abovementioned preparative protocols using PB as the reductant (Supporting information, S9). ^{1}H-NMR spectra of purified (GFC) and fully reduced A_5M-ADH and A_5M-PDHA conjugates are given in Figure 8. Annotations in the spectra are based on literature data [19] and the NMR characterization of purified and fully reduced A_2M-PDHA (Supporting information, S10), where one of the alternative forms of the M residue was structurally elucidated (showed and annotated in Figure 8 as M'). In contrast to the main M residue, M' can appear in equilibrium with the open ring with two vicinal aldehydes at the reducing end. However, conjugates corresponding to the open form were not identified and hence, it appears that the oligomers with the alternative form of the M residue react with both ADH and PDHA in the same way as oligomers with the main form (with the possible exception of a bit slower kinetics discussed above). The different forms cannot be separated during purification and without further investigation, we assume that the alternative forms cannot be distinguished when part of a diblock polysaccharide.
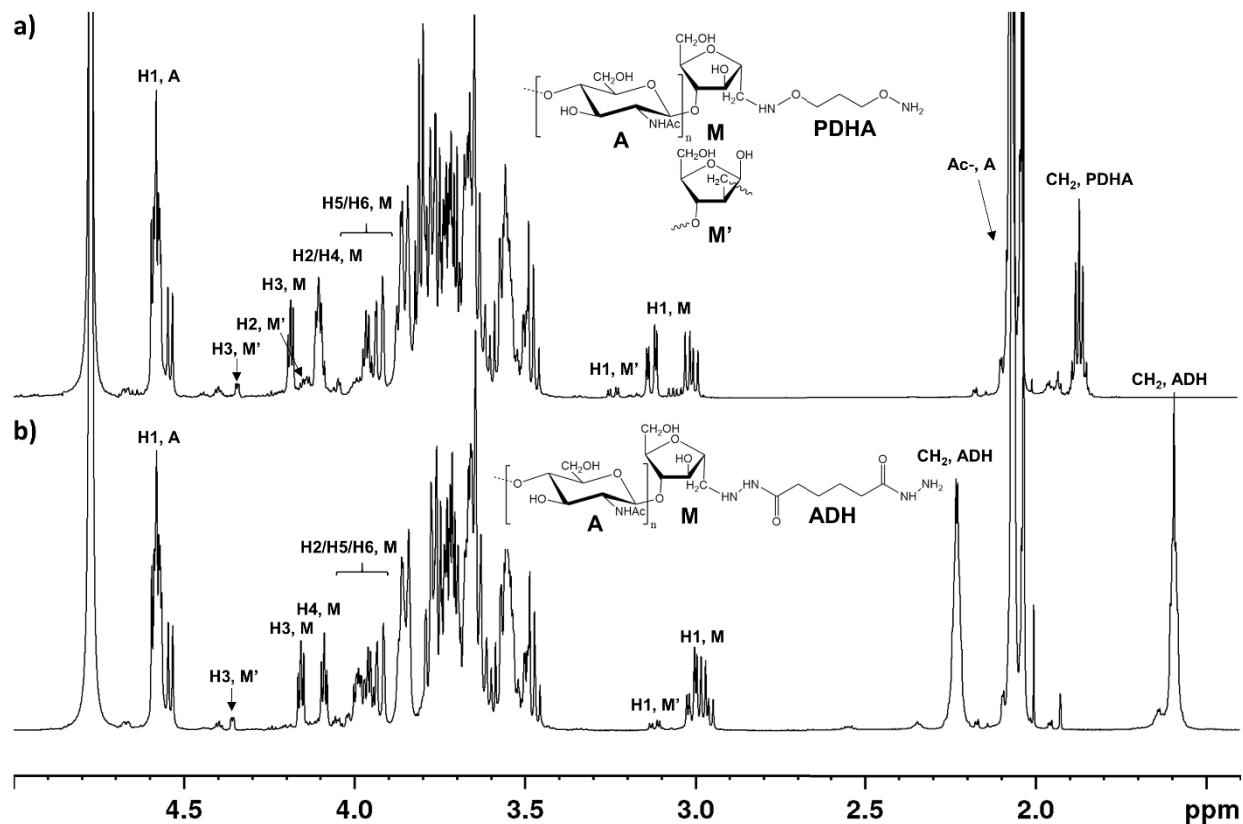
Figure 8: ^{1}H-NMR spectra of reduced and purified **a)** A_5M-PDHA and **b)** A_5M-ADH conjugates.

Attaching a second block: A_nM-*b*-MA_n diblock oligosaccharides

An efficient protocol to prepare A_nM-ADH/PDHA conjugates paves the way for attaching a second oligosaccharide in order to prepare a chitin-based diblock oligo- or polysaccharides (A_nM-*b*-X). We first investigated the formation of A_nM-ADH-MA_n. To study this, reduced A_4M-ADH conjugates was prepared, and subsequently reacted with an equimolar amount of A_4M (conditions otherwise as above). The choice of equimolar proportions is based on the general need to use minimum amounts of oligosaccharide and also to simplify the following purification step. The amination was studied by time course NMR as above, and rate constants are included

in Table 1. The total equilibrium yield of hydrazones was as high as 75% with only one equivalent of the second block. To allow a more direct comparison, we used the rate constants for the conjugation of A_2M and A_5M to free ADH (2 equivalents) to simulate the rate ($t_{0.5}$ and $t_{0.9}$) and yield for the reaction with *equimolar* proportions of oligomers and amines (Supporting information, S11). Interestingly, the equilibrium yield was lower, and the rate was slower than for the conjugation of A_4M to the A_4M-ADH conjugate, indicating that the reactivity of the free hydrazide group towards terminal M-residues is higher for A_nM-ADH than for free ADH. After subsequent reduction with PB (3 equivalents) the yield of diblocks was approximately 83% (Supporting information, S11). Unreacted A_4M oligomers were completely reduced, hence, preventing the diblock formation from going to completion.

The diblock formation was further investigated in the special case of 0.5 equivalents of ADH or PDHA to A_2M oligomers. These conditions should at completion give only disubstituted ADH/PDHA, i.e. the diblocks A_2M-ADH-MA_2 and A_2M-PDHA-MA_2. Here, faster conjugation was observed, especially for ADH, supporting the theory of different kinetics for the attachment of the second block (Table 1 and Supporting information, S12). High equilibrium yields of hydrazones and oximes were obtained (73% with ADH and 86% with PDHA). Interesting, the yield of diblocks after reduction was not increased above these values (Supporting information, S12). Hence, the yield of diblocks corroborates with the statistical amount of disubstituted species expected for the systems (as equimolar concentration of amine and oligomer was used).

Attaching a second block: A_nM-*b*-dextran diblock oligosaccharides

The final step was to study the attachment of a second block of a different kind, namely dextran, using purified and reduced A_5M-ADH and A_5M-PDHA conjugates to form chitin-*b*-dextran

23

diblocks. Dextran oligomers (Dext$_m$) of defined DP (m = DP) were obtained by partial hydrolysis of dextran and fractionation of oligomers by gel filtration chromatography (Supporting information, S13). Reactions were monitored by time course NMR, again using *equimolar* amounts of the two blocks.

By this strategy the reactivity of the reducing end of Dext$_m$ governs the conjugation. Therefore, the kinetics of the conjugation of Dext$_5$ to free ADH and PDHA (2 equivalents) was included for comparison (Supporting Information, S14). Importantly, dextran forms *N*-pyranosides in addition to E- and Z-oximes with PDHA, whereas it forms almost exclusively *N*-pyranosides with ADH [5, 30]. Kinetic constants are given in Table 3.

Table 3: Kinetic parameters obtained from the modelling of the conjugation of A (Dext$_m$) to B (ADH, PDHA or A$_5$M-ADH or A$_5$M-PDHA) using different equivalents of B. Reactions were performed at pH 4.0, RT. E: E-hydrazone/oxime. Z: Z-hydrazone/oxime. Pyr: *N*-pyranoside.

A	B (2x)	A+B ↔ E		A+B ↔ Z		E ↔ Pyr		Z ↔ Pyr		Equilibrium yield [%]
		k_1 [h^{-1}]	k_{-1} [h^{-1}]	k_2 [h^{-1}]	k_{-2} [h^{-1}]	k_3 [h^{-1}]	k_{-3} [h^{-1}]	k_4 [h^{-1}]	k_{-4} [h^{-1}]	
Dext$_5$	ADH	1.5×10^{-3}	1.0×10^{1}	1.5×10^{-4}	1.0×10^{1}	1.1×10^{2}	1.1×10^{0}	1.1×10^{2}	1.1×10^{0}	35
Dext$_5$	PDHA	2.9×10^{-3}	2.0×10^{-3}	4.0×10^{-4}	1.5×10^{-1}	2.0×10^{0}	6.8×10^{0}	2.7×10^{1}	2.0×10^{1}	87
A	**B (1x)**									
Dext$_6$	A$_5$M-ADH	3.0×10^{-3}	1.7×10^{1}	3.0×10^{-4}	1.7×10^{1}	1.1×10^{2}	1.1×10^{0}	1.1×10^{2}	1.1×10^{0}	15
Dext$_6$	A$_5$M-PDHA	1.1×10^{-2}	5.0×10^{-2}	1.5×10^{-3}	1.0×10^{-1}	1.9×10^{0}	4.5×10^{0}	2.7×10^{1}	1.5×10^{1}	66

It may first be noted that dextran oligomers, in agreement with previous findings [5], are much less reactive towards ADH and PDHA compared to A$_n$M oligomers (data for A$_n$M in Table 1). This is due to the pending aldehyde of the reducing end of the latter, being more reactive, as it does

not participate in an aldehyde/hemiacetal equilibrium. Secondly, the rate constants for forming N-pyranosides (k_3 and k_4) are two orders of magnitude larger for ADH compared to PDHA. For ADH they are 5-6 orders of magnitude larger than k_1 and k_2. Hence, the first step (E- and Z-formation) is rate limiting although E- and Z-hydrazones are hardly detected during the reaction with ADH.

The rate constants in Table 3 suggest that dextran oligomers react faster with A_nM-ADH and A_nM-PDHA compared to free ADH and PDHA. To allow a more direct comparison, we used the rate constants for the conjugation of $Dext_5$ to free ADH (2 equivalents) to simulate the rate ($t_{0.5}$ and $t_{0.9}$) and yield for the reaction with *equimolar* proportions of $Dext_5$ and amines (Supporting information, S15). As observed for the A_nM oligomers, dextran reacted faster, and resulted in a higher yield, with the A_5M-ADH or -PDHA conjugates than with free ADH or PDHA. Hence, the second attachment is indeed faster in both cases.

Equilibrium yields obtained with equimolar amounts of dextran and A_5M-ADH/PDHA were only 15% for ADH, but 66% for PDHA. However, improved yields can be expected during reduction of the equilibrium mixture because of the slow reduction of unreacted dextran. Since dextran-based hydrazones and oximes are slowly reduced by PB at RT [5], the reduction was performed using 20 equivalents PB at increased temperature (40°C). Reaction products were fractioned by GFC and analysed by ^{1}H-NMR (Supporting information, S15).

By integration of the GFC chromatogram, the yield of A_5M-PDHA-$Dext_6$ diblocks was 92% after 72 hours, whereas for A_5M-ADH-$Dext_6$ we obtained about 85% diblocks after 144 hours of reduction (Supporting information, S15). The higher yield and shorter reaction times for PDHA diblocks is partly ascribed to the higher equilibrium yield prior to reduction. Moreover, the

almost complete formation of *N*-pyranosides reduces the reduction rate of dextran-ADH

conjugates considerably [5]. It may also be noted that at 40°C some reduction of unreacted dextran

occurred (Supporting information, S15), but the rate was low compared to reduction of unreacted

A_nM. Hence, an increased yield of diblocks can be obtained after addition of reductant in the

dextran systems compared to the A_nM systems. The general structures of chitin-*b*-dextran

diblocks prepared with ADH and PDHA and ^{1}H-NMR spectra of reduced and purified A_5M-*b*-

$Dext_6$ diblocks are given in Figure 9.
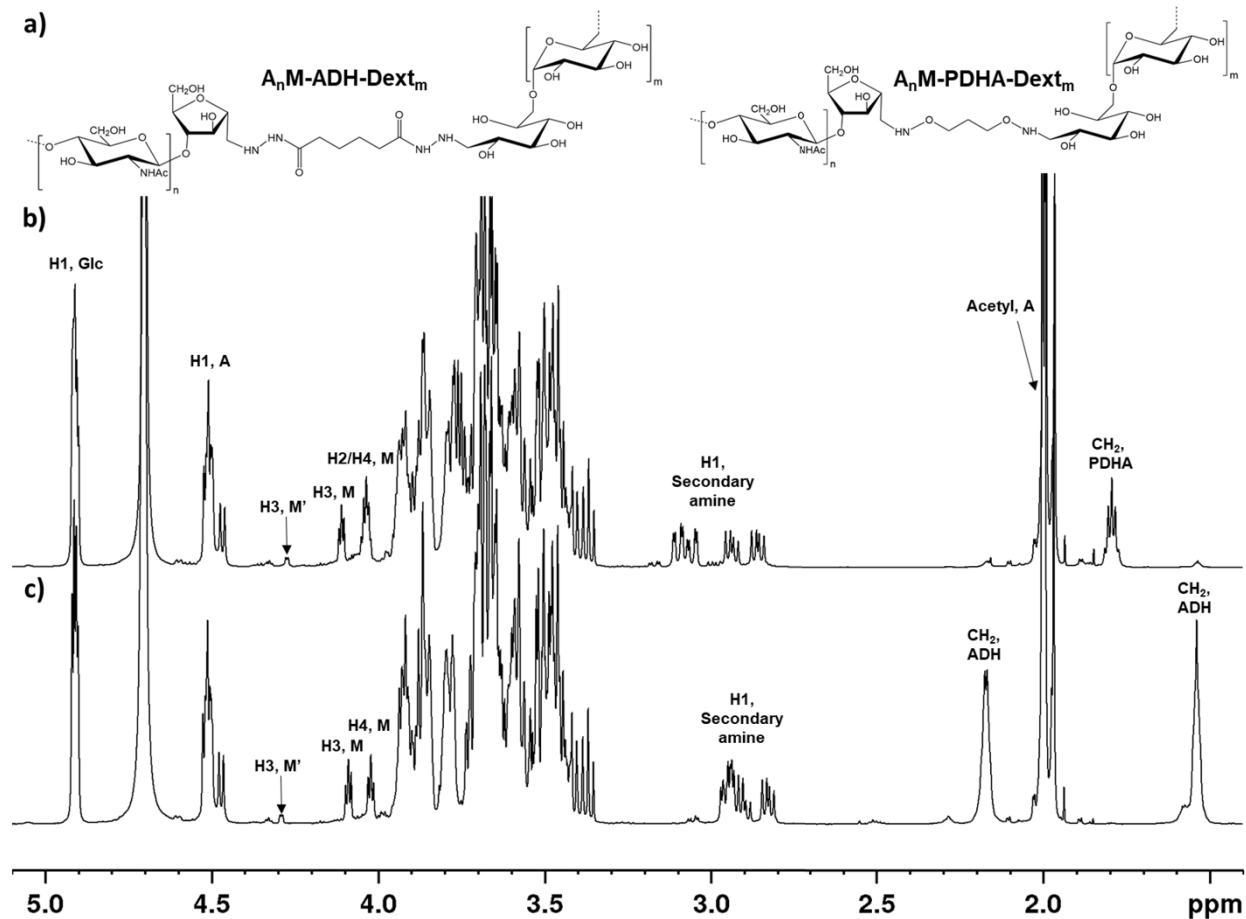
Figure 9: a) General structure of chitin-*b*-dextran diblocks prepared with ADH or PDHA. ^{1}H-

NMR spectra of the reduced and purified **b)** A_5M-PDHA-$Dext_6$ diblock and the **b)** A_5M-ADH-

$Dext_6$ diblock.

Based on the results of this study, two strategies for the preparation of A_nM-*b*-dextran block polysaccharides can be proposed. For the strategy where dextran is conjugated to the free end of ADH or PDHA in A_nM conjugates (discussed above), the attachment of the second block is time consuming since dextran oligomers react more slowly with ADH/PDHA compared to the highly reactive A_nM oligomers. Moreover, the reduction of dextran-based hydrazones and oximes also is slow. However, in contrast to the A_nM oligomers, unreacted dextran oligomers are reduced with a low rate under the given conditions and hence, a high yield of diblocks can be obtained (even under equimolar proportions), even though this strategy requires long reaction times for attachment of the second block.

An alternative strategy is to reverse the protocol and prepare ADH or PDHA activated dextran oligomers in the first step. Due to the slow reduction of dextran oligomers, activation using a large excess of ADH or PDHA can be performed as a conventional one pot reductive amination. The subsequent conjugation of A_nM oligomers to the free end of ADH or PDHA takes advantage of the high reactivity of the terminal M residue of the A_nM oligomers, and the attachment of the second block (both conjugation and reduction) is time efficient compared to opposite strategy. However, this strategy is restricted by the rapid reduction of unreacted A_nM oligomers, which will limit the yield of diblocks (if reacted in an equimolar ratio).

An excess of one of the blocks will in both strategies lead to faster kinetics and higher yield of diblocks. However, an excess of the second block will render some or all the unreacted oligomers inactive after reduction (most relevant for an excess of A_nM oligomers but also relevant for dextran oligomers as shown above). An excess of the activated oligomer conjugate will in contrast be beneficial in both strategies as activated oligomers can be recycled. Both the abovementioned strategies require purification after diblock formation and in this study, GFC

was proven useful. However, purification by block-specific solvents is clearly a possibility deserving future attention. Hence, which strategy is the better therefore depends on factors such as which oligomer or conjugate can be used in excess ("value" of reactants), and available purification steps. It may also be noted that improved equilibrium yields can be obtained by increasing the absolute concentrations of reactants. However, higher concentrations are not compatible with very long chains due to solubility and viscosity issues, and in any case the reductant (PB) will certainly be insoluble at very high concentrations. Heterogeneous systems may be worth exploring further but this is outside the scope of the present work.

The strategies described above should also be relevant for chitosan oligomers prepared by nitrous acid degradation (D_nM type). However, self-branching is an issue for such oligomers [18]. Hence, the strategy where an excess of activated conjugates is used will be advantageous for such oligomers.

CONCLUSIONS

In this work we have first studied in detail the activation of chitin oligosaccharides with the highly reactive 2,5-anhydro-D-mannose at the reducing end (A_nM) by ADH and PDHA as a basis for the preparation of chitin-based diblock polysaccharides. Kinetic constants for both the formation and dissociation of oximes and hydrazones, as well as for their irreversible reduction to the corresponding secondary amines using PB were determined. Rate constants were essentially independent of the chain length and could be used to model the reactions for a wide range of concentrations of reagents. The high susceptibility to reduction of M residues (by both PB and $NaCNBH_3$) was circumvented by a two-step procedure thanks to the excellent equilibrium yields prior to reduction. The free ends of ADH or PDHA activated oligomers had

higher reactivities compared to free ADH or PDHA. Hence, attachment of a second block to form diblocks was therefore feasible and could easily be modelled kinetically. Examples include A_nM-*b*-MA_n and A_nM-*b*-dextran. For the latter, a 'reverse' strategy of reacting A_nM with ADH- or PDHA-activated dextran is also a viable alternative thanks to the high reactivity of the terminal M residue.

ASSOCIATED CONTENT

Supporting Information.

Additional data and explanations are given in Supporting information, S1– S15.

AUTHOR INFORMATION

Corresponding Authors

Christophe Schatz - Laboratoire de Chimie des Polymères Organiques (LCPO), Université de Bordeaux, CNRS, Bordeaux INP, UMR 5629, 33600 Pessac, France. Email: schatz@enscbp.fr

Bjørn E. Christensen - NOBIPOL, Department of Biotechnology and Food Science, NTNU – Norwegian University of Science and Technology, Sem Saelands veg 6/8, NO-7491 Trondheim, Norway. Email: bjorn.e.christensen@ntnu.no

ACKNOWLEDGMENTS

REFERENCES

1.	Volokhova, A. S.; Edgar, K. J.; Matson, J. B., Polysaccharide-containing block copolymers: synthesis and applications. *Mater. Chem. Front.* **2020,** 4, 99-112.

2.	Schatz, C.; Lecommandoux, S., Polysaccharide-Containing Block Copolymers: Synthesis, Properties and Applications of an Emerging Family of Glycoconjugates. *Macromol. Rapid Commun.* **2010,** 31, (19), 1664-1684.

3.	Novoa-Carballal, R.; Muller, A. H. E., Synthesis of polysaccharide-b-PEG block copolymers by oxime click. *Chem. Commun.* **2012,** 48, (31), 3781-3783.

4.	Bondalapati, S.; Ruvinov, E.; Kryukov, O.; Cohen, S.; Brik, A., Rapid End-Group Modification of Polysaccharides for Biomaterial Applications in Regenerative Medicine. *Macromol. Rapid Commun.* **2014,** 35, (20), 1754-1762.

5.	Mo, I. V.; Feng, Y.; Dalheim, M. Ø.; Solberg, A.; Aachmann, F. L.; Schatz, C.; Christensen, B. E., Activation of enzymatically produced chitooligosaccharides by dioxyamines and dihydrazides. *Carbohydr. Polym.* **2020,** 232, 115748.

6.	Xiao, Y.; Chinoy, Z. S.; Pecastaings, G.; Bathany, K.; Garanger, E.; Lecommandoux, S., Design of Polysaccharide-b-Elastin-Like Polypeptide Bioconjugates and Their Thermoresponsive Self-Assembly. *Biomacromolecules* **2020,** 21, (1), 114-125.

7.	Rosselgong, J.; Chemin, M.; Almada, C. C.; Hemery, G.; Guigner, J.-M.; Chollet, G.; Labat, G.; Da Silva Perez, D.; Ham-Pichavant, F.; Grau, E.; Grelier, S.; Lecommandoux, S.; Cramail, H., Synthesis and Self-Assembly of Xylan-Based Amphiphiles: From Bio-Based Vesicles to Antifungal Properties. *Biomacromolecules* **2019,** 20, (1), 118-129.

8.	Tiwari, V. K.; Mishra, B. B.; Mishra, K. B.; Mishra, N.; Singh, A. S.; Chen, X., Cu-Catalyzed Click Reaction in Carbohydrate Chemistry. *Chem. Rev.* **2016,** 116, (5), 3086-3240.

9.	Breitenbach, B. B.; Schmid, I.; Wich, P. R., Amphiphilic Polysaccharide Block Copolymers for pH-Responsive Micellar Nanoparticles. *Biomacromolecules* **2017,** 18, (11), 3844-3845.

10.	Feng, F.; Sun, J.; Radhakrishnan, G. V.; Lee, T.; Bozsoki, Z.; Fort, S.; Gavrin, A.; Gysel, K.; Thygesen, M. B.; Andersen, K. R.; Radutoiu, S.; Stougaard, J.; Oldroyd, G. E. D., A combination of chitooligosaccharide and lipochitooligosaccharide recognition promotes arbuscular mycorrhizal associations in Medicago truncatula. *Nat. Commun.* **2019,** 10, (1), 5047.

11.	Ahmed, A. B. A.; Taha, R. M.; Mohajer, S.; Elaagib, M. E.; Kim, S. K., Preparation, properties and biological applications of water soluble chitin oligosaccharides from marine organisms. *Russ. J. Mar. Biol.* **2012,** 38, (4), 351-358.

12.	Roby, D.; Gadelle, A.; Toppan, A., Chitin oligosaccharides as elicitors of chitinase activity in melon plants. *Biochem. Biophys. Res. Commun.* **1987,** 143, (3), 885-892.

13.	Azuma, K.; Osaki, T.; Minami, S.; Okamoto, Y., Anticancer and Anti-Inflammatory Properties of Chitin and Chitosan Oligosaccharides. *J. Funct. Biomater.* **2015,** 6, (1), 33-49.

14.   Kadokawa, J.-I.; Karasu, M.; Tagaya, H.; Chiba, K., Synthesis of a Block Copolymer Consisting of Oligocellulose and Oligochitin. *J. Macromol. Sci. A* **1996,** 33, (11), 1735-1743.

15.   Kadokawa, U.-I.; Yamashita, K.; Karasu, M.; Tagaya, H.; Chiba, K., Preparation and Enzymatic Hydrolysis of Block Copolymer Consisting of Oligochitin and Poly(Propylene Glycol). *J. Macromol. Sci. A* **1995,** 32, (7), 1273-1280.

16.   Allan, G. G.; Peyron, M., Molecular-Weight Manipulation of Chitosan .1. Kinetics of Depolymerization by Nitrous-Acid. *Carbohydr. Res.* **1995,** 277, (2), 257-272.

17.   Tømmeraas, K.; Vårum, K. M.; Christensen, B. E.; Smidsrød, O., Preparation and characterisation of oligosaccharides produced by nitrous acid depolymerisation of chitosans. *Carbohydr. Res.* **2001,** 333, (2), 137-144.

18.   Tømmeraas, K.; Strand, S. P.; Christensen, B. E.; Smidsrød, O.; Vårum, K. M., Preparation and characterization of branched chitosans. *Carbohydr. Polym.* **2011,** 83, (4), 1558-1564.

19.   Moussa, A.; Crepet, A.; Ladaviere, C.; Trombotto, S., Reducing-end "clickable" functionalizations of chitosan oligomers for the synthesis of chitosan-based diblock copolymers. *Carbohydr. Polym.* **2019,** 219, 387-394.

20.   Pickenhahn, V. D.; Darras, V.; Dziopa, F.; Biniecki, K.; De Crescenzo, G.; Lavertu, M.; Buschmann, M. D., Regioselective thioacetylation of chitosan end-groups for nanoparticle gene delivery systems. *Chem. Sci.* **2015,** 6, (8), 4650-4664.

21.   Coudurier, M.; Faivre, J.; Crepet, A.; Ladaviere, C.; Delair, T.; Schatz, C.; Trombotto, S., Reducing-End Functionalization of 2,5-Anhydro-d-mannofuranose-Linked Chitooligosaccharides by Dioxyamine: Synthesis and Characterization. *Molecules* **2020,** 25, (5), 1143.

22.   Ruhaak, L. R.; Steenvoorden, E.; Koeleman, C. A. M.; Deelder, A. M.; Wuhrer, M., 2-Picoline-borane: A non-toxic reducing agent for oligosaccharide labeling by reductive amination. *Proteomics* **2010,** 10, (12), 2330-2336.

23.   Cosenza, V. A.; Navarro, D. A.; Stortz, C. A., Usage of α-picoline borane for the reductive amination of carbohydrates. *ARKIVOC* **2011,** 12, 182-194.

24.   Fang, J.; Qin, G.; Ma, J.; She, Y.-M., Quantification of plant cell wall monosaccharides by reversed-phase liquid chromatography with 2-aminobenzamide pre-column derivatization and a non-toxic reducing reagent 2-picoline borane. *J. Chromatogr. A* **2015,** 1414, 122-128.

25.   Unterieser, I.; Mischnick, P., Labeling of oligosaccharides for quantitative mass spectrometry. *Carbohydr. Res.* **2011,** 346, (1), 68-75.

26.   Chen, J.; Spiering, G.; Mosquera-Giraldo, L.; Moore, R. B.; Edgar, K. J., Regioselective Bromination of the Dextran Nonreducing End Creates a Pathway to Dextran-Based Block Copolymers. *Biomacromolecules* **2020**.

27.   Li, B.; Wang, Q.; Wang, X.; Wang, C.; Jiang, X., Preparation, drug release and cellular uptake of doxorubicin-loaded dextran-b-poly(ε-caprolactone) nanoparticles. *Carbohydr. Polym.* **2013,** 93, (2), 430-437.

28.   Vårum, K. M.; Antohonsen, M. W.; Grasdalen, H.; Smidsrød, O., Determination of the degree of N-acetylation and the distribution of N-acetyl groups in partially N-deacetylated chitins (chitosans) by high-field n.m.r. spectroscopy. *Carbohydr. Res.* **1991,** 211, (1), 17-23.

29.   Lindberg, B.; Lönngren, J.; Svensson, S., Specific Degradation of Polysaccharides. In *Advances in Carbohydrate Chemistry and Biochemistry*, Tipson, R. S.; Derek, H., Eds. Academic Press: 1975; Vol. Volume 31, pp 185-240.

30.   Kwase, Y. A.; Cochran, M.; Nitz, M., Protecting-Group-Free Glycoconjugate Synthesis: Hydrazide and Oxyamine Derivatives in N-Glycoside Formation. In *Modern synthetic methods in carbohydrate chemistry: From monosaccharides to complex glycoconjugates*, Werz, D. B.; Vidal, S., Eds. Wiley: 2013; pp 67-96.

31.   Baudendistel, O. R.; Wieland, D. E.; Schmidt, M. S.; Wittmann, V., Real-Time NMR Studies of Oxyamine Ligations of Reducing Carbohydrates under Equilibrium Conditions. *Chem. Eur.* **2016,** 22, (48), 17359-17365.

32.   Gilmore, K.; Vukelić, S.; McQuade, D. T.; Koksch, B.; Seeberger, P. H., Continuous Reductions and Reductive Aminations Using Solid NaBH4. *Org. Process Res. Dev.* **2014,** 18, (12), 1771-1776.

TABLE OF CONTENTS GRAPHIC
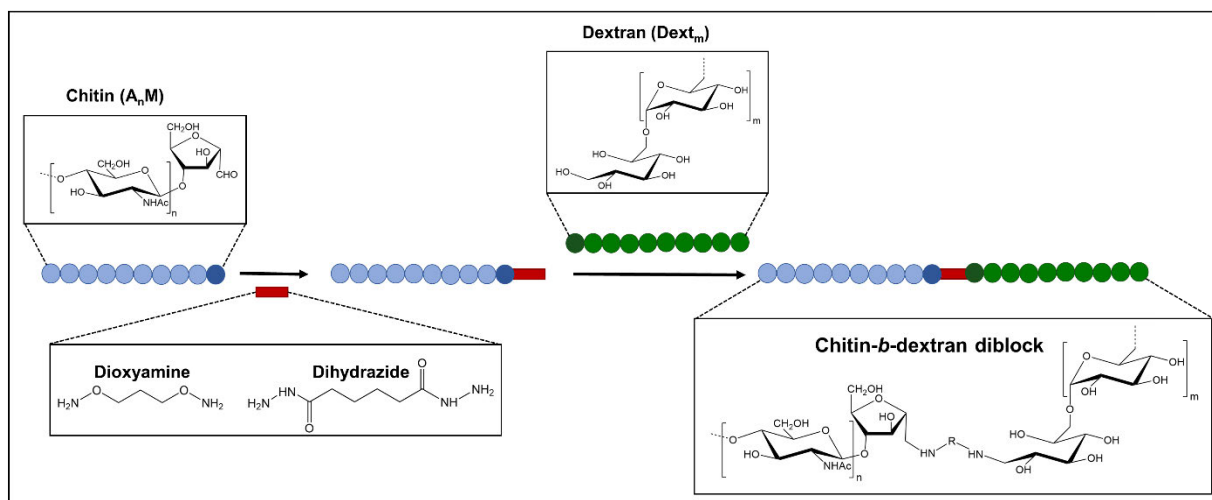
Supporting Information

2,5-Anhydro-D-mannose end-functionalised chitin oligomers activated by dioxyamines or dihydrazides as precursors of diblock oligosaccharides

Ingrid Vikøren Mo, Marianne Øksnes Dalheim, Finn L. Aachmann, Christophe Schatz, Bjørn E. Christensen

Contents

S1 Preparation and characterization of A_nM oligomers

Chitin oligomers of the type A_nM, where A_n represent uninterrupted sequences of *N*-acetyl D-glucosamine (A) residues with a 2,5-anhydro-D-mannose (M) residue at the reducing end, were prepared by nitrous acid (HONO) depolymerisation of chitosan ($F_A = 0.48$), using an excess HONO (1.3 equivalents) to the fraction of D-glucosamine (D) residues [1, 2]. The excess of HONO converts all the D residues into M residues, whereas A residues are unaffected, providing solely A_nM oligomers. The water-soluble oligomers (DP < 10) were fractionated by preparative gel filtration chromatography (GFC) to obtain purified low molecular weight A_nM oligomers of specific DPs (Figure S1a). The chitosan with $F_A = 0.48$ provided mainly trimers (A_2M) and dimers (AM) (Figure S1). Separation of the oligomer mixture by analytical GFC (Figure S1b) showed shoulder peaks for all the oligomer fractions in the chromatogram. Without further investigation, shoulder peaks were suggested to be caused by the alternative forms of M (discussed below).
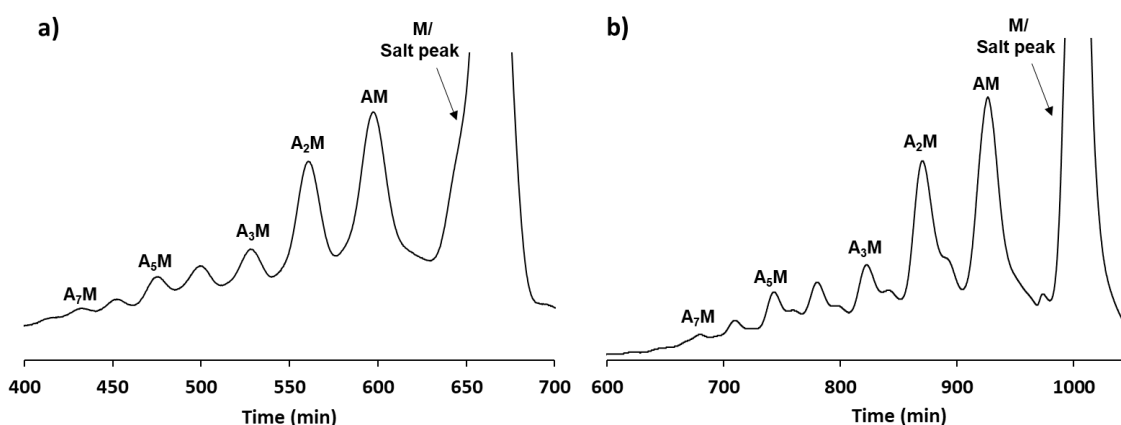
Figure S1: a) preparative and **b)** analytical GFC fractionation of the mixture of water-soluble A_nM (n = 1-8) oligomers obtained by nitrous acid degradation of chitosan ($F_A = 0.48$) using an excess (1.3x) of nitrous acid.

Oligomers were purified (by dialysis), freeze-dried and characterized by ^{1}H-NMR (Figure S2). The ^{1}H-NMR spectra were annotated according to literature [2, 3]. The doublet at approximately 4.9 ppm was assigned to the gem-diol (hydrated aldehyde) of the reducing end M residue. Additional doublets in the anomeric region (4.95-5.1 ppm) were assigned to alternative forms of the as M residue suggested in the literature by Lindberg et al [4] marked as M' in all figures. Purified A_nM oligomers were slightly polydisperse due to the incomplete baseline separation by the preparative GFC (Figure S1a). The polydispersity of the oligomers was confirmed by the ^{1}H-NMR characterization of A_4M and A_2M in Figure S2a and S2b, respectively, where the integral of H1, A was higher than expected relative to the sum of the integrals of H1, M and H1, M' (expected ratio 4:1 and 2:1 for A_4M and A_2M, respectively).
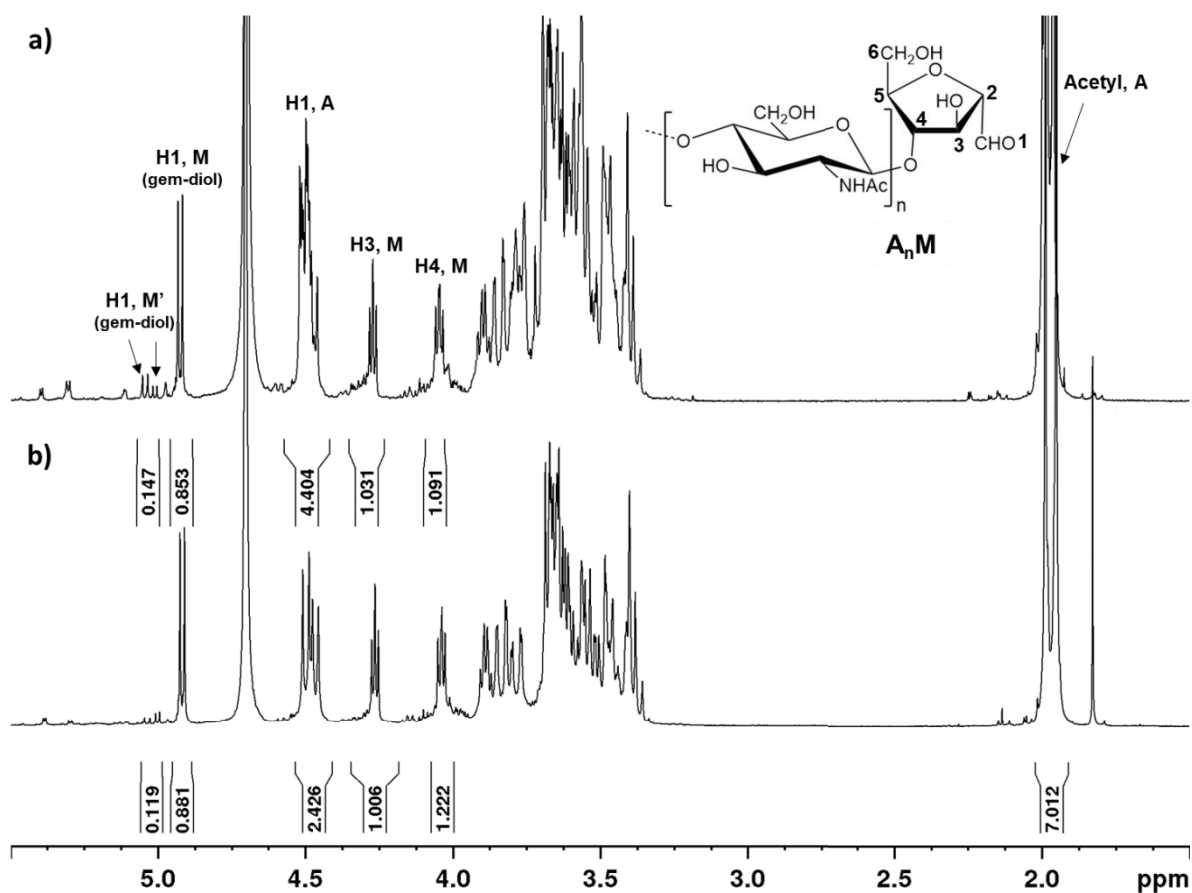
Figure S2: ^{1}H-NMR characterization of fractionated and purified **a)** A_4M and **b)** A_2M in D_2O including annotations and integrals (600 MHz). M' refers to alternative (minor) forms of M (see S2).

S2 Conjugation of A_nM oligomers to ADH and PDHA studied by time course NMR

Conjugation of A_nM oligomers to ADH and PDHA was monitored by time course NMR as described earlier [5]. In brief, conjugation reactions were performed in deuterated NaAc-buffer (with TSP added as internal standard) at pH 3.0, 4.0 or 5.0 using 2 equivalents of ADH or PDHA relative to the concentration of oligomers (20.1 mM). ^{1}H-NMR spectra were recorded at specific time points (Figure S3 and S4) and yields of conjugates were determined by integration of the obtained spectra. Minor resonances close to the major resonances from the hydrazones/oximes (H1, M E or Z) were attributed to the conjugation of oligomers with alternative forms of the M residue (H1, M' E or Z) (assigned in Figure S3 and S4). Both the major and minor resonances from the E and Z hydrazones or oximes were integrated to obtain the yield of conjugates. Due to overlapping resonances (e.g. H2, M Z overlapping with H1, M (gem-diol) in Figure S4), yields could not be calculated from the sum of integrals from the H1 reducing end proton resonances in each individual spectrum. Due to the slight polydispersity of the oligomers, the yields could not be calculated from the integrals of the resonances resulting from

3

the oligomers. Therefore, the integral of the resonance from the internal standard (TSP, 0 ppm) was used as reference to calculate yields. As the conjugates were reduced in a subsequent step (see below) the integral value of the TSP resonance was related to the integrals of the resonances from the completely reduced conjugates (for each individual reaction mixture). The TSP integral value was set to this specific value in all the spectra obtained during the time course NMR study for the conjugation and reduction to calculate the yields of conjugates and subsequently reduced secondary amine conjugates during the reactions. The yields were calculated based on the assumption of 100 % yield of reduced secondary amine conjugates. Integrals of overlapping resonances were calculated by subtraction.
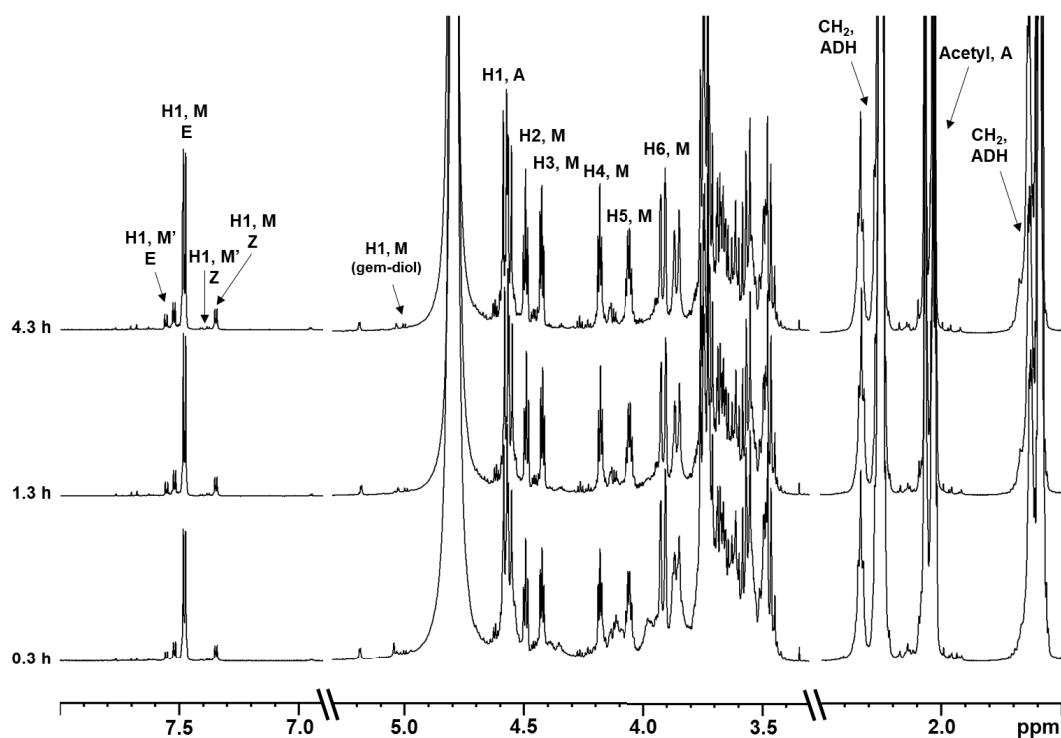
Figure S3: ^{1}H-NMR spectra obtained at defined time points for the conjugation reaction with A_2M (20.1 mM) and 2 equivalents ADH at pH 4.0, RT.
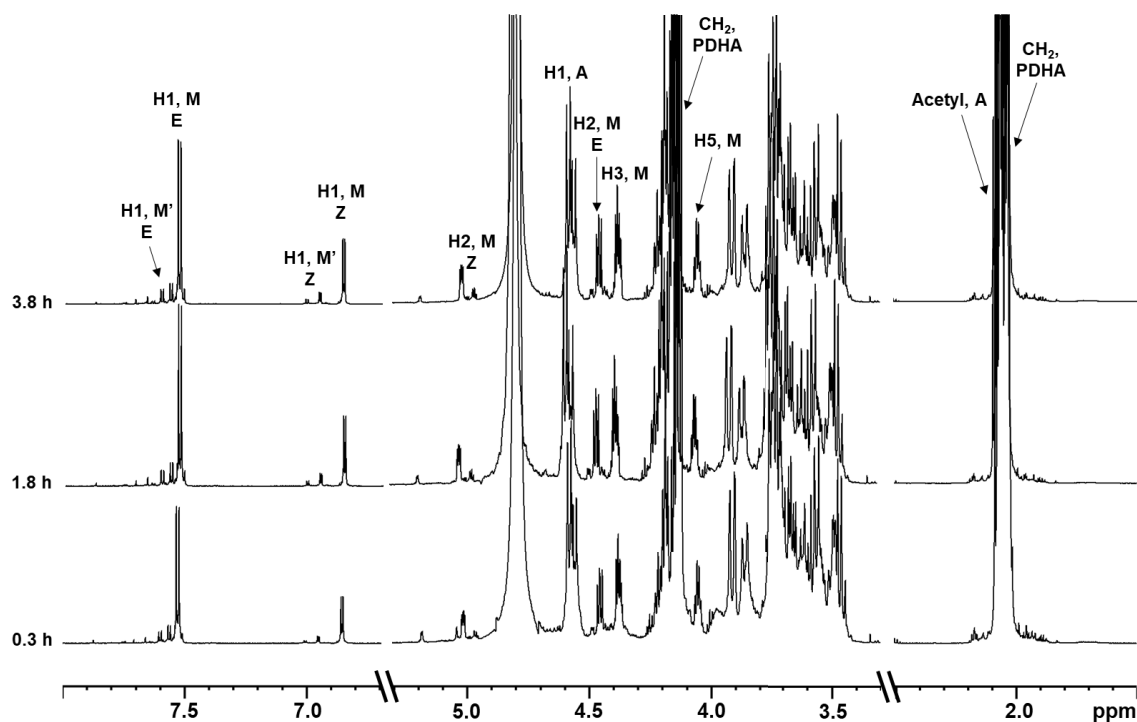
Figure S4: ^{1}H-NMR spectra obtained at defined time points for the conjugation reaction with A_2M (20.1 mM) and 2 equivalents PDHA at pH 4.0, RT.

S3 Kinetic modelling of the reductive amination reaction

The reductive amination of oligosaccharides with different amines (e.g. oxyamines (PDHA) or hydrazides (ADH)) is comprised of several individual reactions with independent rates and rate constants. The overall reaction involves the conjugation (amination) of the oligosaccharide, where E- and Z- oximes or hydrazones (Schiff bases) are formed for oxyamines or hydrazides, respectively. For oligosaccharides where the reducing end aldehyde is in equilibrium with a hemiacetal (normal reducing end), the acyclic Schiff bases are in equilibrium with cyclic *N*-glycosides (e.g. *N*-pyranosides). By adding a reducing agent, the Schiff bases will be irreversibly reduced forming secondary amine conjugates. Irreversible reduction of oligosaccharides by the reducing agent will prevent the reductive amination reaction from going to completion. The general reaction scheme is shown in Figure S5.
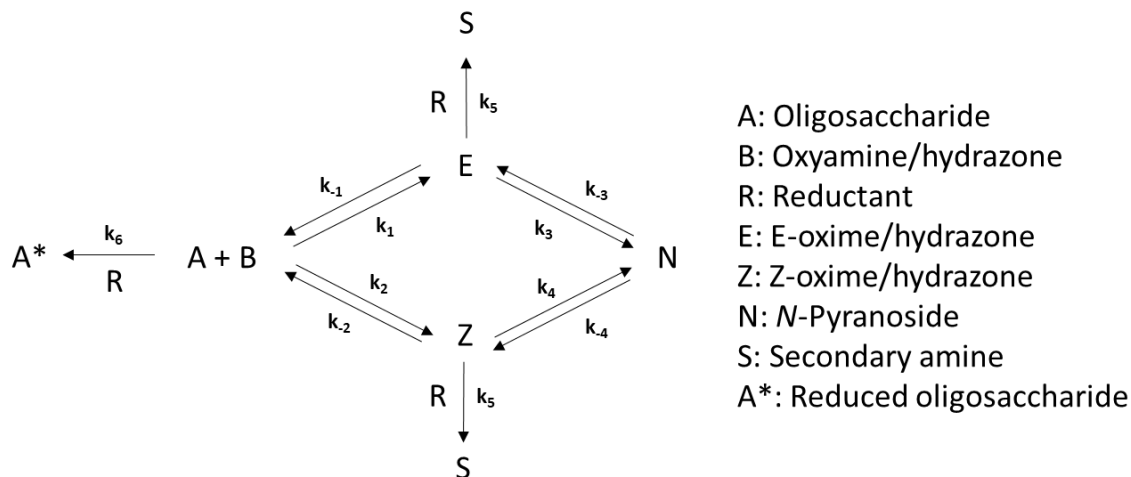
Figure S5: General reaction scheme for the reductive amination of oligosaccharides with normal reducing ends including assigned rate constants for each independent reaction involved. Reversible reactions are described by two rate constants (forward and reverse), whereas irreversible reactions are described by one rate constant (the scheme indicates the assumption that reduction of E and Z had the same rate constant (k_5)).

When considering the reactions to be *first order* with respect to each reactant, reaction rates can be determined by the following equations

$$\frac{d\,[A]}{dt} = -k_1[A][B] + k_{-1}[E] - k_2[A][B] + k_{-2}[Z] - k_6[A][R]$$

$$\frac{d\,[B]}{dt} = -k_1[A][B] + k_{-1}[E] - k_2[A][B] + k_{-2}[Z]$$

$$\frac{d\,[R]}{dt} = -k_5[E][R] - k_5[Z][R] - k_6[A][R]$$

$$\frac{d\,[E]}{dt} = k_1[A][B] - k_{-1}[E] - k_3[E] + k_{-3}[N] - k_5[E][R]$$

$$\frac{d\,[Z]}{dt} = k_2[A][B] - k_{-2}[Z] - k_4[Z] + k_{-4}[N] - k_5[Z][R]$$

$$\frac{d\,[N]}{dt} = k_3[E] - k_{-3}[N] + k_4[Z] - k_{-4}[N]$$

$$\frac{d\,[A^*]}{dt} = k_6[A][R]$$

The concentration of each reactant or product at specific time points, $[X]_t$, can be obtained from the reaction rates by the following equation

$$[X]_t = [X]_{t-\Delta t} + \frac{d[X]}{dt}\Delta t$$

6

where, t is the time, and Δt is the time difference from last modelled time point. The numeric modelling was carried out using Excel, generally substituting differentials of the type $d[X]/dt$ with $\Delta[X]/\Delta t$. From starting concentrations $[A]_0$, $[B]_0$ etc, the concentrations at successive time increments $t_{i+1} = t_i + \Delta t$ were inductively calculated as $[X]_{i+1} = [X]_i + (\Delta[X]_i/\Delta t)\Delta t$. The time interval ($\Delta t$) was chosen sufficiently small to result in a simulation which did not further change when choosing an even smaller time interval. All reactions were modelled using this approach, and the model was fitted to the experimental data by adjusting the rate constants to give the minimum sum of squares.

In the special case of reductive amination with chitin or chitosan oligosaccharides prepared by nitrous acid degradation, only Schiff bases (oximes/hydrazones) can be formed. Hence, the general reaction scheme for these reactions is simplified as showed in Figure S6.
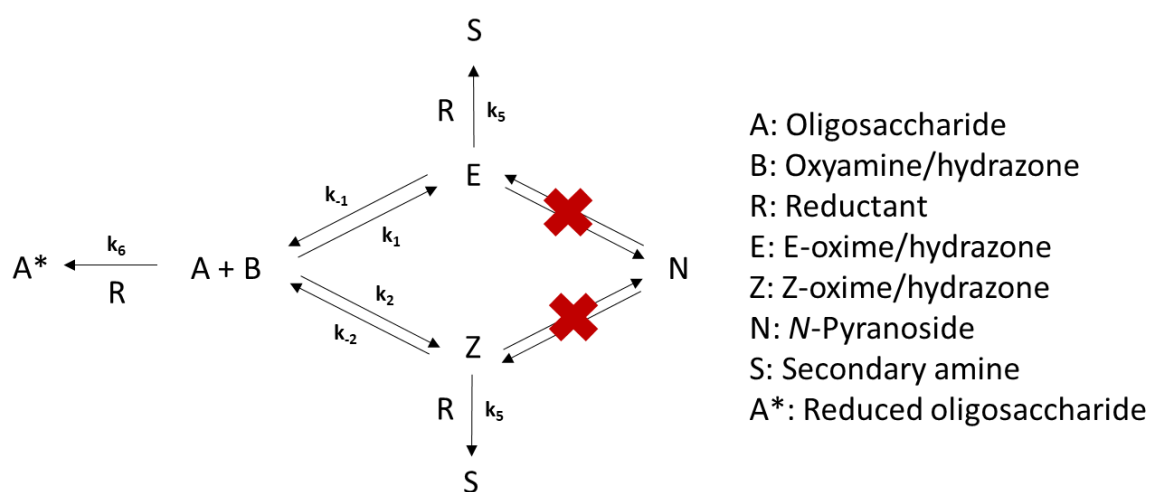
Figure S6: General reaction scheme for the reductive amination of oligosaccharides with M residue at the reducing end including assigned rate constants for each independent reaction involved.

S4 Modelling of A_nM conjugation reactions

Conjugation reactions (no reducing agent present) with A_nM oligomers were studied by time course NMR (S2). The experimental data obtained for the conjugation reactions were fitted using the model described in S3 (based on the reaction scheme presented in Figure S6). Examples of the data fitting for the conjugation of A_2M oligomers to ADH and PDHA (2 equivalents) at pH 4.0 are given in Figure S7.
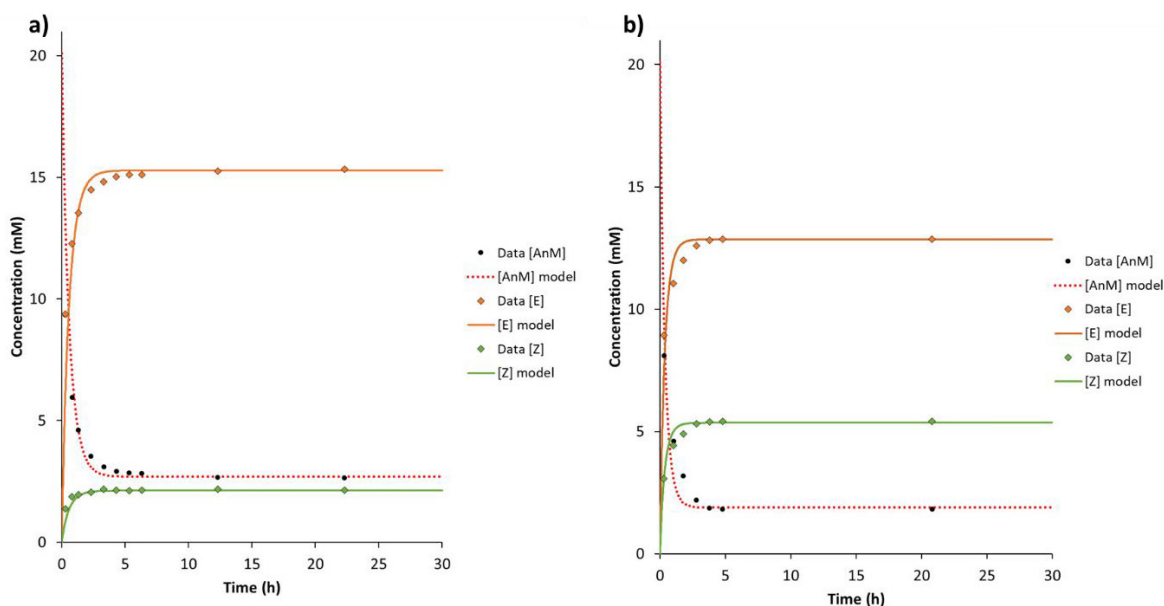
Figure S7: Model fitting of experimental data obtained at pH 4.0, RT for the reactions with A_2M and 2 equivalents of **a)** ADH or **b)** PDHA.
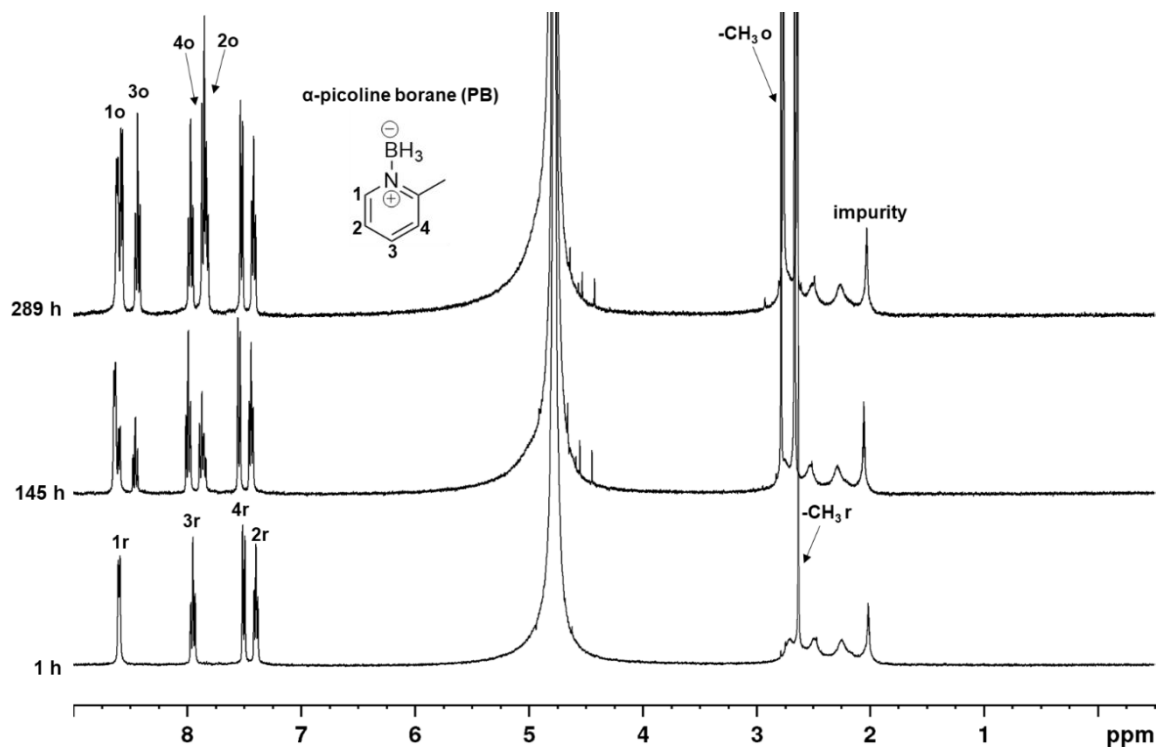
S5 Spontaneous decomposition of reducing agents

The decomposition of α-picoline borane (PB) and sodium cyanoborohydride ($NaCNBH_3$) in 500 mM deuterated NaAc-buffer, pH 4.0, was monitored by NMR. The two reducing agents have distinct resonances in the ^{1}H-NMR spectrum and hence, their decomposition was studied. In contrast to $NaCNBH_3$, which is completely dissolved in the buffer, PB has low initial solubility, but dissolves slowly over time (observed by increased intensity of the resonances over time).

The protons of the pyridine ring in PB give resonances with chemical shifts in the range 7.2 to 8.7 ppm, whereas the protons of the methyl group give one resonance with a chemical shift of approximately 2.6 ppm (Figure S8). The protons of the $-BH_3$ group are not visible in the ^{1}H-NMR spectrum due to negative chemical shifts. When PB is oxidised (o), the proton resonances are moved slightly downfield as seen in Figure S8. The relative reductive power (%) for PB over time was calculated by relating the intensity of the protons resulting from the reduced form of PB (r) to the total amount of dissolved PB (r+o) (Figure S8).

In contrast to PB, the proton resonances of the $-BH_3$ group in $NaCNBH_3$ are within the NMR scale (0 – 8 ppm). $NaCNBH_3$ lacks other protons and hence, it was not possible to study the oxidation of this reducing agent. Therefore, the decomposition was related to the reduced intensity of the resonances from the protons in the $-BH_3$ group relative to an impurity in the buffer (Figure S9). As the first spectrum was obtained after one hour, the intensity of the resonances at t = 0 was obtained by extrapolation. The relative reductive power (%) for $NaCNBH_3$ was related to the decomposition of the reducing agent. By comparing the change in relative reductive power (%) for the two reducing agents
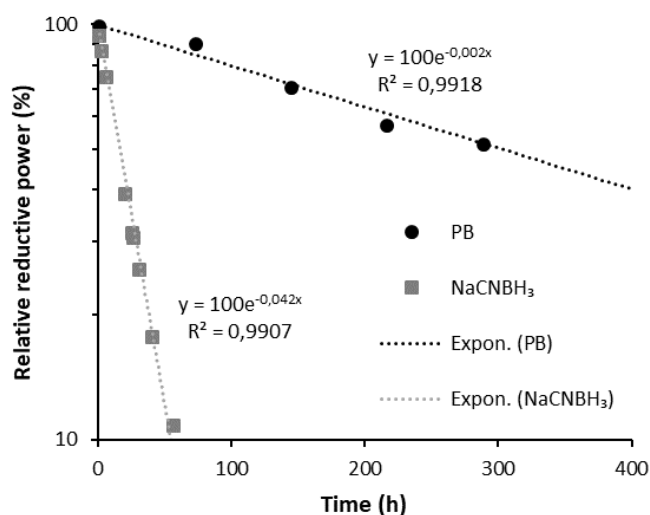
8

over time (Figure S10), NaCNBH$_3$ was shown to decompose approximately 20 times faster than PB in the buffer.

Figure S8: Spontaneous decomposition of PB in deuterated acetate buffer (500 mM, pH 4.0, RT) monitored by time course NMR.
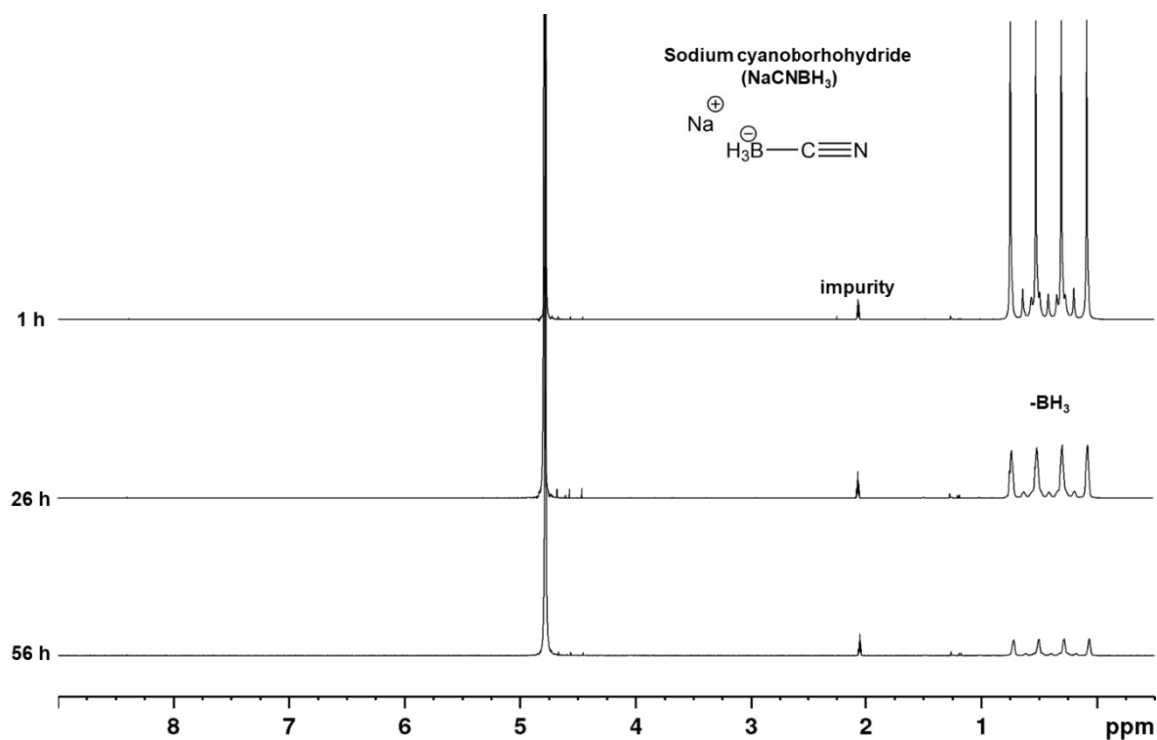
Figure S9: Spontaneous decomposition of NaCNBH$_3$ in deuterated NaAc-buffer (500 mM, pH 4.0, RT) monitored by time course NMR.

Figure S10: Change in relative reductive power (%) of PB and NaCNBH$_3$ over time in deuterated NaAc-buffer (500 mM, pH 4.0, RT).

S6 Reduction of A$_n$M oligomers

Reduction of A$_n$M oligomers was performed by adding 3 equivalents reducing agent (PB or NaCNBH$_3$) to oligomers dissolved in deuterated NaAc-buffer. The course of the reduction was studied by monitoring the disappearance of reducing end gem-diol resonances (H1, M and H1, M'). Resonance intensities were related to the internal standard (TSP). Reduction of A$_n$M oligomers by PB was studied at pH 3.0, 4.0 or 5.0 (Figure S11-S13) or by NaCNBH$_3$ at pH 4.0 (Figure S14).

For comparison, reduction of AA oligomers (normal reducing end) was studied using 3 equivalents PB (Figure S15) or NaCNBH$_3$ (Figure S16) at pH 4.0. In contrast to the A$_n$M oligomers, no detectable reduction in the intensity of the reducing end resonances for AA was observed. However, the relative ratio of the α- to β- reducing end resonances gradually changed (Figure S15). For this experiment AA was dissolved in the buffer shortly before PB was added and the first spectrum was obtained.
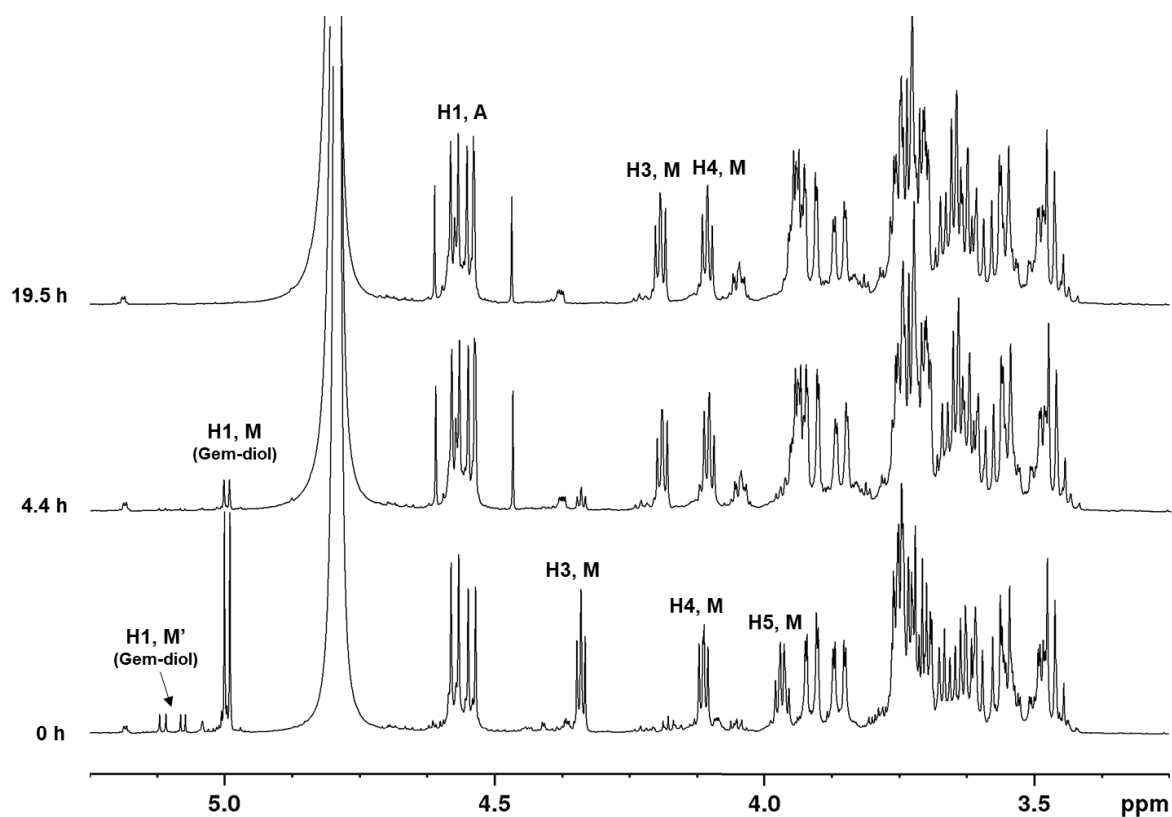
Figure S11: ^{1}H-NMR spectra obtained at defined time points for the reduction of A_2M oligomers (20.1 mM) in deuterated acetate buffer, pH 3.0, RT using 3 equivalents PB (60.3 mM).
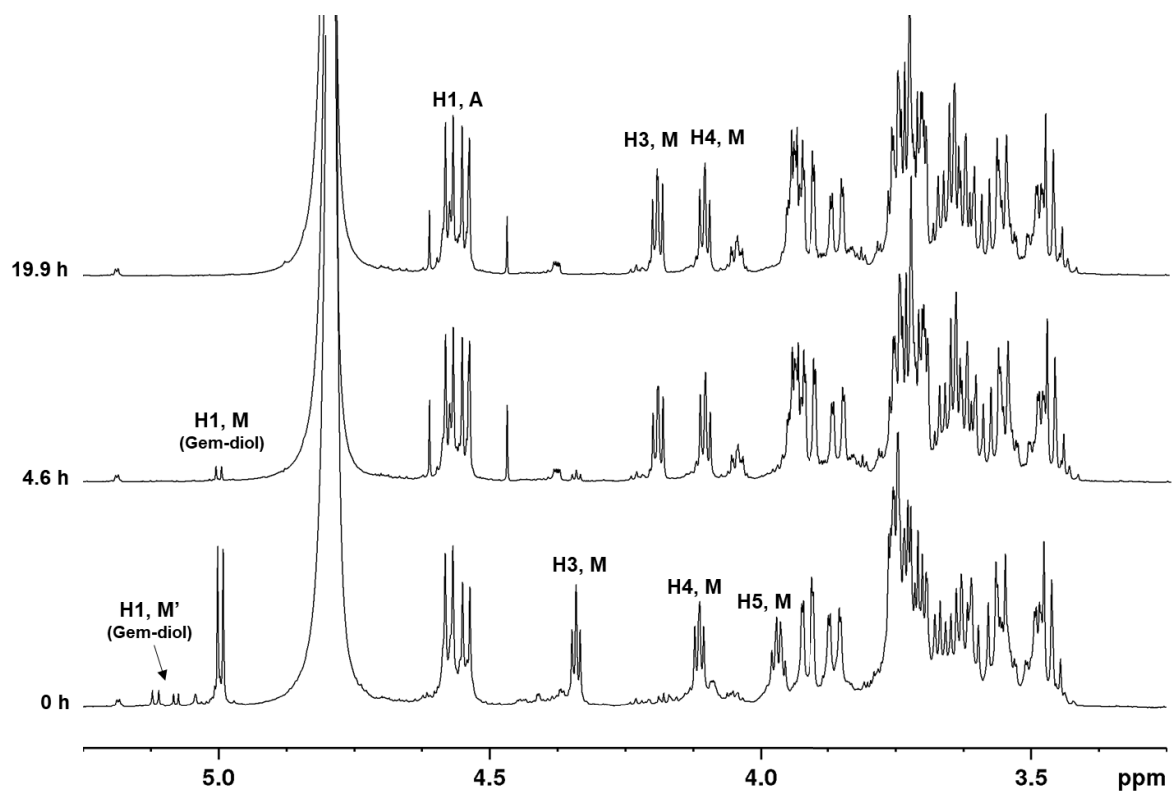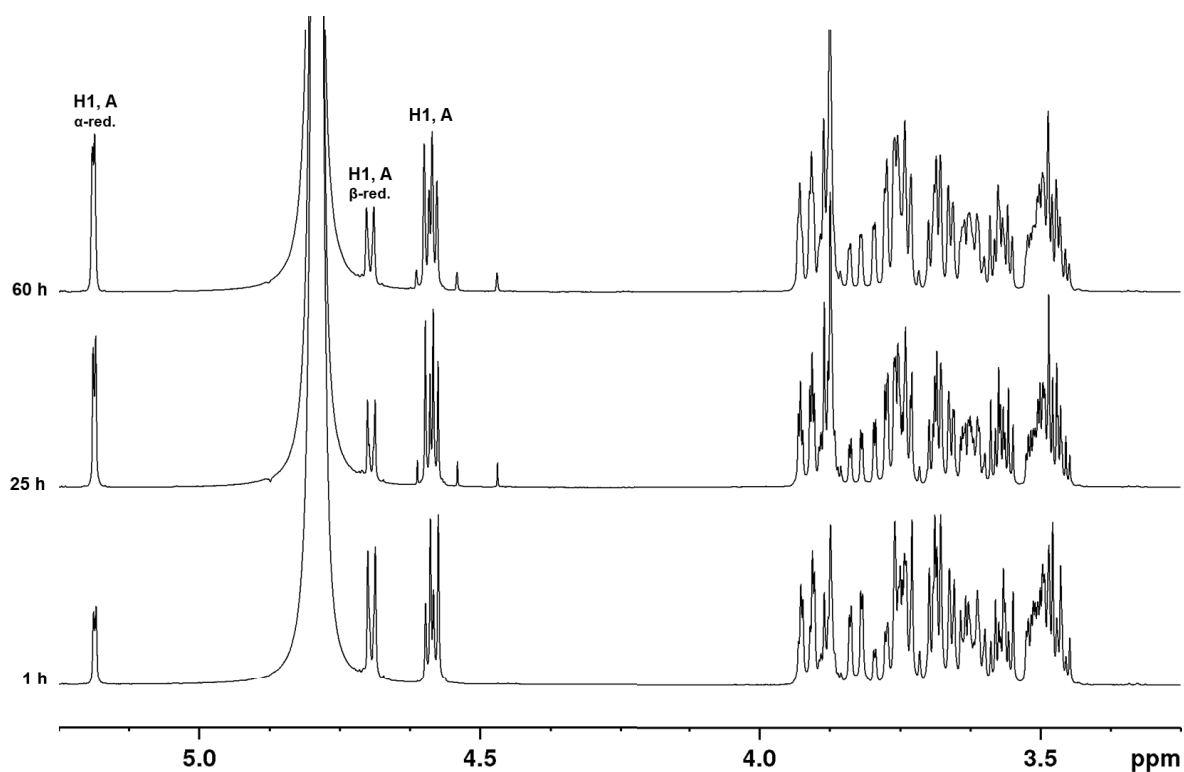

Figure S12: ^{1}H-NMR spectra obtained at defined time points for the reduction of A_2M oligomers (20.1 mM) in deuterated acetate buffer, pH 4.0, RT using 3 equivalents PB (60.3 mM).
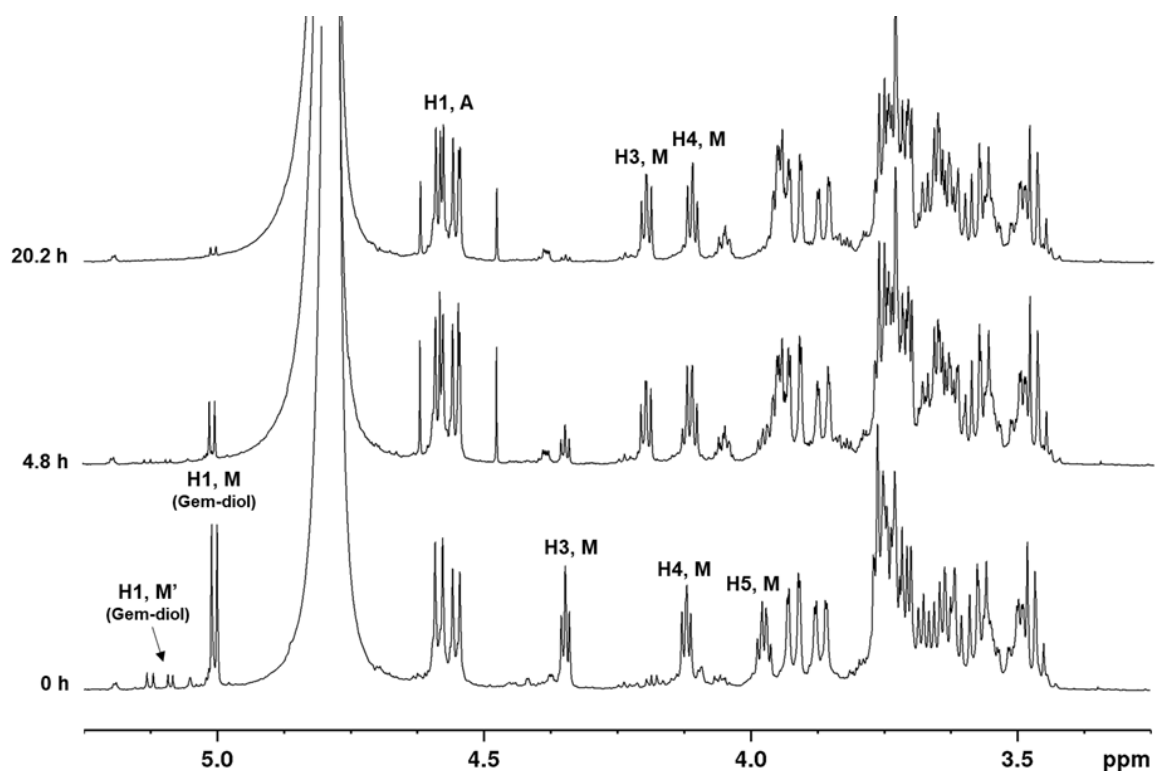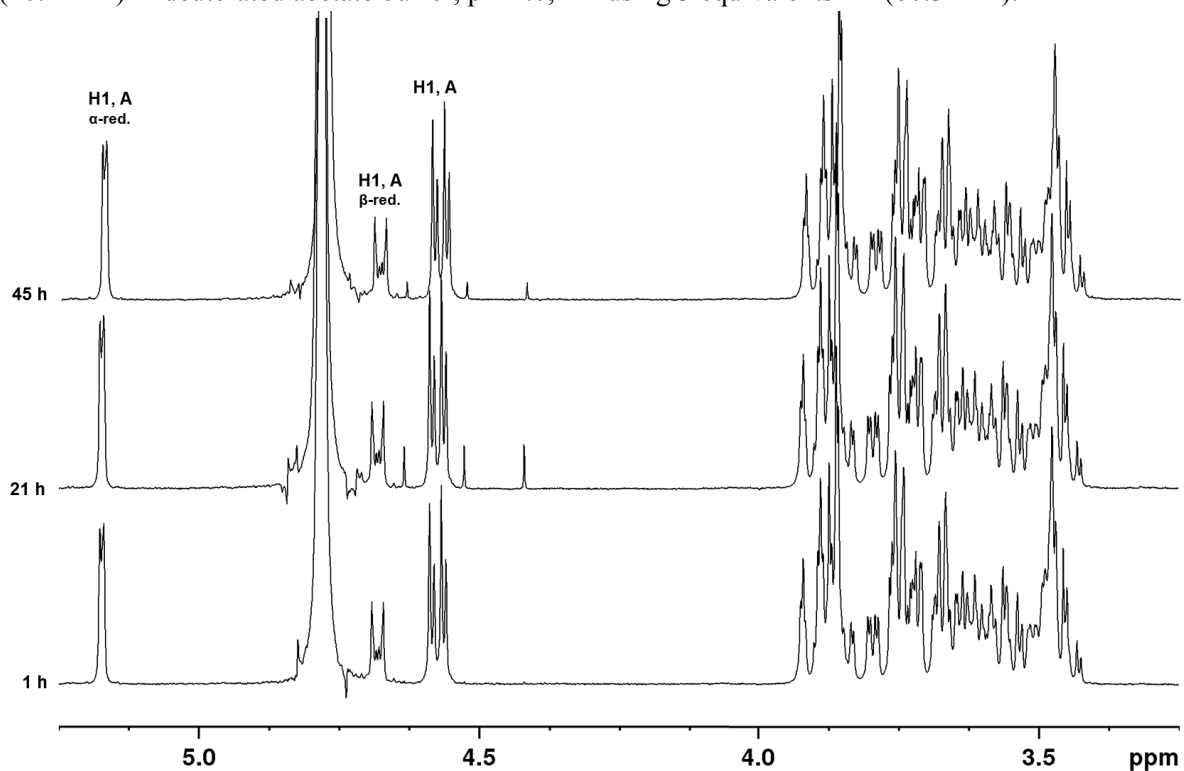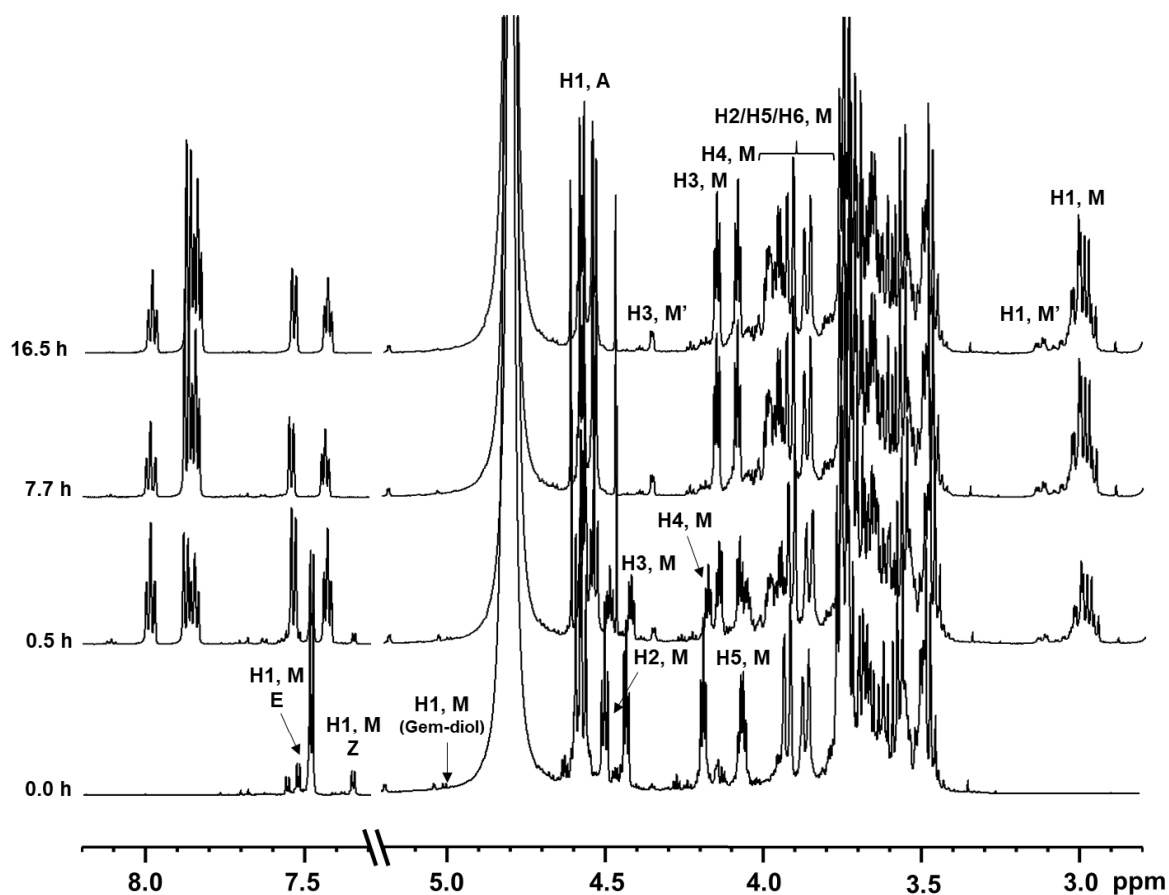
Figure S13: ^{1}H-NMR spectra obtained at defined time points for the reduction of A_2M oligomers (20.1 mM) in deuterated acetate buffer, pH 5.0, RT using 3 equivalents PB (60.3 mM).
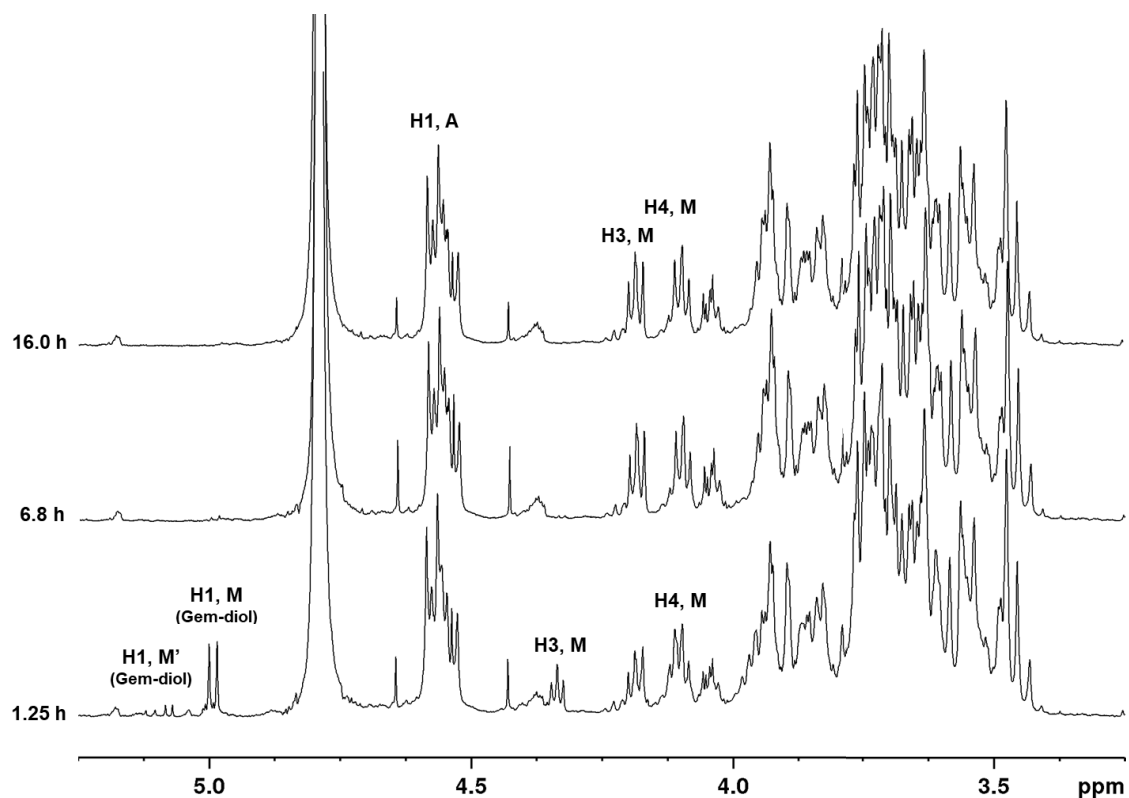
Figure S14: ^{1}H-NMR spectra obtained at defined time points for the reduction of A_3M oligomers (20.1 mM) in deuterated acetate buffer, pH 4.0, RT using 3 equivalents NaCNBH$_3$ (60.3 mM).

Figure S15: ^{1}H-NMR spectra obtained at defined time points for the reduction of AA oligomers (20.1 mM) in deuterated acetate buffer, pH 4.0, RT using 3 equivalents PB (60.3 mM).

Figure S16: ^{1}H-NMR spectra obtained at defined time points for the reduction of AA oligomers (20.1 mM) in deuterated acetate buffer, pH 4.0, RT using 3 equivalents NaCNBH$_3$ (60.3 mM).

S7 Reduction of AₙM conjugates

Reduction of A_nM conjugates was studied by adding 3 equivalents reducing agent (PB or $NaCNBH_3$) to the equilibrium mixtures of conjugates (pH 3.0, 4.0 or 5.0). The course of the reduction was studied by monitoring the disappearance of hydrazone or oxime proton resonances and the appearance methylene proton resonances from the reduced secondary amine conjugates (at approximately 3 ppm) over time. Due to the overlap of the methylene proton resonances from the different forms of the M residue after reduction, the total resonance area (2.9 – 3.35 ppm) was integrated to give the yield of reduced conjugates. ^{1}H-NMR spectra obtained at different time points for the reduction of A_2M-ADH and A_2M-PDHA conjugates by 3 equivalents PB at pH 4.0 are given in Figure S17 and S18, respectively. The kinetics of the reduction is given in Figure S19 a and b, respectively. For the reduction of A_nM-PDHA conjugates, E-oxime resonances (H1, M E) overlapped with one of the resonances from the reduced form of PB (Figure S18). Hence, this integral was obtained by subtraction.


Figure S17: ^{1}H-NMR spectra obtained at defined time points for the reduction of A_2M-ADH conjugates (prepared using 2 equivalents ADH) by 3 equivalents (60.3 mM) PB at pH 4.0, RT. Resonances from the unreduced conjugate and unreacted oligomer are annotated in the first two spectra, whereas resonances from the reduced secondary amine conjugate are annotated in the last obtained spectrum (16.5 h).

Figure S18: ^{1}H-NMR spectra obtained at defined time points for the reduction of A_2M-PDHA conjugates (prepared using 2 equivalents PDHA) by 3 equivalents (60.3 mM) PB at pH 4.0, RT. Resonances from the unreduced conjugate and unreacted oligomer are annotated in the first two spectra, whereas resonances from the reduced secondary amine conjugate are annotated in the last obtained spectrum (178 h).

Figure S19: Kinetics of the reaction obtained from the spectra in Figure S17 and S18 for the reduction of **a)** A_2M-ADH (hydrazone) conjugates and **b)** A_2M-PDHA (oxime) conjugates by 3 equivalents PB at pH 4.0, RT, respectively.

15

S8 Modelling of A_nM reduction reactions

Using the rate constants and equilibrium yields obtained for the conjugation of A_nM to 2 equivalents ADH or PDHA, the experimental data obtained for the reduction of conjugates (studied by time course NMR, S7) were fitted using the model described in S3 (based on the reaction scheme presented in Figure S6). Examples for the data fitting for the reduction A_2M-ADH or A_2M-PDHA conjugates using 3 equivalents PB at pH 4.0 (RT) are given in Figure S20 a and b, respectively. The addition of reducing agent to the equilibrium mixture of conjugates was set as $t = 0$. Due to overlapping resonances and low resolution in the NMR spectra, the yield of unreacted oligomers ($[A_nM]$ in the model) was not monitored. However, the model also predicts the consumption of unreacted oligomers based on the yield of conjugates and the rate of reduction (Figure S20).
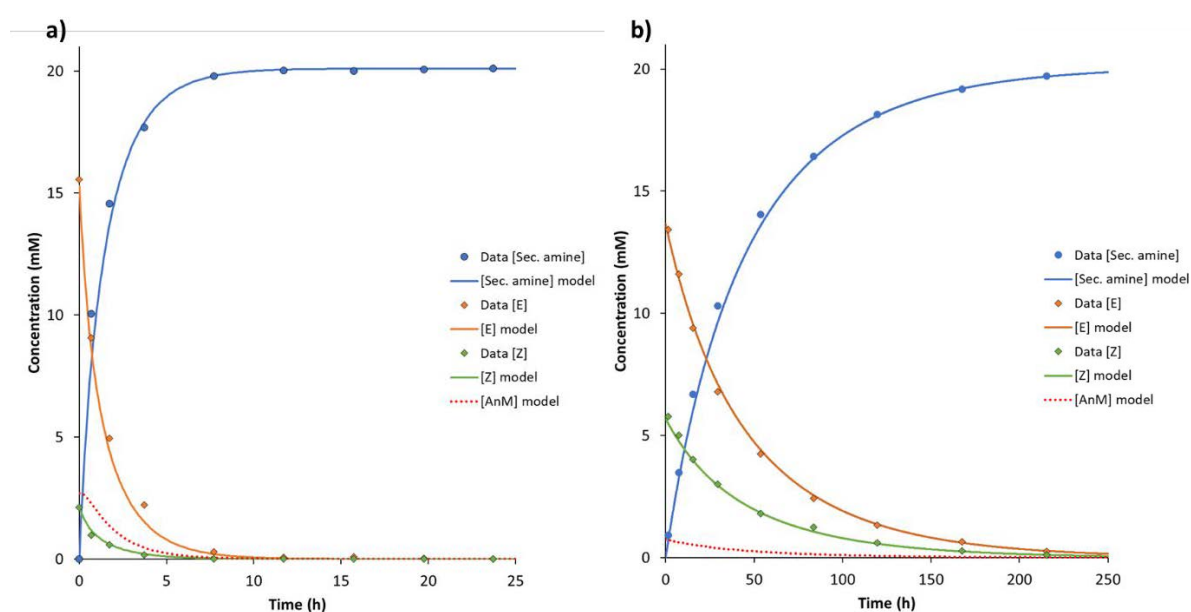
Figure S20: Model fitted to the experimental data obtained for reduction of A_2M-ADH (a) and A_2M-PDHA (b) conjugates using 3 equivalents PB at pH 4.0, RT.

S9 Optimisation of preparative protocols

Statistical distribution of mono-, di- and unsubstituted ADH and PDHA

The relative amount of unsubstituted, monosubstituted and disubstituted ADH and PDHA can be calculated assuming the reactivities of the two termini are identical. Such estimates are primarily intended to determine how much ADH or PDHA should be used for mono-substitution (activation) without producing too much disubstituted species.

Definitions and main relations:

$[A_nM]_0$: Initial molar concentration of oligosaccharide

$[L]_0$: Initial molar concentration of ADH or PDHA

[-NH$_2$]$_0$: Initial molar concentration of terminal amine

Let a be defined as the equivalence of linker (ADH or PDHA) relative to oligosaccharide before reaction. Hence:

$$[L]_0 = a[A_nM]_0$$

Since we treat each terminal amine as a separate and independent reactant we may further write:

$$[-NH_2]_0 = 2[L]_0 = 2a[A_nM]_0$$

Let b be defined as the fraction of oligosaccharide that has become substituted. b is obtained directly from the equilibrium yields listed in Table 1. Hence, $b[A_nM]_0$ becomes the molar concentration of substituted oligosaccharide, which must necessarily equal the molar concentration of substituted amine. The fraction of substituted amines (p) thus becomes:

$$p = b\frac{[A_nM]_0}{[-NH_2]_0} = b\frac{[A_nM]_0}{2[L]_0} = \frac{b}{2a}$$

Hence, p is a simple function of the fraction of substituted oligosaccharide (b) and the molar equivalence of linker (a). For statistical distributions fractions and probabilities are interchangeable. Hence:

The probability that both ends are substituted, fraction of disubstituted species (f_{DS}) = p^2
The probability that none of the ends are substituted, fraction of unsubstituted species (f_{US}) = $(1 - p)^2$
The probability that one end is substituted, fraction of monosubstituted species (f_{MS}) = $1 - p^2 - (1 - p)^2 = 2p - 2p^2 = 2p(1-p)$

b is obtained directly from the equilibrium yields given in Table 1. As an example, the reaction between A$_2$M and 2 equivalents of ADH ($a = 2$) at pH 4.0 is considered. The equilibrium yield of substituted oligosaccharides obtained by NMR was 87 % and hence, $b = 0.87$. Then p becomes:

$$p = \frac{0.87}{4} = 0.22$$

and f_{DS} is $(0.22)^2 = 0.0484 = 5$ %. When 10 equivalents of ADH is used (i.e. $a = 10$) and we assume $b = 0.87$, f_{DS} is reduced to $0.002 = 0.2$ %. Examples of th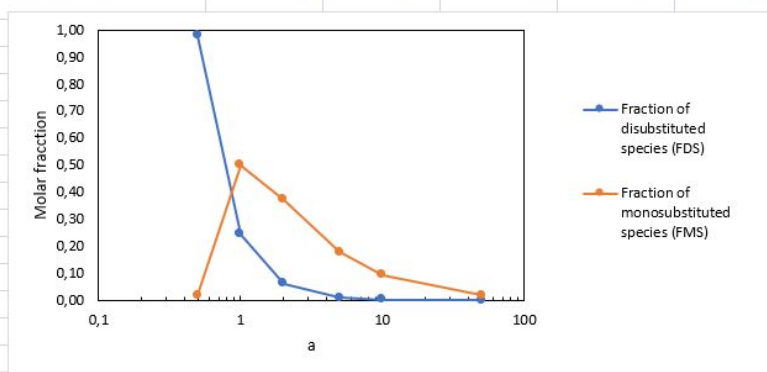e statistical distribution of mono-, di- and unsubstituted species with different equivalents of linker (a) and fractions of substituted oligomer (b) are given in Figure S21-S23.

17

a	Equivalents linker	0,5	1	2	5	10	50
b	Fraction substituted oligomer	0,70	0,70	0,70	0,70	0,70	0,70
p		0,700	0,350	0,175	0,070	0,035	0,007
Fraction of disubstituted species (F_{DS})		0,490	0,123	0,031	0,005	0,001	0,000
Fraction of monosubstituted species (F_{MS})		0,420	0,455	0,289	0,130	0,068	0,014
Fraction of unsubstituted species (F_{US})		0,090	0,423	0,681	0,865	0,931	0,986
Ratio mono-/disubstituted species		0,86	3,71	9,43	26,57	55,14	283,71
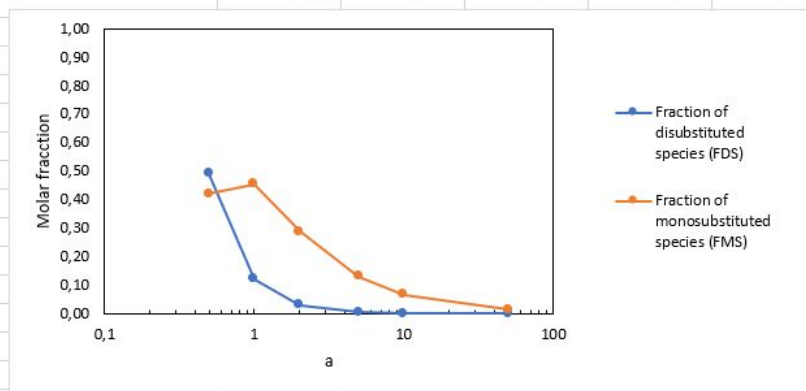
Figure S21: Statistical distribution of mono-, di- and unsubstituted species with different equivalents of linker (a) and $b = 0.70$.

a	Equivalents linker	0,5	1	2	5	10	50
b	Fraction substituted oligomer	0,87	0,87	0,87	0,87	0,87	0,87
p		0,870	0,435	0,218	0,087	0,044	0,009
Fraction of disubstituted species (F_{DS})		0,757	0,189	0,047	0,008	0,002	0,000
Fraction of monosubstituted species (F_{MS})		0,226	0,492	0,340	0,159	0,083	0,017
Fraction of unsubstituted species (F_{US})		0,017	0,319	0,612	0,834	0,915	0,983
Ratio mono-/disubstituted species		0,30	2,60	7,20	20,99	43,98	227,89
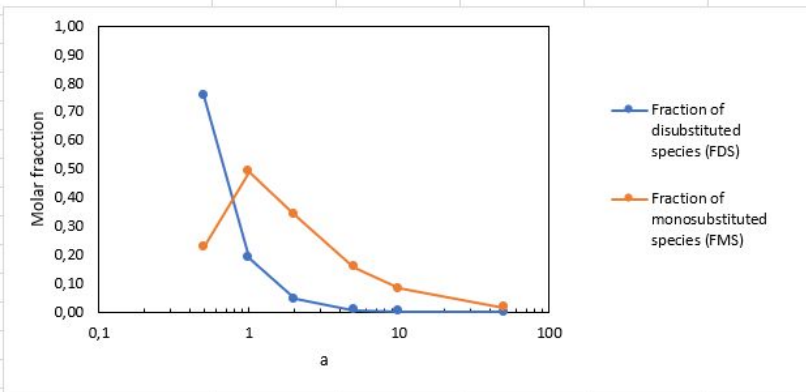
Figure S22: Statistical distribution of mono-, di- and unsubstituted species with different equivalents of linker (a) and $b = 0.87$.

18

a	Equivalents linker	0,5	1	2	5	10	50
b	Fraction substituted oligomer	0,99	0,99	0,99	0,99	0,99	0,99
p		0,990	0,495	0,248	0,099	0,050	0,010
Fraction of disubstituted species (F_{DS})		0,980	0,245	0,061	0,010	0,002	0,000
Fraction of monosubstituted species (F_{MS})		0,020	0,500	0,372	0,178	0,094	0,020
Fraction of unsubstituted species (F_{US})		0,000	0,255	0,566	0,812	0,903	0,980
Ratio mono-/disubstituted species		0,02	2,04	6,08	18,20	38,40	200,02

Figure S23: Statistical distribution of mono-, di- and unsubstituted species with different equivalents of linker (a) and $b = 0.99$.

Minimisation of disubstituted ADH or PDHA

As shown above the statistical amount of disubstituted ADH or PDHA is significant (5-6 %) when 2 equivalents are used, especially for high reaction yields, but decreases below 1% for 10 equivalents. This was qualitatively verified by GFC fractionation of A_nM-PDHA conjugates prepared with 2 or 10 equivalents of PDHA, respectively (Figure S24). A significant decrease in disubstituted species was observed when 10 equivalents were used. Hence, a large excess ($\geq$ 10 equivalents) is necessary to minimise the amount of disubstituted species.
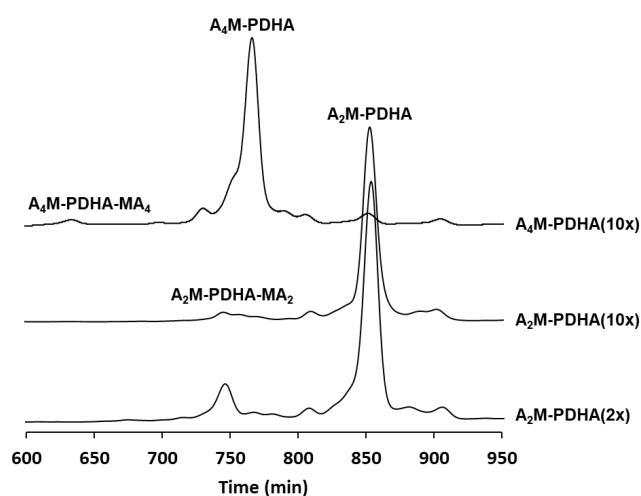
Figure S24: GFC fractionation of the reaction mixtures obtained for the conjugation of A_nM oligomers to 2 or 10 equivalents (2x or 10x, respectively) PDHA under otherwise standard conditions (20.1 mM oligomer, pH 4.0, RT).

Optimisation of reduction conditions for PDHA conjugates

The reduction of PDHA conjugates was optimised by varying the concentration of reducing agent (PB). However, due to the low solubility of PB in the buffer, reduction of A_4M-PDHA conjugates (equilibrium mixture with 10 equivalents PDHA) using 20 equivalents PB was performed in deuterated buffer in a separate vial (not in the NMR tube). The reaction was performed on a shaking device to increase the collision frequency of undissolved reducing agent and conjugates. NMR spectra of the dissolved phase of the reaction mixture was obtained after 24 and 48 hours revealing complete reduction after 48 hours.

Preparation of A_nM conjugates using optimised protocols

Reduced A_nM conjugates (A_nM-ADH and A_nM-PDHA) were prepared using optimised protocols. In brief, conjugation was carried out for 6 hours at RT using 10 equivalents ADH and PDHA at pH 4.0. For ADH conjugates, reduction was performed for 24 hours at RT by adding 3 equivalents PB to the equilibrium mixture, whereas for the PDHA conjugates, 20 equivalents PB were added to the equilibrium mixture and the reduction was performed for 48 hours at RT to ensure complete reduction. Reaction mixtures were fractionated by GFC and purified conjugates were characterized by ^{1}H-NMR. Fractionation of reduced A_5M-ADH and A_5M-PDHA conjugates is shown in Figure S25. Fractionation of the A_nM oligomer mixture is included in the figure for comparison. Small amounts of disubstituted ADH/PDHA were formed in both reactions. The relative amount of disubstituted species seemed higher than obtained for the optimised protocol using A_2M oligomers (Figure S24), which may be a result of higher reactivity of oligomers with higher DP and the higher fraction of substituted amine (equilibrium yield of conjugates). In addition, conjugates with shorter and longer A_nM oligomers were present in the reaction mixture reflecting a slight polydispersity of the starting oligomer (A_5M), due to the lower resolution of the preparative GFC system. However, pure A_5M-ADH/PDHA conjugates were obtained after fractionation, verified by the ^{1}H-NMR characterization of A_5M-ADH and A_5M-PDHA given in Figure S26 and S27, respectively.
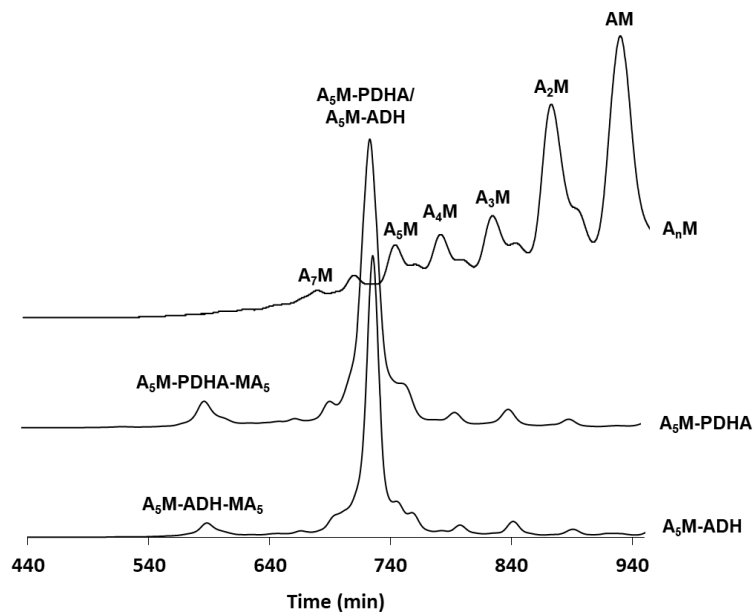
Figure S25: GFC fractionation of the reaction mixtures obtained for the preparation of A_5M-ADH and A_5M-PDHA conjugates using optimised conditions. Fractionation of the mixture of A_nM oligomers is included for comparison.
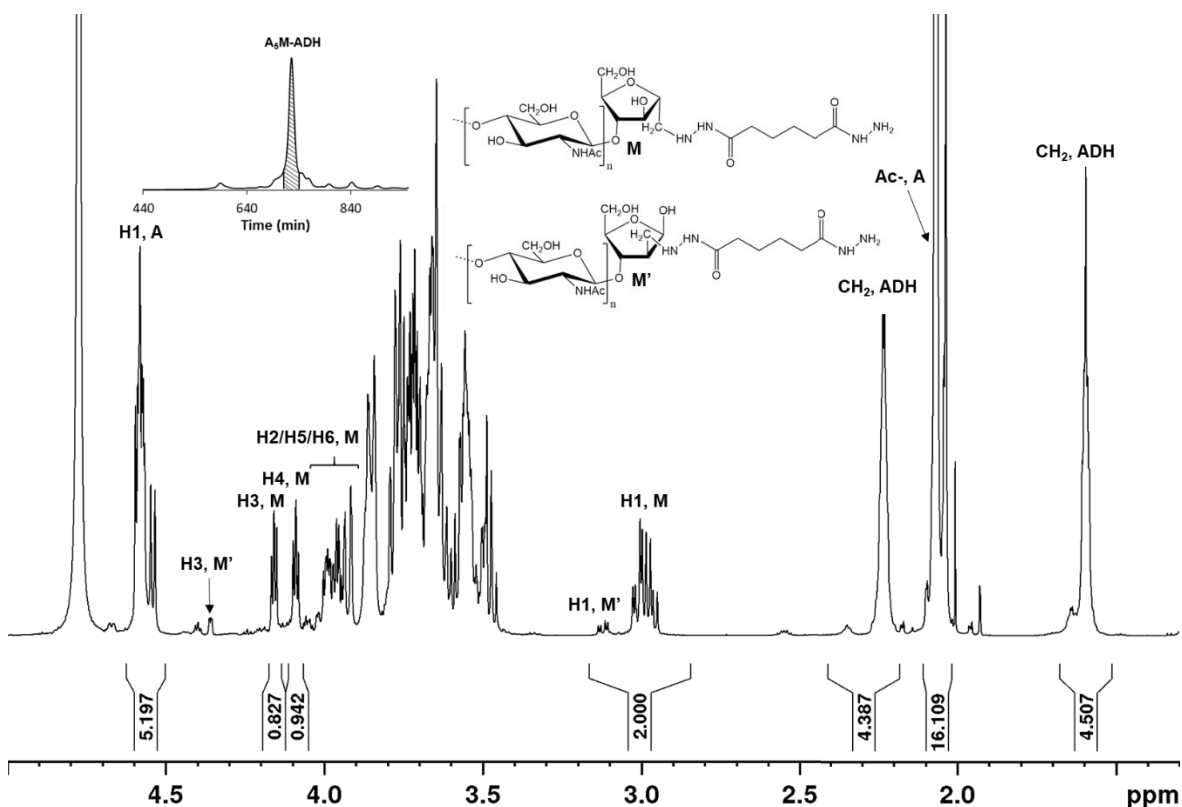
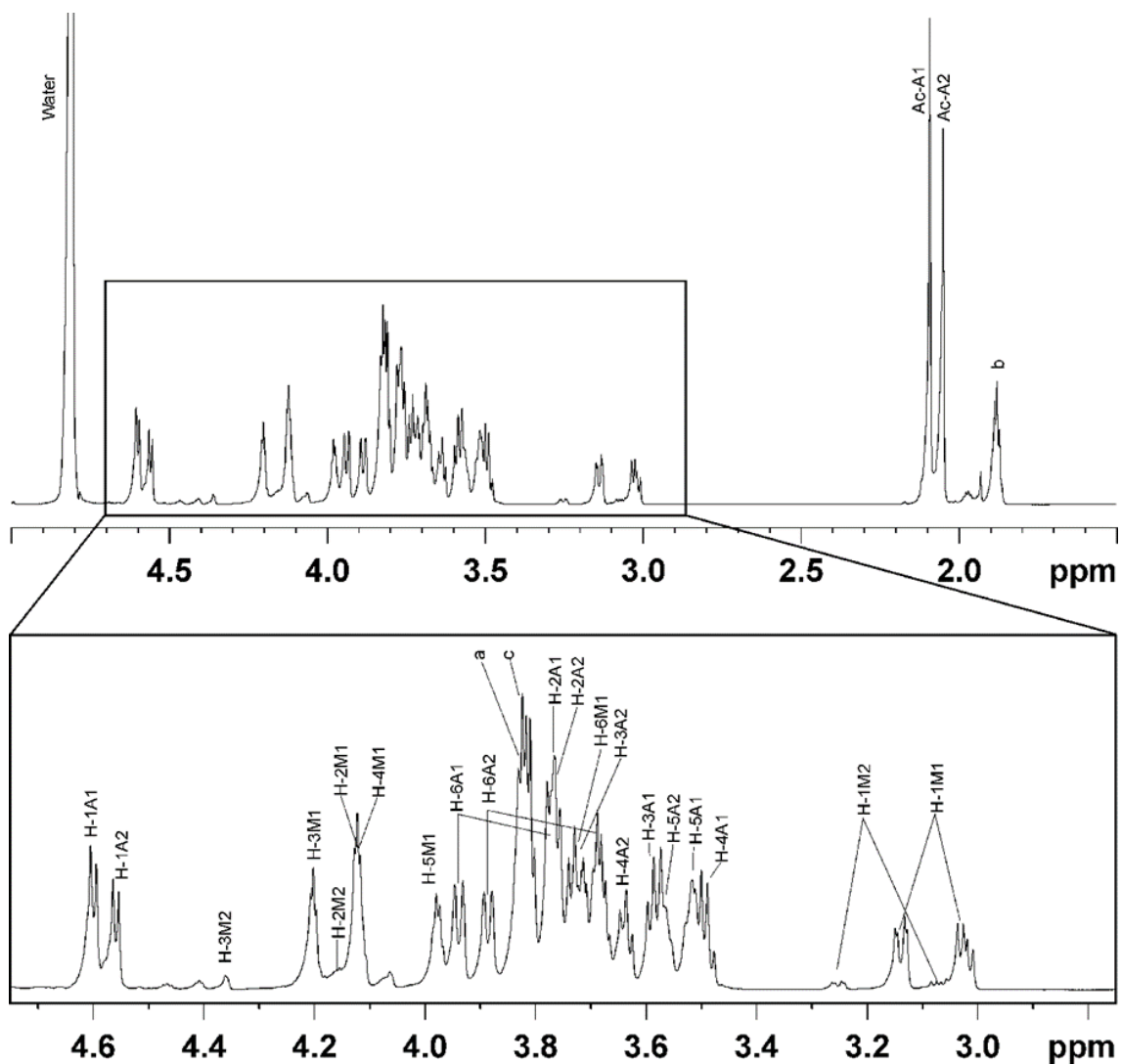**Figure S26:** ^{1}H-NMR spectrum of the purified A_5M-ADH conjugate (D_2O, 300K, 600 MHz)
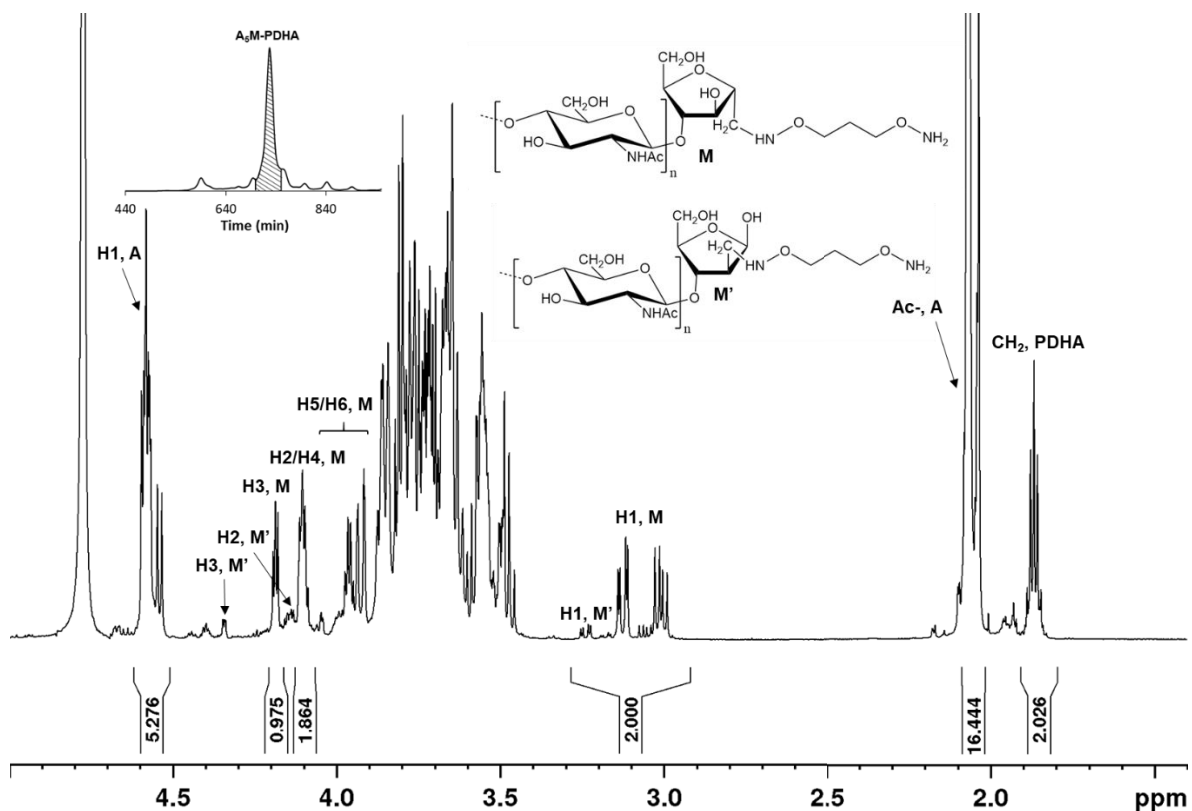
**Figure S27:** ^{1}H-NMR spectrum of the purified A_5M-PDHconjugate (D$_2$O, 300K, 600 MHz)

S10 2D NMR characterization of the reduced and purified A$_2$M-PDHA

The reduced and purified A$_2$M-PDHA conjugate was characterized by homo- and heteronuclear NMR correlation experiments. The conjugate was dissolved in D$_2$O and the NMR analysis was carried out using the 800 MHz spectrometer in a 3 mm NMR tube. Resonances were assigned by starting at the anomeric proton signal and then following the proton-proton connectivity using TOCSY, DQF-COSY/IP-COSY, ^{13}C H2BC and ^{13}C HSQC-[^{1}H,^{1}H] TOCSY spectra. ^{13}C-HSQC was used for assigning the carbon chemical shifts. The ^{13}C HMBC spectrum provided information of connections between the sugars. One of the alternative forms of the M residue was structurally elucidated to be 3,5-anhydro-D-mannose. The following designations are used in the spectra displayed in Figure S28 and S29 and Table S1: A1 (*N*-acetylglucosamine (A) residue at the non-reducing end), A2 (middle *N*-acetylglucosamine (A) residue), M1 (2,5-anhydro-D-mannose (M) residue), M2 (3,5-anhydro-D-mannose (M') residue), -Ac (*N*-acetyl groups of A residues) a, b and c (unique identified methylene groups of PDHA). H/C# refers to the proton-carbon pairs with the ring carbon number for the monosaccharides. TSP was used for chemical shift reference. Chemical shifts are reported in Table S1. The structure of the A$_2$M-PDHA conjugate is included in Figure S29.

22

Figure S28: ^{1}H-NMR spectrum of the reduced and purified A_2M-PDHA conjugate recorded at 298 K. Designations as described above.
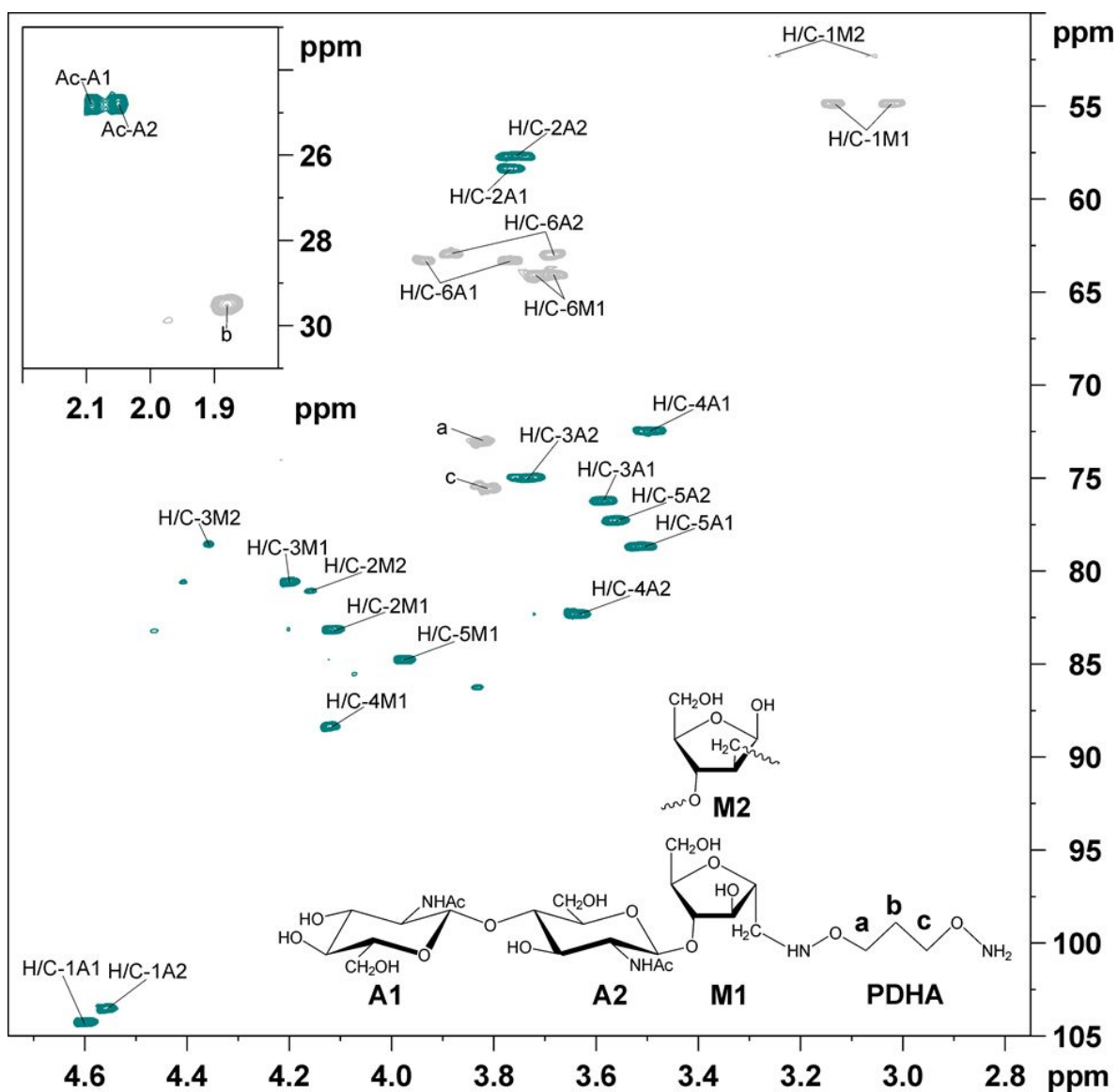
Figure S29: ^{13}C HSQC spectrum of the reduced and purified A_2M-PDHA conjugate recorded at 298 K. Designations as described above.

Table S1: Chemical shift assignment for the reduced and purified A_2M-PDHA conjugate at 298 K. The chemical shifts are related to TSP. Designations as described above.

Structural unit	Assignment						
	H-1; C-1	**H-2; C-2**	**H-3; C-3**	**H-4; C-4**	**H-5; C-5**	**H-6; C-6**	**Ac-H; C**
A1	4.60,104.2	3.75;57.5	3.59;76.2	3.49;72.4	3.51;78.6	3.93,3.77;63.2	2.09; 24.8
A2	4.56; 103.4	3.77;58.2	3.74;74.9	3.98;84.7	3.56;77.2	3.88,3.69;62.9	2.05; 24.8
M1	3.14,3.02;54.8	4.11;83.1	4.20;80.5	4.12;88.3	3.98;84.7	3.73,3.69;64.0	-
M2	3.25,3.07;52.2	4.16;80.9	4.36; 78.4	3.62; 82.3	n.d	n.d	-
	a	b	c				
PDHA	3.82;72.9	1.88;29.6	3.81;75.6	-	-	-	-

n.d: Not determined.

S11 Preparation of chitin-*b*-chitin diblocks from activated chitin oligomers (A$_4$M-ADH)

Chitin-*b*-chitin diblocks were prepared by reacting A$_4$M-ADH conjugates (reduced and purified) with A$_4$M oligomers in an equimolar molar ratio. The conjugation of the second block (A$_4$M) was monitored by NMR (as described in S2). The kinetics was compared to simulated values for the corresponding reaction using rate constants obtained for the conjugation of A$_2$M and A$_5$M to free ADH. The results are summarised in Table S2 and kinetic plots are given in Figure S30. The comparison suggests the second conjugation proceeds somewhat faster than the first.

Table S2: Kinetic parameters obtained from the modelling of the reaction of A$_4$M with an equimolar proportion of A$_4$M-ADH. Simulated parameters for the corresponding reactions with equimolar proportions of oligomers and amines (0.5 equivalents ADH) using rate constants obtained for the conjugation of A$_2$M and A$_5$M to free ADH are given in italics.

| Equivalents				A+B $\leftrightarrow$ E		A+B $\leftrightarrow$ Z		A+B $\leftrightarrow$ E + Z		Equilibrium yield [%]
								$t_{0.5}$ [h]	$t_{0.9}$ [h]	
A	B	B	pH	k_1 [h^{-1}]	k_{-1} [h^{-1}]	k_2 [h^{-1}]	k_{-2} [h^{-1}]			
A$_4$M	A$_4$M-ADH	1	4.0	7.3 x 10^{-2}	1.5x10^{-1}	1.1x10^{-2}	1.5x10^{-1}	0.35	1.57	74
A$_2$M	*ADH*	*0.5*	*4.0*	*1.8x10^{-2}*	*2.0x10^{-1}*	*2.5x10^{-3}*	*2.0x10^{-1}*	*0.91*	*3.34*	*51*
A$_5$M	*ADH*	*0.5*	*4.0*	*3.0x10^{-2}*	*3.5x10^{-1}*	*4.0x10^{-3}*	*3.5x10^{-1}*	*0.54*	*1.96*	*50*
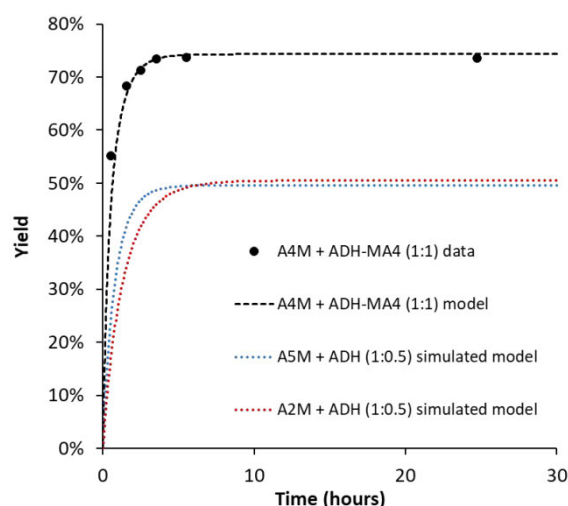
Figure S30: Kinetics of the reaction of A$_4$M with an equimolar proportion of A$_4$M-ADH. Simulated data for the corresponding reactions of A$_2$M and A$_5$M with free ADH and PDHA (0.5 equivalents, equimolar proportions of oligomers and amines) is included for comparison.

Reduction of the obtained equilibrium mixture was performed using 3 equivalents PB for 24 hours (RT). The reaction mixture was fractionated by GFC (Figure S31) and main products were purified. ^{1}H-NMR characterization of the main fraction (Figure S32) confirmed formation of the completely reduced A$_4$M-ADH-MA$_4$ diblock. Due to slight polydispersity of the A$_4$M oligomer (containing

oligomers of lower and higher DP), some longer and shorter diblocks were consequently formed. ^{1}H-NMR characterization of the fraction holding unreacted A_4M oligomers and A_4M-ADH conjugates (Figure S33) revealed complete reduction of the unreacted oligomers (no H1, M reducing end resonances). Hence, the fast reduction of oligomers prevented the diblock formation from going to completion. By integration of the chromatogram (Figure S31), the chitin-*b*-chitin diblock (A_4M-ADH-MA_n) area was found to accounted for 70 % of the total area, whereas unreacted conjugates (A_4M-ADH) and unreacted oligomers (A_nM) accounted for the resisting 30 % of the area. By assuming an equimolar ratio of oligomers and conjugates, the weight yield of diblocks in the reaction was 82.5 %.

	Diblock area	Conjugate/oligomer area
Time (min)	440-685	685-822
Area	17.9	7.6
Area (%)	70.2	29.8
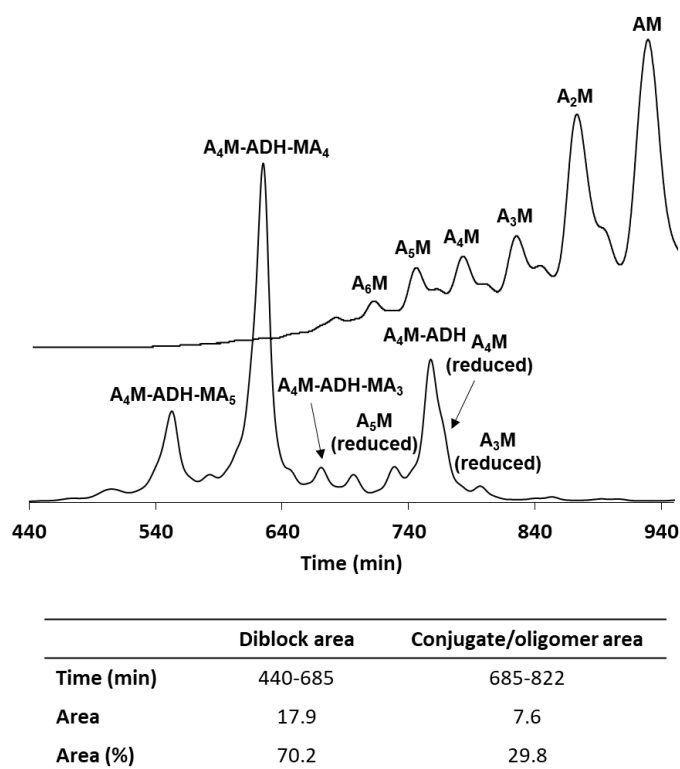
Figure S31: GFC fractionation of the reaction mixture obtained for the preparation of chitin diblocks by reacting A_4M-ADH with A_4M oligomers in an equimolar ratio. Fractionation of the mixture of A_nM oligomers is included for comparison.
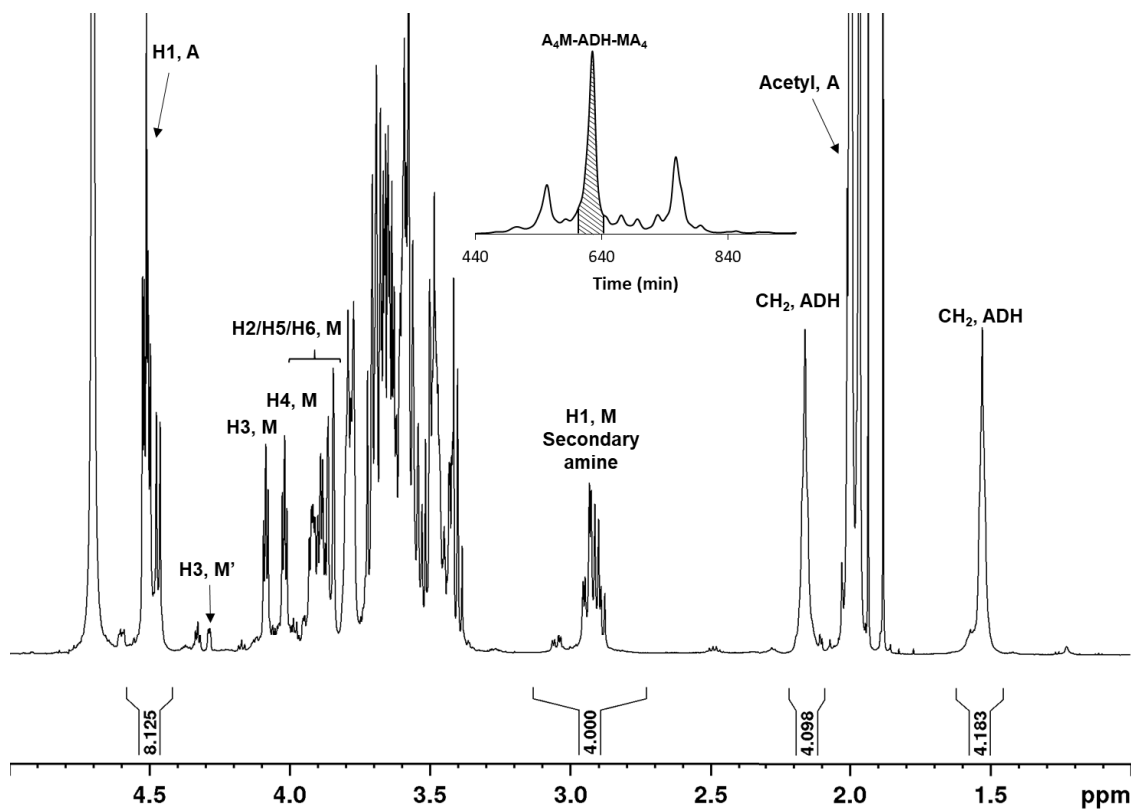
Figure S32: ¹H-NMR spectrum of the purified A_4M-PDHA-MA_4 diblock fraction (D_2O, 300K, 600 MHz) from the chromatogram in Figure S31.
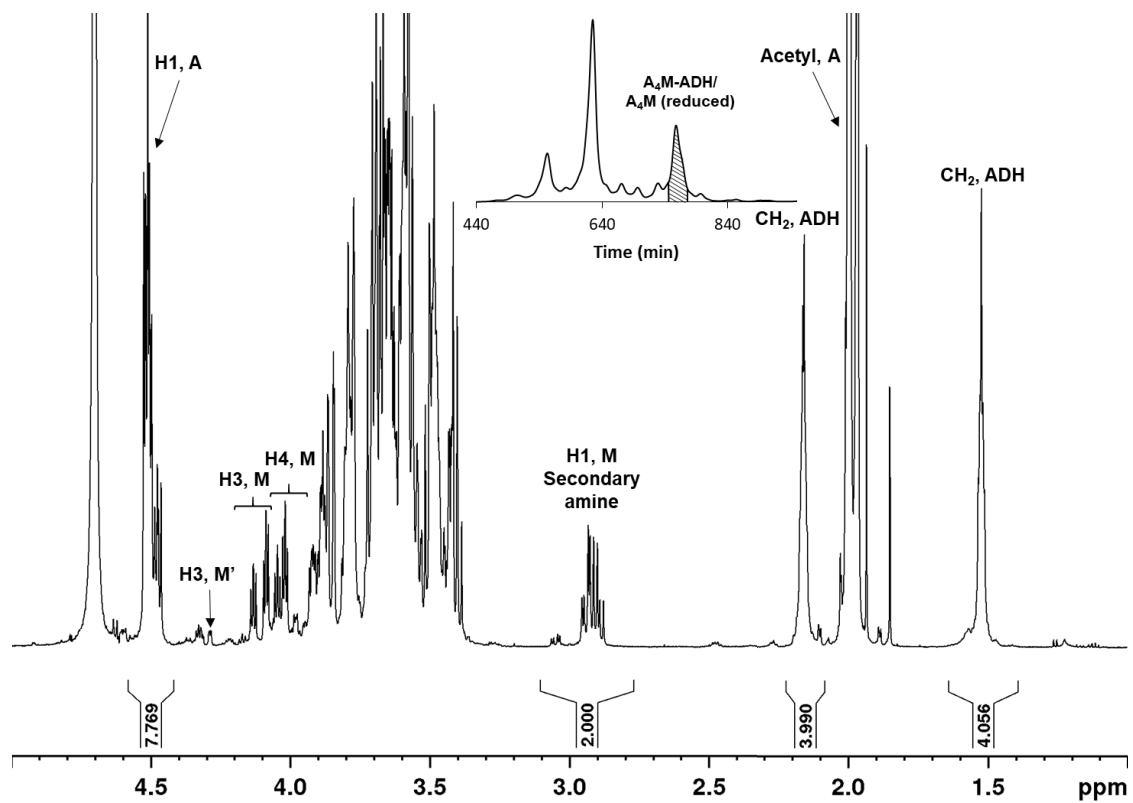
Figure S33: ¹H-NMR spectrum of the A_4M-PDHA/A_4M (reduced) fraction (D_2O, 300K, 600 MHz) from the chromatogram in Figure S31.

S12 Preparation of chitin-*b*-chitin diblocks using a sub-stoichiometric amount of ADH or PDHA

Chitin-*b*-chitin diblocks were prepared using A_2M oligomers and a sub-stoichiometric amount of ADH or PDHA (0.5 equivalents). The conjugation of oligomers was monitored by NMR. The kinetics was compared to simulated values using rate constants obtained for the conjugation of A_2M to free ADH or PDHA (2 equivalents). The results are summarised in Table S3 and the kinetic plots are given in Figure S34.

Table S3: Kinetic parameters obtained from the modelling of the reaction of A_2M with 0.5 equivalents of ADH or PDHA (equimolar proportions of oligomers and amines). Simulated parameters for the corresponding reactions using rate constants obtained for the conjugation of A_2M to free ADH or PDHA are given in italics.

| Equivalents				A+B ↔ E		A+B ↔ Z		A+B ↔ E + Z		Equilibrium yield [%]
								$t_{0.5}$ [h]	$t_{0.9}$ [h]	
A	B	B	pH	k_1 [h^{-1}]	k_{-1} [h^{-1}]	k_2 [h^{-1}]	k_{-2} [h^{-1}]			
A_2M	ADH	0.5	4.0	4.0×10^{-1}	9.0×10^{-1}	5.8×10^{-2}	9.0×10^{-1}	0.06	0.28	73
A_2M	*ADH*	*0.5*	*4.0*	*1.8×10^{-2}*	*2.0×10^{-1}*	*2.5×10^{-3}*	*2.0×10^{-1}*	*0.91*	*3.35*	*51*
A_2M	PDHA	0.5	4.0	1.2×10^{-1}	6.0×10^{-2}	5.2×10^{-2}	6.0×10^{-2}	0.22	1.21	88
A_2M	*PDHA*	*0.5*	*4.0*	*2.4×10^{-2}*	*2.2×10^{-1}*	*1.0×10^{-2}*	*2.2×10^{-1}*	*0.64*	*2.41*	*57*
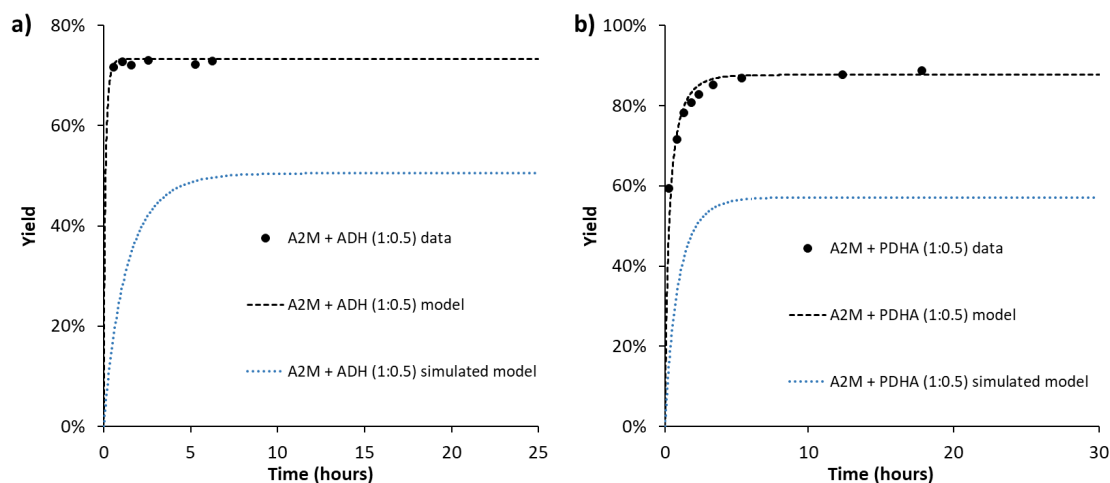
Figure S34: Kinetics of the reactions of A_2M with 0.5 equivalents of **a)** ADH and **b)** PDHA. Simulated data for the corresponding reactions of A_2M with free ADH and PDHA (0.5 equivalents, equimolar proportions of oligomers and amines) is included for comparison.

Reduction of the equilibrium mixtures was performed using 3 equivalents PB for 24 hours or 20 equivalents PB for 48 hours at room temperature for the reaction with ADH and PDHA, respectively. Reaction mixtures were fractionated by GFC (Figure S35) and the main fractions were purified and characterized by ^{1}H-NMR (Figure S36 – S40). Products from the ADH reaction were completely reduced (no hydrazone resonances in the spectra) whereas minor oxime resonances were observed in

the products from the PDHA reaction, indicating incomplete reduction. Impurity of the A_2M oligomers gave additional fractions in the GFC chromatograms obtained for both reactions. The yield of diblocks was obtained by integrating the chromatograms (Figure S35) as described above. The weight yield of diblocks was 74 % and 87 % for the reaction with ADH and PDHA, respectively. The yield of diblocks corresponds well to the statistical amount of diblocks expected (73 % for ADH and 88 % for PDHA). Unreacted oligomers were completely reduced (no H1, M resonances observed in the ^{1}H-NMR spectra), confirming the fast reduction of A_nM oligomers preventing the diblock formation form going to completion.

	Diblock area	Conjugate/oligomer area
Time (min)	613-780	780-918
Area	4.2	3.0
Area (%)	58.5	41.5

	Diblock area	Conjugate/oligomer area
Time (min)	600-784	784-910
Area	7.7	2.3
Area (%)	77.0	23.0
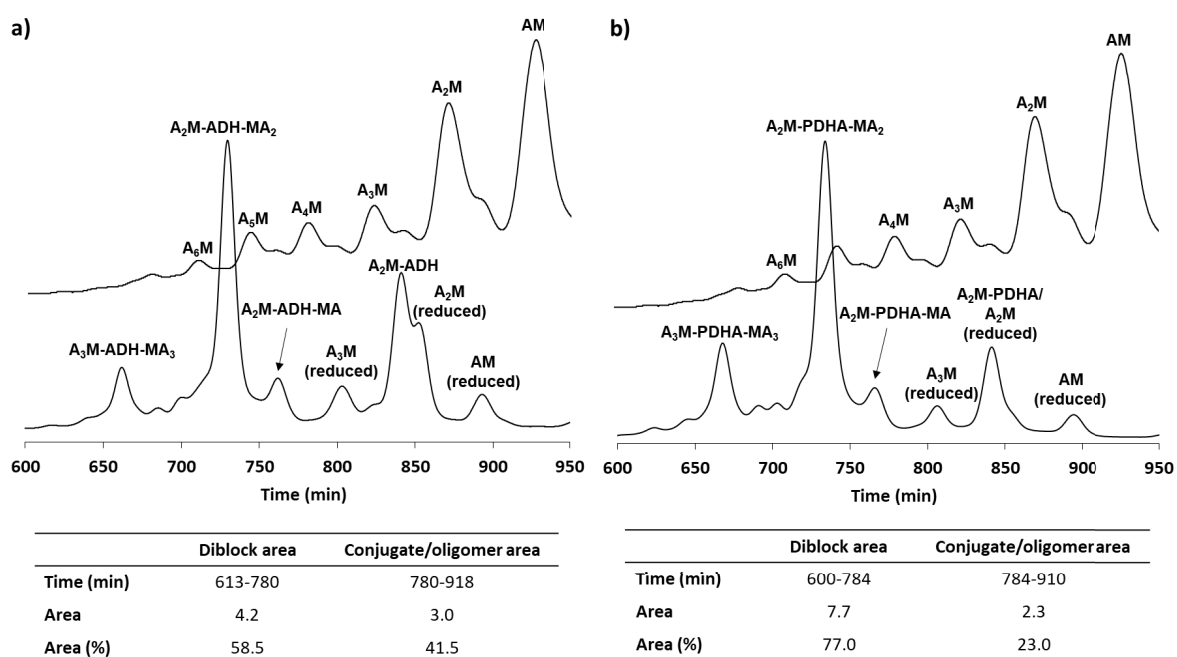
Figure S35: GFC fractionation of the reaction mixture obtained for the preparation of chitin diblocks by reacting A_2M oligomers with a sub stoichiometric amount (0.5 equivalents) of **a)** ADH or **b)** PDHA. Fractionation of the mixture of A_nM oligomers is included for comparison.
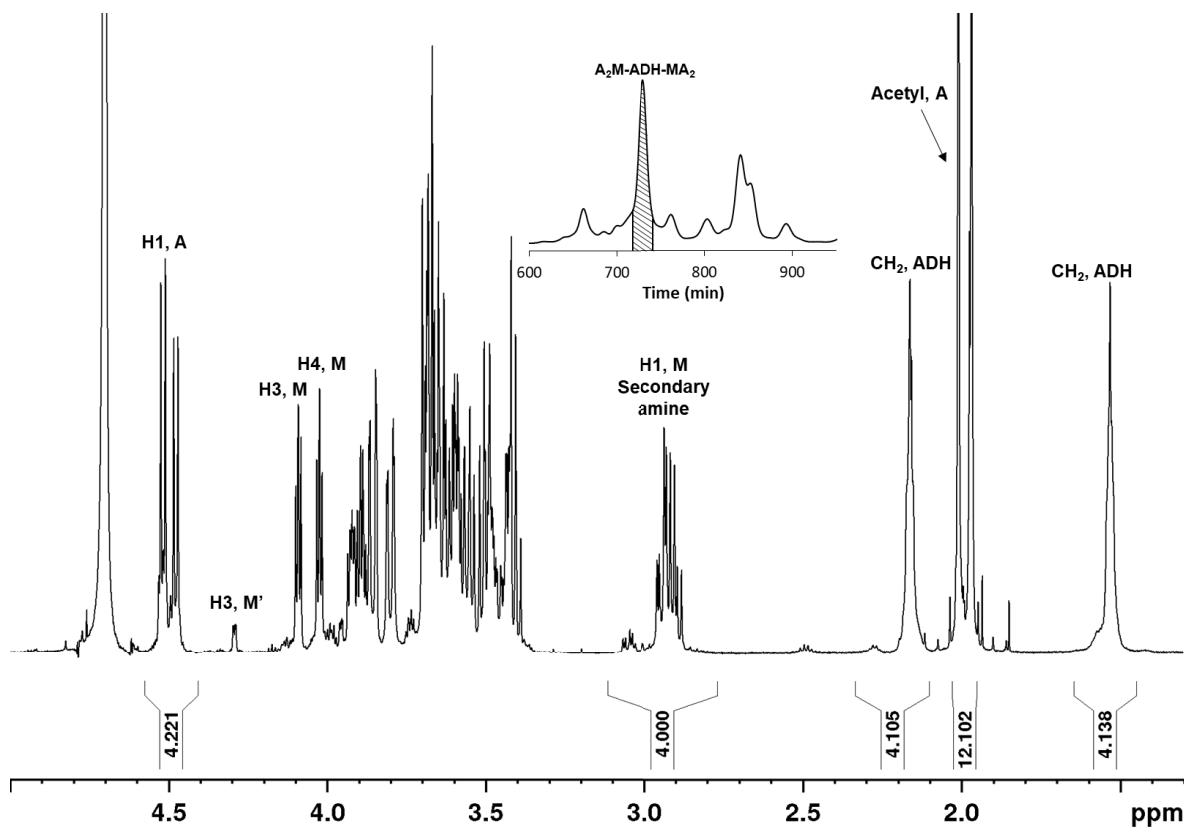
Figure S36: ^{1}H-NMR spectrum of the purified A_2M-ADH-MA_2 diblock fraction (D_2O, 300K, 600 MHz) from the chromatogram in Figure S35a.
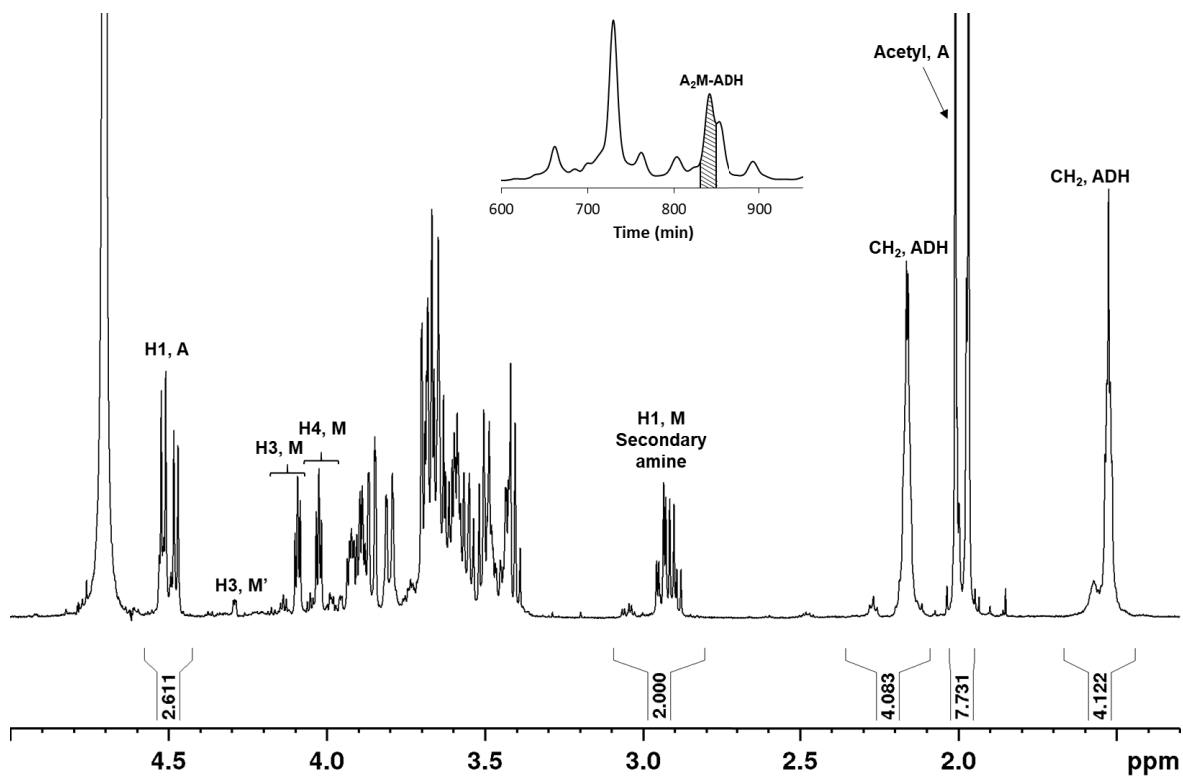
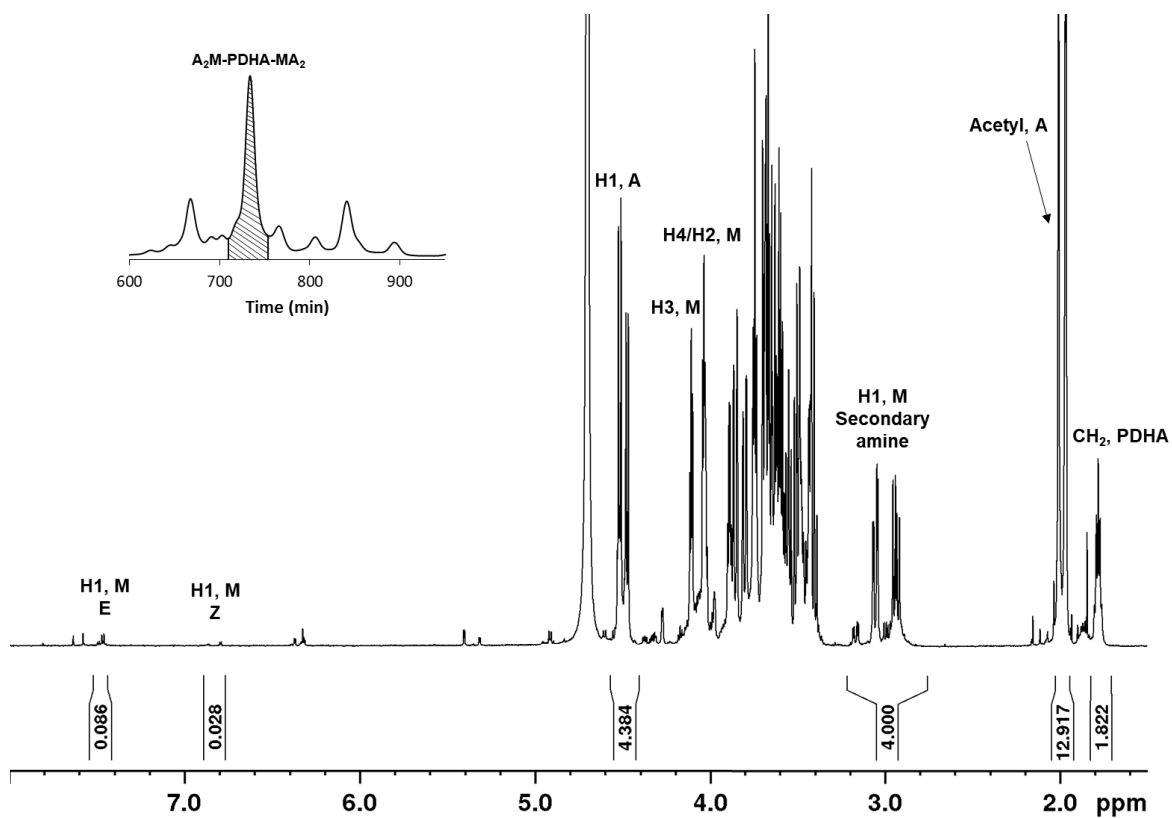**Figure S37:** ^{1}H-NMR spectrum of the A_2M-ADH fraction (D_2O, 300K, 600 MHz) from the chromatogram in Figure S35a.

30
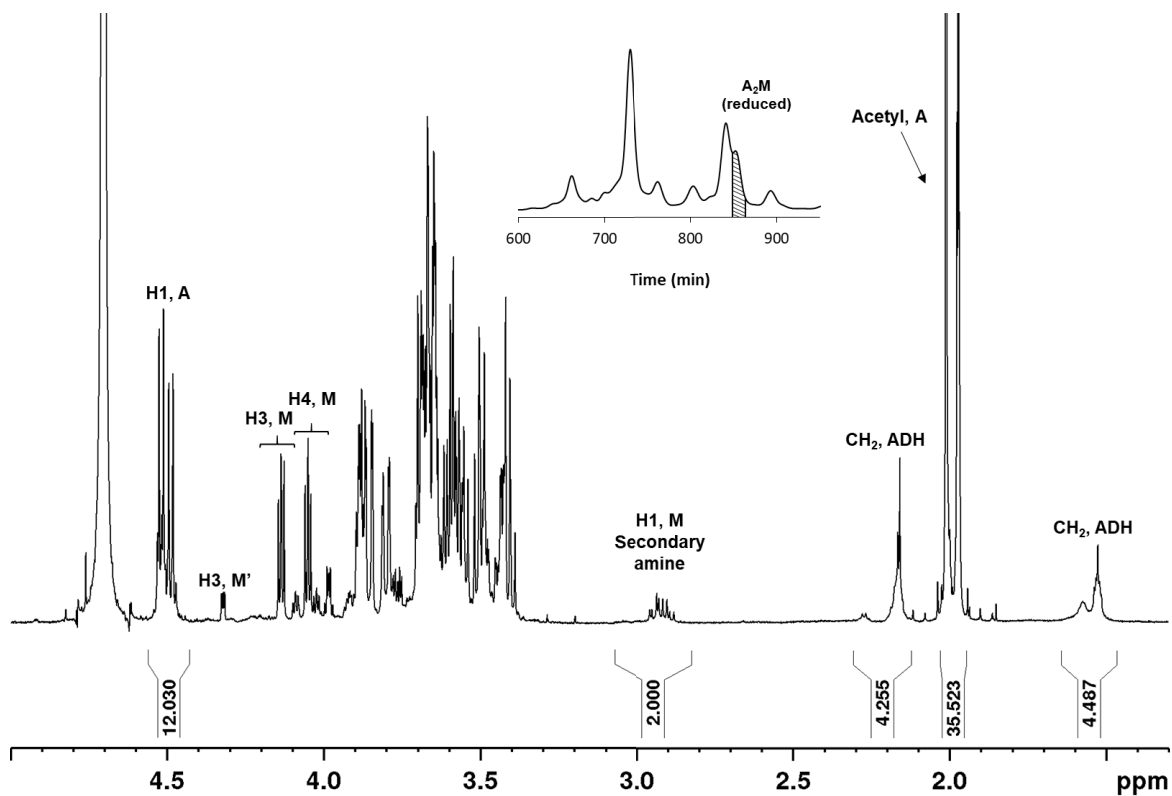
**Figure S38:** ^{1}H-NMR spectrum of the A$_2$M (reduced) fraction (D$_2$O, 300K, 600 MHz) from the chromatogram in Figure S35a.

Figure S39: ^{1}H-NMR spectrum of the purified A$_2$M-PDHA-MA$_2$ diblock fraction (D$_2$O, 300K, 600 MHz) from the chromatogram in Figure S35b.
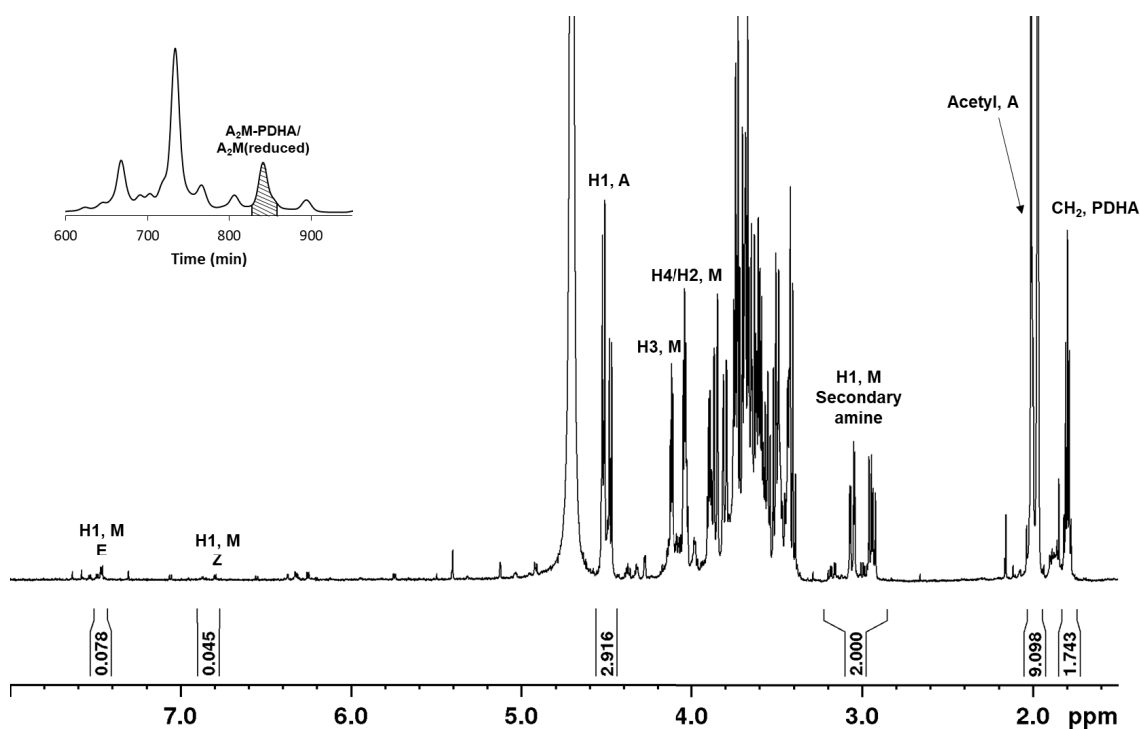
Figure S40: ^{1}H-NMR spectrum of the A$_2$M-PDHA/A$_2$M (reduced) fraction (D$_2$O, 300K, 600 MHz) from the chromatogram in Figure S35b.

## S13 Preparation and characterization of dextran (Dext$_m$) oligomers

Dextran (Dext$_m$) oligomers were prepared by acid hydrolysis of dextran (Dextran T-2000, M$_w$ = 2,000,000). ^{1}H-NMR characterisation of Dextran T-2000 is given in Figure S41. The degree of branching was estimated from the integral of the H1 resonance of internal glucose residues in the main chain and the H1 of the glucose residues at the branching points (BP) to 3.6 % [6]. The degradation mixture was fractionated by preparative GFC to obtain isolated Dext$_m$ oligomers (Figure S42a). The isolated Dext$_6$ oligomer (DP = 6) was characterized by ^{1}H-NMR (Figure S43) and fractionated by analytical GFC (Figure S42b) to show the slight polydispersity of the oligomer. The degree of branching of the oligomer was estimated to approximately 0.8 % showing that the branches are more rapidly hydrolysed than the linkages in the main chain.
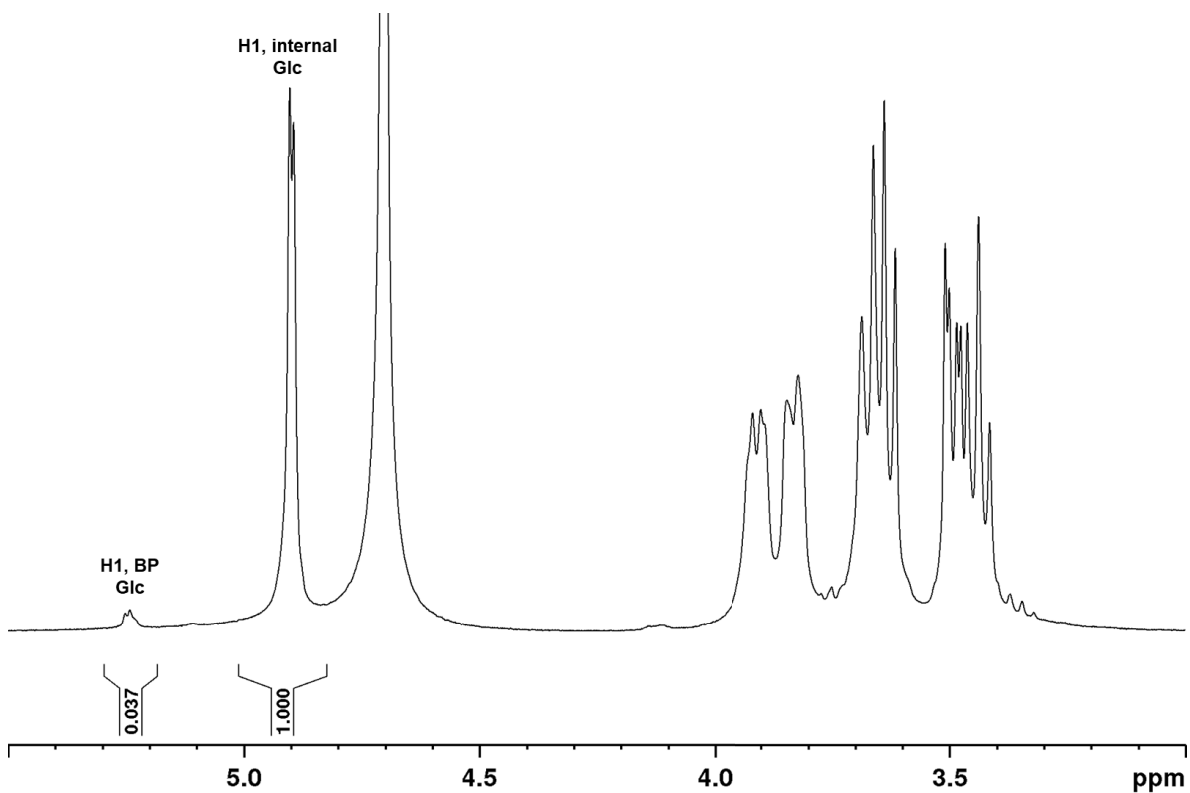
**Figure S41:** ^{1}H-NMR characterization of Dextran T-2000 (D$_2$O, 300K, 600 MHz).
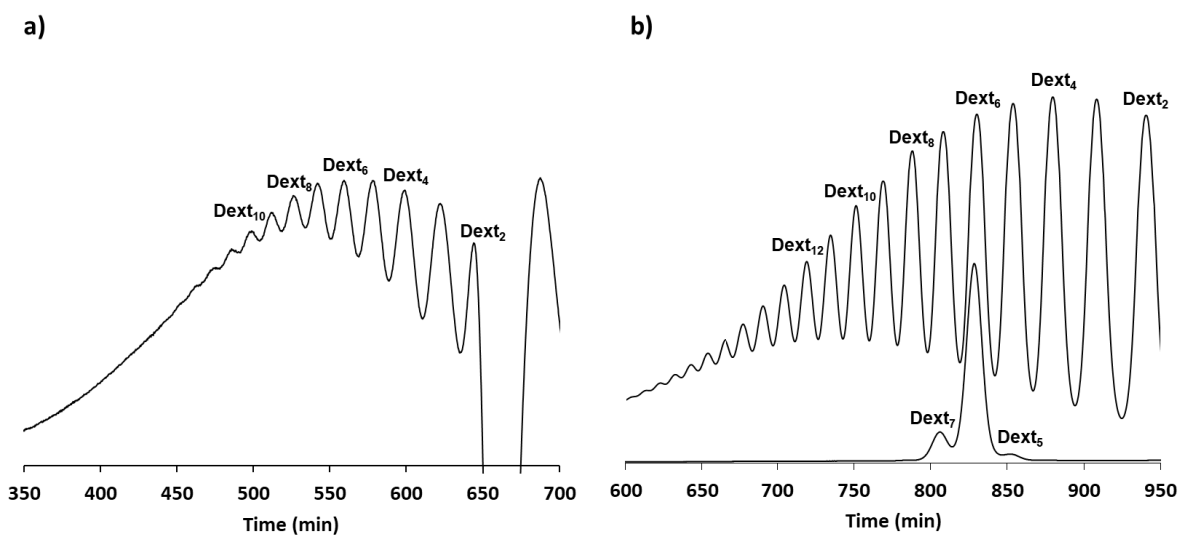
Figure S42: a) Preparative GFC fractionation of the mixture of Dext$_m$ oligomers **b)** analytical GFC fractionation of isolated Dext$_6$. Fractionation of the mixture of Dext$_m$ oligomers is included for comparison.
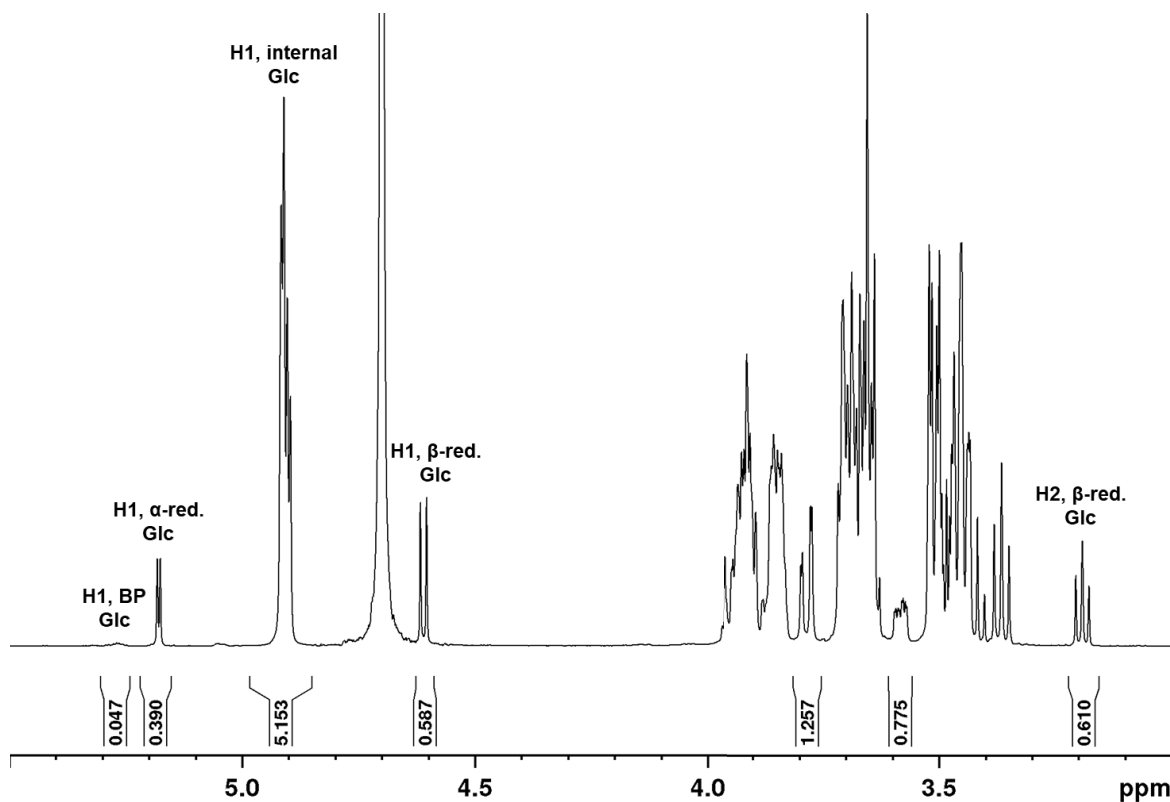
Figure S43: ^{1}H-NMR spectrum of the isolated Dext$_6$ oligomer (in D$_2$O, 300 K, 600 MHz) obtained from the preparative GFC fractionation in Figure S42a.

## S14 Conjugation of Dext$_m$ oligomers to ADH and PDHA studied by time course NMR

Conjugation of Dext$_5$ oligomers (DP = 5) to ADH and PDHA (2 equivalents) at pH 4.0, RT was monitored by NMR (Figure S44 and S45, respectively). Here, the reducing end of dextran (Glc, normal reducing end), governs the conjugation and hence, the acyclic hydrazones and oximes are in equilibrium with cyclic *N*-glycosides. As previously shown [5], dextran formed almost exclusively *N*-pyranosides with ADH, whereas it formed *N*-pyranosides in addition to E- and Z-oximes with PDHA. The equilibrium yield of conjugates (E-/Z-hydrazones or oximes + *N*-pyranosides) obtained for the reactions was 35% for Dext$_5$ with ADH and 87% for Dext$_5$ with PDHA. The experimental data obtained in the conjugation reactions were fitted using the model described in S3 (based on the reaction scheme presented in Figure S5). The data fitting for the conjugation Dext$_5$ oligomers to ADH and PDHA (2 equivalents) at pH 4.0 (RT) are given in Figure S46. Rates ($t_{0.5}$ and $t_{0.9}$) and equilibrium yields for the total conjugation reaction are given in Table S4.

34
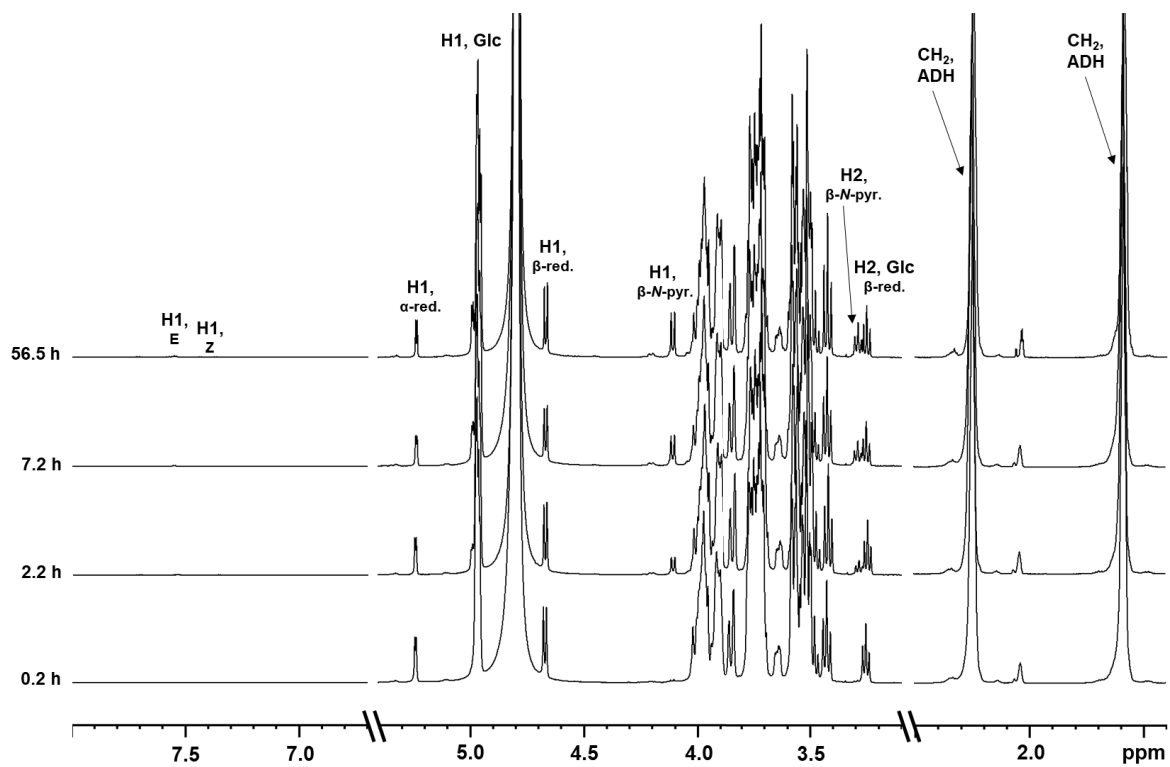
Figure S44: ^{1}H-NMR spectra obtained at defined time points for the conjugation reaction with Dext$_5$ (20.1 mM) and 2 equivalents ADH at pH 4.0, RT.
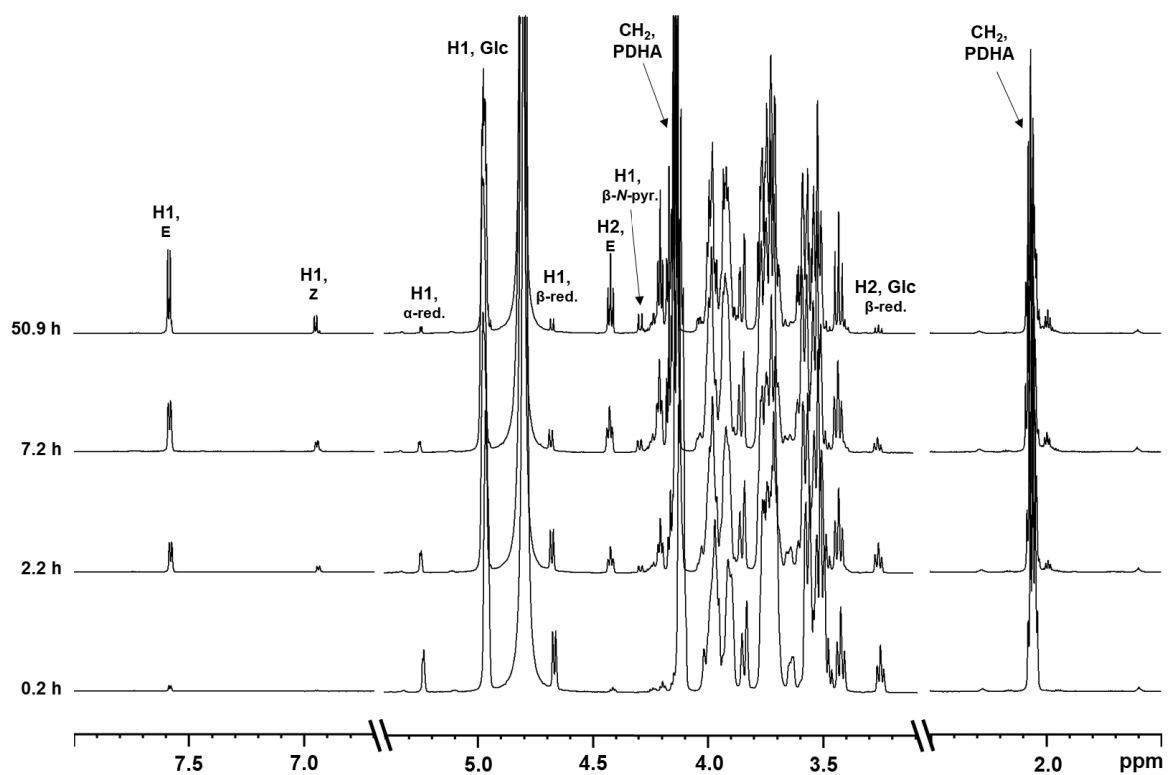
Figure S45: ^{1}H-NMR spectra obtained at defined time points for the conjugation reaction with Dext$_5$ (20.1 mM) and 2 equivalents PDHA at pH 4.0, RT.
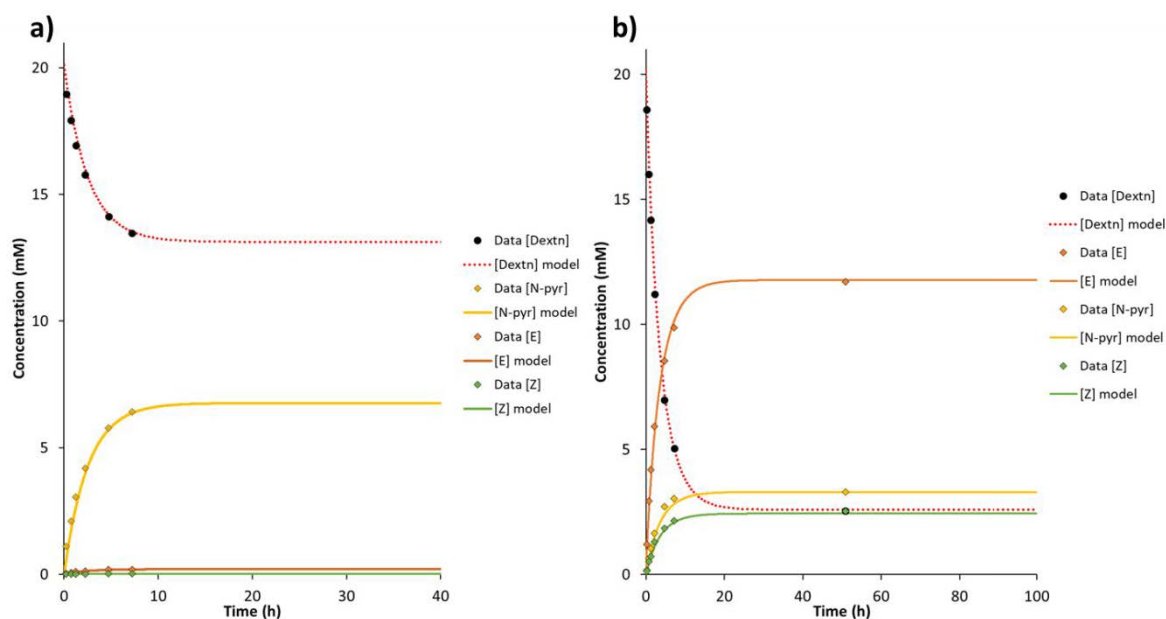
Figure S46: a) Model fitted to the experimental data obtained for the conjugation of Dext$_5$ to ADH (2 equivalents) at pH 4.0, RT. **b)** Model fitted to the experimental data obtained for the conjugation of Dext$_5$ to PDHA (2 equivalents) at pH 4.0, RT.

**Table S4:** Kinetic parameters obtained from the modelling of the reaction of Dext$_5$ with 2 equivalents ADH or PDHA.

		Equivalents			A+B ↔ E + Z+Pyr		Equilibrium yield [%]
A	**B**	**B**	**pH**	$t_{0.5}$ [h]	$t_{0.9}$ [h]		
Dext$_5$	ADH	2	4.0	1.74	5.84		35
Dext$_5$	PDHA	2	4.0	2.38	8.54		87

S15 Preparation of chitin-*b*-dextran diblocks

Chitin-*b*-dextran diblocks were prepared by reacting A$_5$M-ADH or A$_5$M-PDHA conjugates (reduced and purified) with dextran oligomers of DP = 6 (Dext$_6$) in an equimolar ratio. The conjugation of the dextran block was monitored by NMR (as described in S2) and combined equilibrium yields of 15 and 66 % were obtained for the conjugation to A$_5$M-ADH or A$_5$M-PDHA, respectively. The kinetics was (as above) compared to simulated values using rate constants (k$_1$, k$_{-1}$ etc) obtained for the conjugation of Dext$_5$ to free ADH or PDHA. The results are summarised in Table S5 and the kinetic plots are given in Figure S47. Compared to the model, it appears the second conjugation is faster and gives higher yields than the first.

Table S5: Kinetic parameters obtained from the modelling of the reaction of $Dext_6$ with an equimolar proportion of A_5M-ADH or A_5M-PDHA. Simulated parameters for the corresponding reactions with equimolar proportions of oligomers and amine using rate constants obtained for the conjugation of $Dext_5$ to free ADH or PDHA are given in italics.
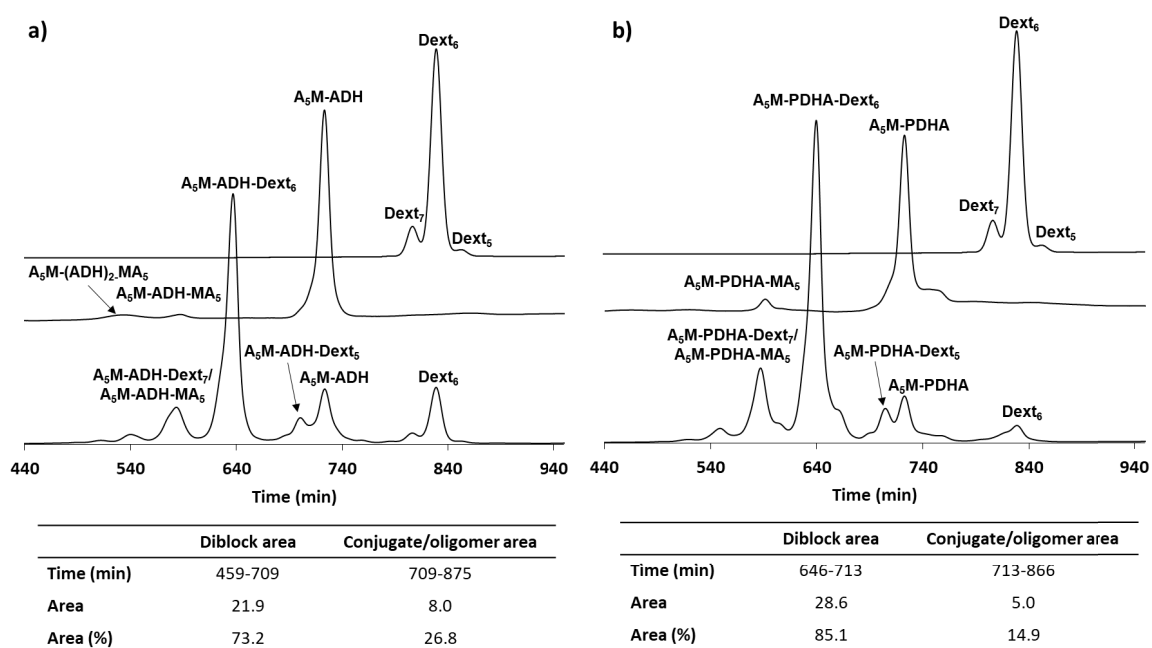
| | | Equivalents | | A+B ↔ E + Z+Pyr | | Equilibrium yield |
| | | | | $t_{0.5}$ | $t_{0.9}$ | |
A	**B**	**B**	**pH**	**[h]**	**[h]**	**[%]**
$Dext_6$	A_5M-ADH	1	4.0	1.72	5.74	15
$Dext_5$	*ADH*	*0.5*	*4.0*	*2.27*	*7.54*	*11*
$Dext_6$	A_5M-PDHA	1	4.0	2.07	8.36	66
$Dext_5$	*PDHA*	*0.5*	*4.0*	*5.76*	*21.30*	*51*
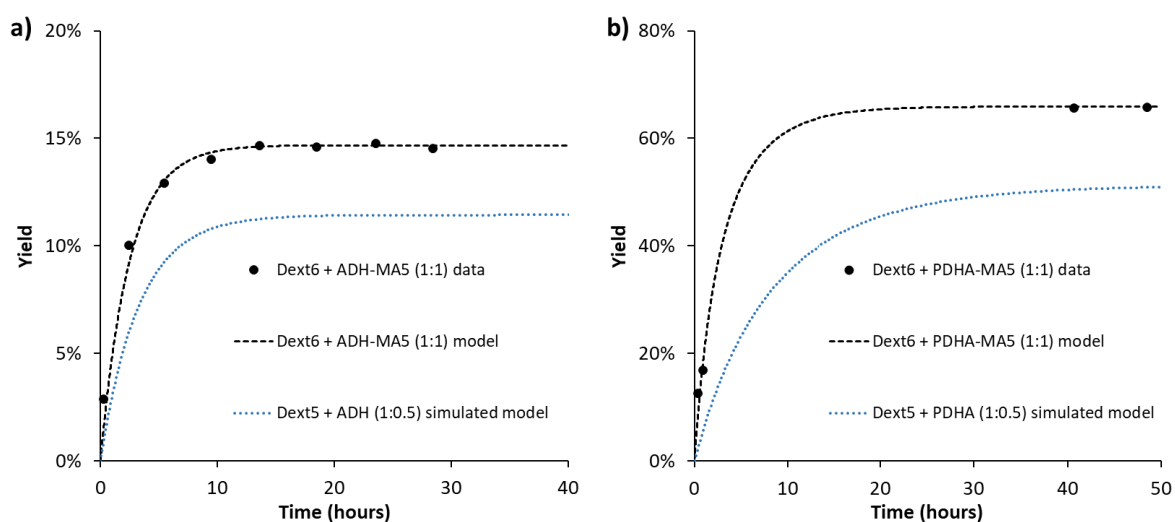
Figure S47: Kinetics of the reactions of Dex_6 with equimolar amounts of **a)** A_5M-ADH and **b)** A_5M-PDHA. Simulated data for the corresponding reactions of Dex_5 with free ADH and PDHA (0.5 equivalents) is included for comparison.

Reduction of the equilibrium mixtures with chitin-*b*-dextran diblocks was performed at 40 °C using 20 equivalents PB due to the slow reduction of conjugates with normal reducing ends [5]. Reduction was terminated after 72 and 144 hours for the preparation A_5M-PDHA-$Dext_6$ and A_5M-ADH-$Dext_6$ diblocks, respectively, due to the slower reduction of ADH conjugates [5]. The reaction mixtures were fractionated by GFC (Figure S48), and main fractions were purified and characterized by ^{1}H-NMR (Figure S49-S53). As purified A_5M conjugates were used for the diblock preparation, the integral for the H1, A resonance was set to 5 in all the ^{1}H-NMR spectra. The yield of diblocks was obtained by integrating the chromatograms (Figure S48) as described above. Due to the slight polydispersity of the $Dext_6$ oligomer, some longer and shorter diblocks were also formed. The weight yield of diblocks was 85 and 92 % for chitin-*b*-dextran diblocks with ADH and PDHA, respectively. The amount of remaining unreduced diblock could not be accurately determined because the resonance

corresponding to the unreduced *N*-pyranoside conjugates overlaps with other resonances in the spectra. However, the integral for the secondary amine resonance balanced the integrals of the resonances from both chitin and dextran, suggesting close to complete reduction of diblocks. Approximately 40 % the unreacted dextran oligomers from the reaction with A_5M-ADH conjugates (20 equivalents PB, 40 °C) were reduced after 144 hours (6 days) (Figure S51). Hence, the dextran oligomers are reduced by PB with a much slower rate than the A_nM oligomers. The slow reduction of dextran oligomers also explains the higher yield of diblocks obtained compared to the low amination yield, as the dextran oligomers can react further after addition of reducing agent.


	Diblock area	Conjugate/oligomer area
Time (min)	459-709	709-875
Area	21.9	8.0
Area (%)	73.2	26.8

	Diblock area	Conjugate/oligomer area
Time (min)	646-713	713-866
Area	28.6	5.0
Area (%)	85.1	14.9

Figure S48: GFC fractionation of the reaction mixture obtained for the preparation of diblocks by reacting $Dext_6$ oligomers with **a)** A_5M-ADH or **b)** A_5M-PDHA conjugates in an equimolar ratio. Fractionation of the $Dext_6$ oligomers and the purified conjugates are included for comparison.
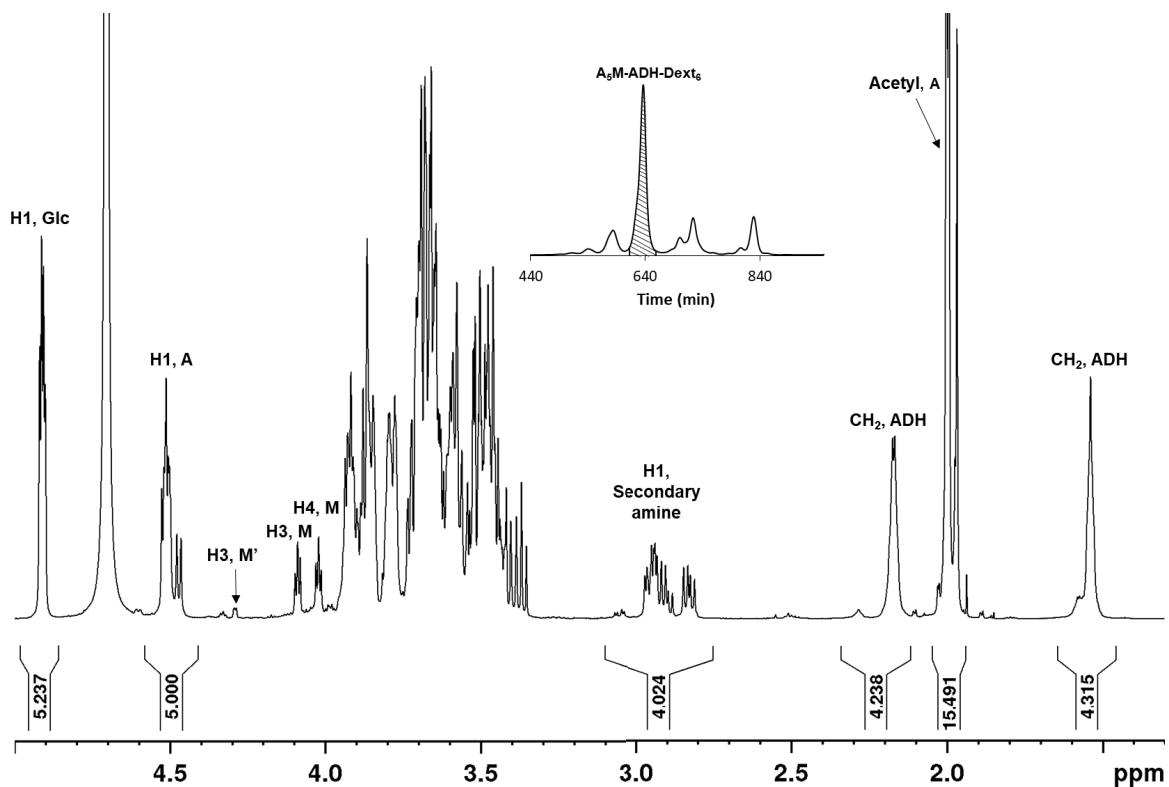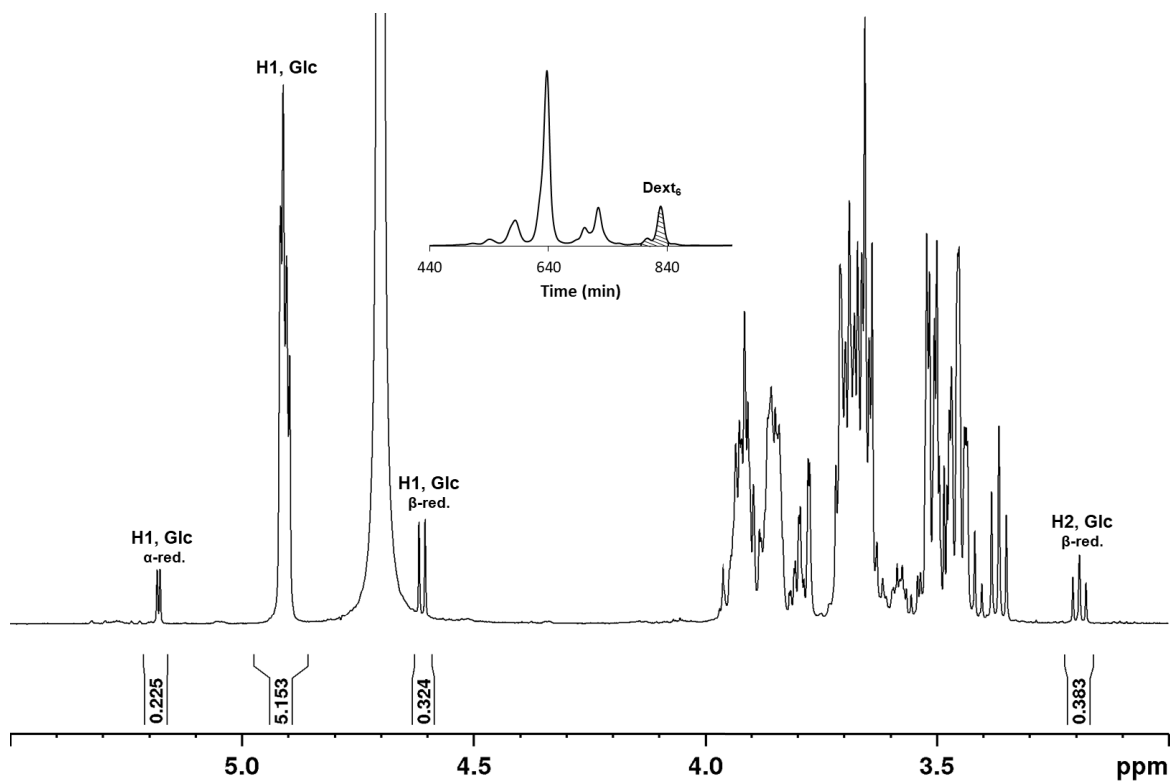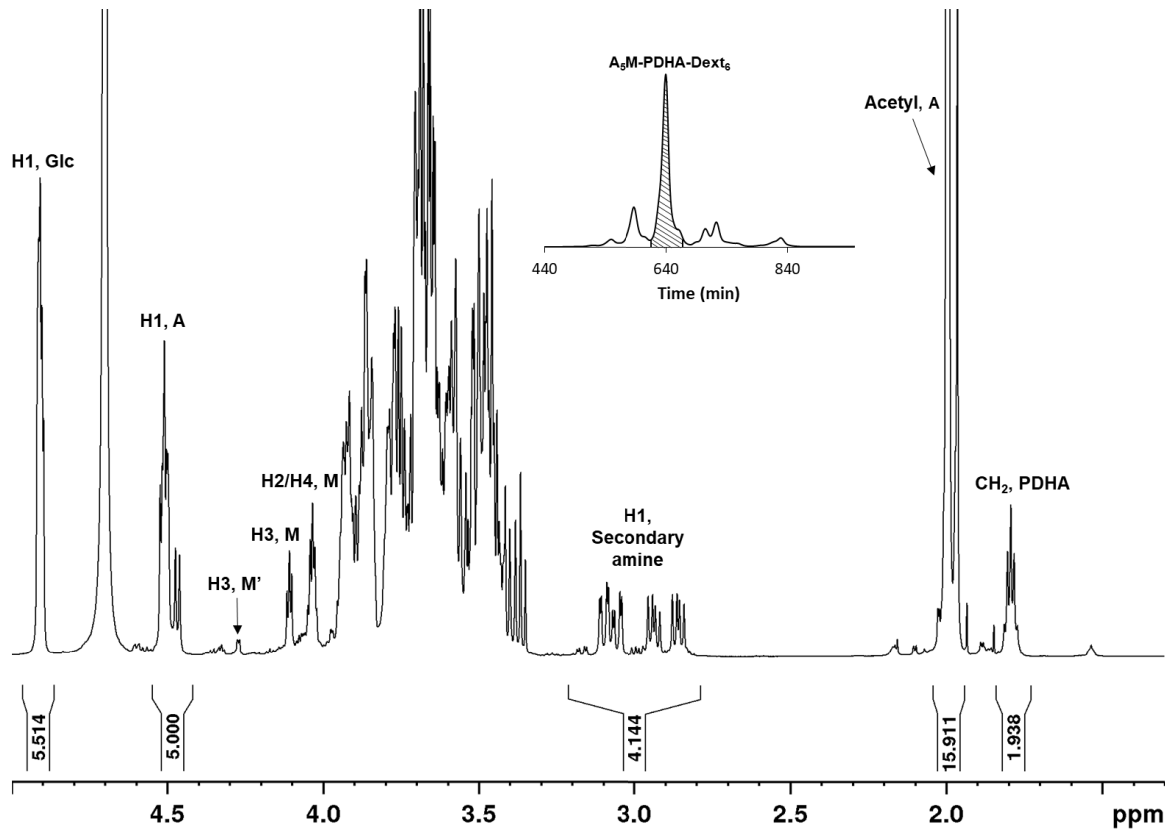
Figure S49: ^{1}H-NMR spectrum of the A_5M-ADH-Dext$_6$ fraction (D$_2$O, 300K, 600 MHz) from the chromatogram in Figure S48a.
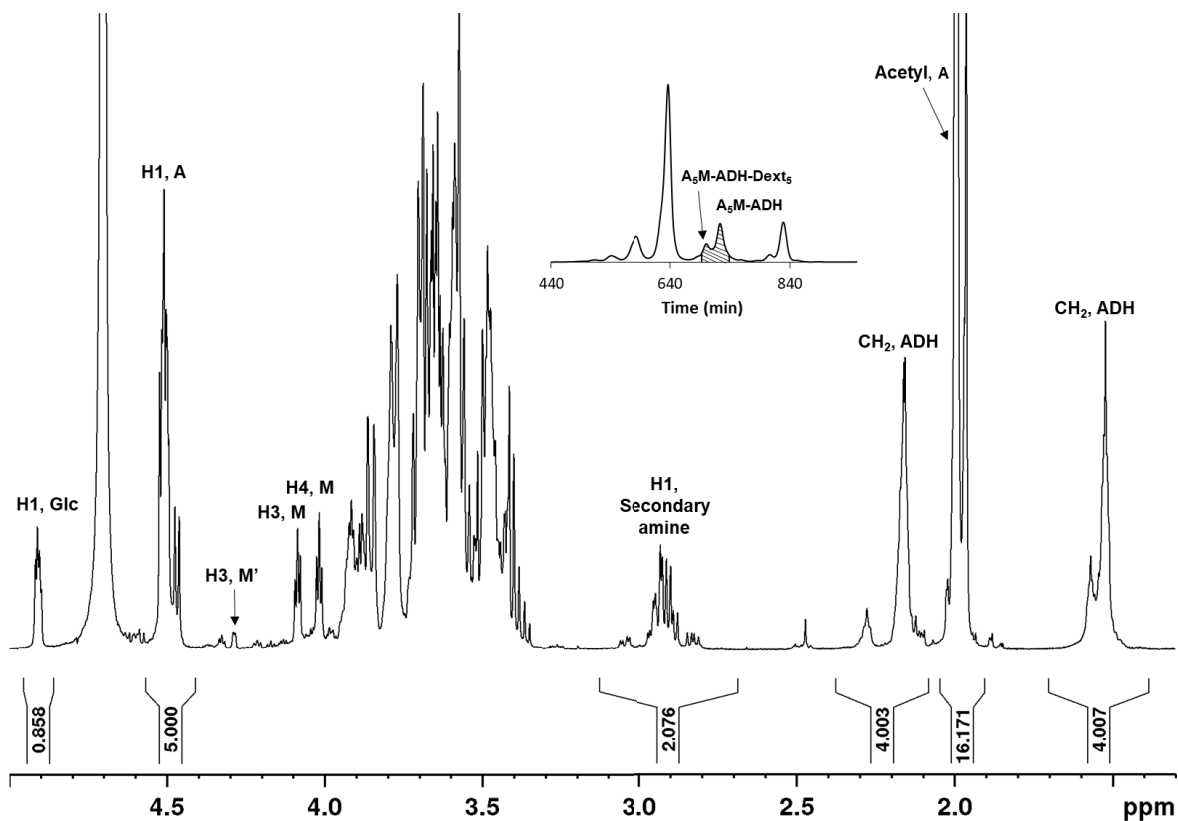
Figure S50: ^{1}H-NMR spectrum of the A_5M-ADH-Dext$_5$/A_5M-ADH fraction (D$_2$O, 300K, 600 MHz) from the chromatogram in Figure S48a.

Figure S51: ^{1}H-NMR spectrum of the Dext$_6$ fraction (D$_2$O, 300K, 600 MHz) from the chromatogram in Figure S48a.

Figure S52: ^{1}H-NMR spectrum of the A$_5$M-PDHA-Dext$_6$ fraction (D$_2$O, 300K, 600 MHz) from the chromatogram in Figure S48b.
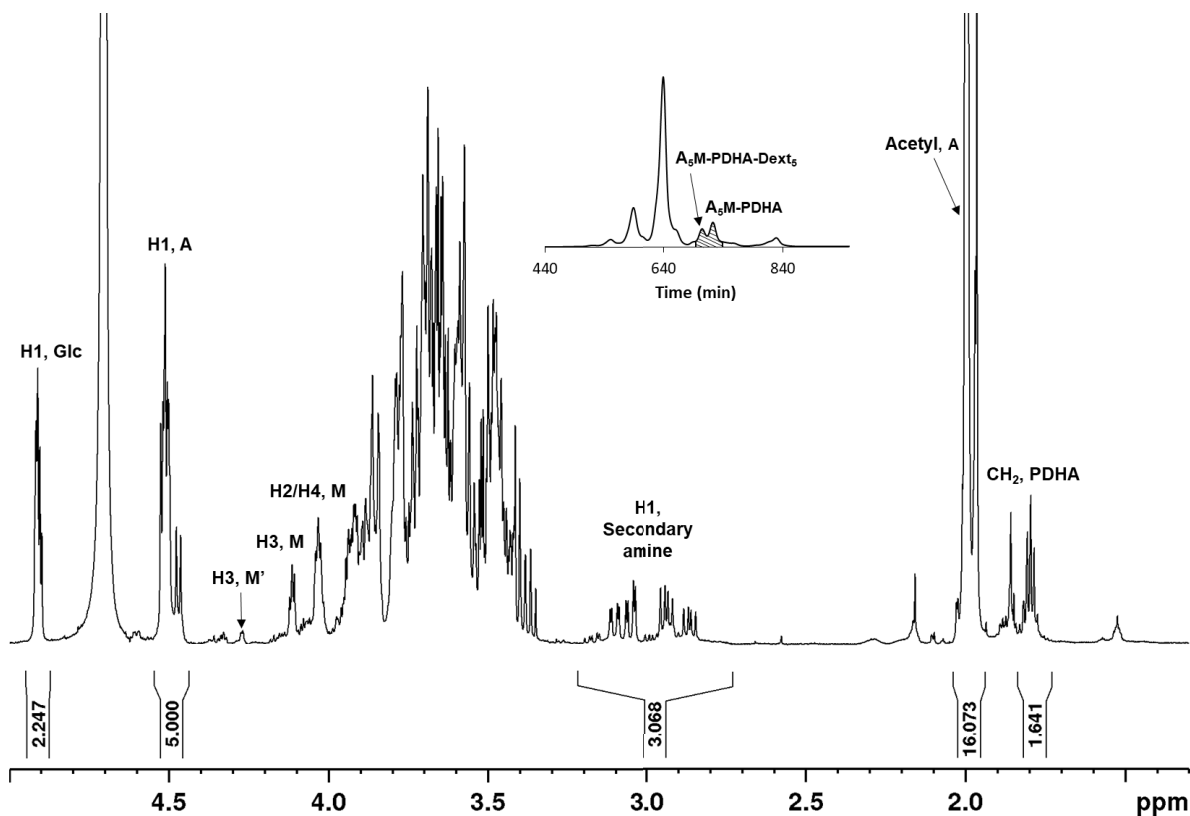
Figure S53: ^{1}H-NMR spectrum of the A_5M-PDHA-Dext$_5$/A_5M-PDHA fraction (D$_2$O, 300K, 600 MHz) from the chromatogram in Figure S48b.

References

1.   Allan, G. G.; Peyron, M., Molecular-Weight Manipulation of Chitosan .1. Kinetics of Depolymerization by Nitrous-Acid. *Carbohydr. Res.* **1995,** 277, (2), 257-272.

2.   Tømmeraas, K.; Vårum, K. M.; Christensen, B. E.; Smidsrød, O., Preparation and characterisation of oligosaccharides produced by nitrous acid depolymerisation of chitosans. *Carbohydr. Res.* **2001,** 333, (2), 137-144.

3.   Sugiyama, H.; Hisamichi, K.; Sakai, K.; Usui, T.; Ishiyama, J.-I.; Kudo, H.; Ito, H.; Senda, Y., The conformational study of chitin and chitosan oligomers in solution. *Bioorg. Med. Chem.* **2001,** 9, (2), 211-216.

4.   Lindberg, B.; Lönngren, J.; Svensson, S., Specific Degradation of Polysaccharides. In *Advances in Carbohydrate Chemistry and Biochemistry,* Tipson, R. S.; Derek, H., Eds. Academic Press: 1975; Vol. Volume 31, pp 185-240.

5.   Mo, I. V.; Feng, Y.; Dalheim, M. Ø.; Solberg, A.; Aachmann, F. L.; Schatz, C.; Christensen, B. E., Activation of enzymatically produced chitooligosaccharides by dioxyamines and dihydrazides. *Carbohydr. Polym.* **2020,** 232, 115748.

6.   van Dijk-Wolthuis, W. N. E.; Franssen, O.; Talsma, H.; van Steenbergen, M. J.; Kettenes-van den Bosch, J. J.; Hennink, W. E., Synthesis, Characterization, and Polymerization of Glycidyl Methacrylate Derivatized Dextran. *Macromolecules* **1995,** 28, (18), 6317-6322.